

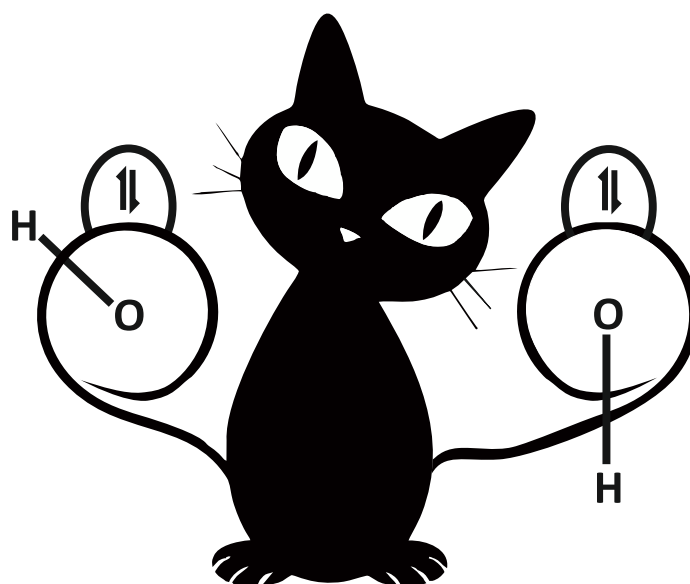
You spin me right round—

Computational and experimental studies on conformer-specific reactivity in hydroxycarbenes

Inauguraldissertation zur Erlangung des Doktorgrades der Naturwissenschaftlichen Fachbereiche

im Fachgebiet Organische Chemie (Fachbereich 08) an der

Justus-Liebig-Universität Gießen



vorgelegt von

Henrik Quanz

aus Hünfeld

angefertigt im Zeitraum von Mai 2015 bis Februar 2021

am Institut für Organische Chemie

der Justus-Liebig-Universität Gießen

Betreuer: Prof. Dr. Peter R. Schreiner, PhD

Eidesstattliche Erklärung

Ich erkläre: Ich habe die vorgelegte Dissertation selbstständig und ohne unerlaubte fremde Hilfe und nur mit den Hilfen angefertigt, die ich in der Dissertation angegeben habe. Alle Textstellen, die wörtlich oder sinngemäß aus veröffentlichten Schriften entnommen sind und alle Angaben, die auf mündlichen Auskünften beruhen, sind als solche kenntlich gemacht. Ich stimme einer evtl. Überprüfung meiner Dissertation durch eine Antiplagiat-Software zu. Bei den von mir durchgeführten und in der Dissertation erwähnten Untersuchungen habe ich die Grundsätze guter wissenschaftlicher Praxis, wie sie in der „Satzung der Justus-Liebig-Universität Gießen zur Sicherung guter wissenschaftlicher Praxis“ niedergelegt sind, eingehalten.

Ort, Datum

Unterschrift

Dekan: Prof. Dr. Thomas Wilke

Erstgutachter: Prof. Dr. Peter R. Schreiner, PhD

Zweitgutachter: Prof. Dr. Bernd Smarsly

„Die Quantenmechanik ist sehr achtung-gebietend. Aber eine innere Stimme sagt mir, daß das doch nicht der wahre Jakob ist. Die Theorie liefert viel, aber dem Geheimnis des Alten bringt sie uns kaum näher. Jedenfalls bin ich überzeugt, daß der nicht würfelt.“

Albert Einstein (1879–1955)

Zusammenfassung

Hydroxycarbene ($R-\ddot{C}-OH$) sind vor allem bekannt als Metall-Liganden in so genannten Fischer-Carbenen. Ihre Existenz als „freies“ Carben war jedoch bis 2008 umstritten, als es Schreiner *et al.* gelang, das einfachste Hydroxycarben, Hydroxymethylen ($R=H$) bei tiefen Temperaturen zu isolieren. Es zeigte sich, dass Hydroxymethylen nicht persistent ist und trotz einer enormen Energiebarriere zu Formaldehyd reagiert, ein Prozess der nur durch quantenmechanisches Tunneln (QMT) zu erklären ist. Da QMT nicht nur von der Höhe, sondern auch von der schwer zu bestimmenden Breite der Reaktionsbarriere abhängt, erschwert es das rationale Design von Reaktionen. Insbesondere die selektive Reduktion der Energiebarrieren von Konformeren zu ihren Produkten haben einen entscheidenden Einfluss auf die Produktverteilung (Curtin-Hammett-Prinzip). Dennoch konnte in allen Fällen bei der Isolation von Hydroxycarbenen niemals das *s-cis*-Konformer nachgewiesen werden. In dieser Arbeit konnten wir zum ersten Mal *s-cis*-Konformere von Hydroxycarbenen isolieren.

In der ersten Veröffentlichung isolierten und charakterisierten wir das *s-cis*-Konformer von Trifluoromethylhydroxycarben ($F_3C-\ddot{C}-OH$), welches wir durch UV-Strahlung des *s-trans*-Konformers erzeugen konnten. Das *s-trans*-Konformer zeigte den typischen [1,2]H-Shift zu Trifluoroacetaldehyd durch QMT. Das *s-cis*-Konformer zeigt dies nicht, weshalb wir von einem konformerspezifischen [1,2]H-Shift durch QMT sprechen. Das bekannte Curtin-Hammett-Prinzip kann nicht angewandt werden, da das *s-cis*-Konformer vom *s-trans*-Konformer durch eine hohe Aktivierungsbarriere getrennt ist, und somit eine schnelle Gleichgewichtsreaktion ausgeschlossen ist. Zum Zeitpunkt der Veröffentlichung zeigte sich, dass Trifluoromethylhydroxycarben die längste gemessene Halbwertszeit ($\tau = 144$ Std.) aller Hydroxycarbene hatte.

In der zweiten Veröffentlichung konnten wir das *s-cis,s-cis*-Konformer des Dihydroxycarbens nach Bestrahlung mit nahem Infrarotlicht (NIR) charakterisieren. Die beiden Konformere, das *s-cis,s-trans*- und das *s-trans,s-trans*-Konformer, waren bekannt, nicht aber das *s-cis,s-cis*-Konformer. Dieses Konformer ist ein Intermediat in der direkten Reaktion von H_2 und CO_2 . Das *s-cis,s-cis*-Konformer ist nicht persistent. Es wandelt sich durch QMT zu dem *s-cis,s-trans*-Konformer innerhalb von 22 Minuten bei 3 K um. Durch die Analyse der Reaktionskinetik konnten wir feststellen, dass diese Reaktion nur partiell stattfindet. Unsere Berechnungen lassen den Schluss zu, dass durch QMT eine Reaktion zu CO_2 und H_2 stattgefunden hat.

In der dritten Veröffentlichung haben wir das Programm *TUNNEX* beschrieben. Mit seiner nutzerfreundlichen Oberfläche ermöglicht es die Tunnelhalbwertszeit mittels Wentzel-Kramers- und Brillouin-Methode (WKB) zu bestimmen. Um die Daten für *TUNNEX* aufzubereiten, bedienen wir uns der Quantenchemiesoftware *Gaussian* und einem von uns entwickelten Tool. Der Nutzer muss die Daten nur noch über die graphische Oberfläche von *TUNNEX* importieren und bestimmte Parameter festlegen. Das Programm ist frei nutzbar und online veröffentlicht. Mit *TUNNEX* ist es möglich eine erste Abschätzung der erwarteten Halbwertszeit auf Basis von standardisierten Berechnungen zu erhalten.

Abstract

Hydroxycarbenes ($R-\ddot{C}-OH$) are known ligands in so-called Fischer-complexes. Still, the scientific community debated the existence of “free” hydroxycarbenes until the isolation of the simplest hydroxycarbene, hydroxymethylene ($R=H$), which Schreiner *et al.* achieved at cryogenic temperatures. Surprisingly, hydroxymethylene is not persistent and reacts quickly to formaldehyde despite a high barrier, concluding that quantum mechanical tunneling (QMT) must be involved. As QMT is not only dependent on the reaction barrier height but also on the reaction barrier width—which hard to model—there is a significant challenge in the rational design of reactions. Especially, the reduction of a conformer's activation barrier to its product has a distinct influence on the product ratio (Curtin-Hammett principle). Nevertheless, we have not observed the *s-cis*-conformer of hydroxycarbenes and their reactivity. Hence, we explored the generation of *s-cis* hydroxycarbenes by applying two different strategies.

In the first publication, we tried to isolate the *s-cis*-conformer of trifluoromethylhydroxycarbene ($F_3C-\ddot{C}-OH$), which is stabilized by an intramolecular H-F bridge. Indeed, after irradiation with UV light, we could observe the *s-cis* conformer. The *s-trans*-conformer displays the typical [1,2]H-shift to trifluoroacetaldehyde through QMT, whereas the *s-cis*-conformer does not transform. Hence, trifluoromethylhydroxycarbene shows conformer-specific tunneling. The established Curtin-Hammett principle is not applicable because a significant activation barrier separates the two conformers, making fast equilibration impossible. At the time of the publication, trifluoromethylhydroxycarbene showed the longest measurable half-life ($\tau = 144$ h) of all previously isolated hydroxycarbenes. Hence, the push-pull substitution of the substituents OH and CF_3 may stabilize carbenes, which was later observed for other hydroxycarbenes.

In the second publication, we addressed whether it was possible to generate conformers in hydroxycarbenes through stimulation with near-infrared light (NIR). We investigated the system of dihydroxycarbene, which has three different conformers and is an essential intermediate on the $[H_2CO_2]$ potential energy surface. The *s-cis,s-trans*-conformer and the *s-trans,s-trans*-conformer were known, but not the *s-cis,s-cis*-conformer, an essential intermediate in the bimolecular reaction of H_2 and CO_2 . We could transform either conformer to the previously unobserved *s-cis,s-cis* conformer through NIR irradiation. At 3 K, the *s-cis,s-cis*-conformer is not stable and undergoes QMT back to the *s-cis,s-trans*-conformer within 22 minutes. We found indications for a second QMT reaction of the *s-cis,s-cis*-conformer, possibly a decomposition to CO_2 and H_2 , which we could confirm by computations.

In the third publication, we presented a program suite to compute tunneling half-lives in a simple fashion (*TUNNEX*) using the Wentzel, Kramers, and Brillouin (WKB) method. The necessity arose during the last project as to accelerate the computation of QMT half-lives. After generating the reaction path using Gaussian—a widely used quantum chemistry program—the user deploys a helper tool to generate the data necessary for WKB computation. After import in *TUNNEX*, the user defines the parameters and computes the QMT half-life. The program is free to use and published online. It uses openly available libraries for interpolation and integration of the tunneling path. *TUNNEX* is the first entry point for computing the QMT half-lives and is as user-friendly as possible.

Meinem Onkel Karl Dieter

Table of Contents

Eidesstattliche Erklärung	III
Zusammenfassung	VII
Abstract	VIII
1 Introduction	1
1.1 Carbenes in chemistry	1
1.2 Characterization of highly reactive carbenes	5
1.3 Quantum mechanical tunneling (QMT)	6
1.4 [1,2]H-tunneling in hydroxycarbenes	10
1.5 Generation of conformers in matrix isolation studies	13
1.6 Our experimental insights concerning conformer chemistry in hydroxycarbenes	16
1.7 Our contributions to the computational determination of tunneling half-lives	19
1.8 Concluding remarks	20
1.9 References	21
2 Publications	25
2.1 Conformer-specific hydrogen atom tunnelling in trifluoromethylhydroxycarbene	25
2.2 TUNNEX: An easy-to-use Wentzel-Kramers-Brillouin (WKB) implementation to compute tunneling half-lives	33
2.3 Identification and reactivity of <i>s-cis,s-cis</i> -dihydroxycarbene, a new [CH ₂ O ₂] intermediate	39
2.4 Further co-authored publications	45
3 Acknowledgement	47

1 Introduction

Hydroxycarbenes ($R-\ddot{C}-OH$, **1**) feature a divalent carbon atom with only six electrons and a hydroxy group in α -position to the carbene center. In 2008, Schreiner *et al.* isolated the simplest conceivable hydroxycarbene, hydroxymethylene ($H-\ddot{C}-OH$, **1a**), which is a high-energy isomer of formaldehyde (**2a**) and possibly involved in prebiotic sugar formation.^[1,2] Schreiner *et al.* obtained **1a** through pyrolysis of glyoxylic acid (**3a**) with subsequent trapping of the products at 11 K in solid Ar.^[1] Caged by insurmountable activation barriers at this temperature ($29.7 \text{ kcal mol}^{-1}$), hydroxymethylene should not undergo any transformation. However, Schreiner *et al.* found that **1a** disappeared within two hours through an [1,2]H-shift to **2a** via quantum mechanical tunneling (QMT). As the rate of QMT depends on the width and height of the barrier (the width includes the mass), it is more likely to find QMT for light particles such as electrons, *e.g.*, in scanning tunneling microscopy (STM) and electron transfer reactions (Marcus theory).^[3-5] Despite many examples wherein hydrogen transfer reactions commonly proceed via QMT,^[6,7] we often neglect this effect to compute accurate rates. The basis for evaluating kinetic rate constants is transition state theory (TST), developed by Eyring, Evans, and Polanyi.^[8,9] Its application to the temperature-dependent *endo-exo*-product ratio in a Diels-Alder reaction by Woodward and Bear^[10] established TST as a successful theory for predicting rates and product ratios for chemical reactions. Undoubtedly, the mechanical picture of TST makes it prone to fail if QMT is involved. Hence, it was only a matter of time when Schreiner *et al.* found a system where the principles derived from TST are invalid. Methylhydroxycarbene ($H_3C-\ddot{C}-OH$, **1b**) prefers the [1,2]H-shift to acetaldehyde (**2b**) over the [1,2]H-shift to vinyl alcohol (**4**). The barrier for the [1,2]H-shift is higher but narrower compared to the [1,2]H-shift to **4** ($28.0 \text{ kcal mol}^{-1}$ vs. $22.6 \text{ kcal mol}^{-1}$), thus establishing *tunneling control* as the third reaction paradigm.^[11,12]

Hence, we attempted to replace the methyl group with a trifluoromethyl (CF_3) group, leading potentially to conformational control of tunneling, as H-F interaction could stabilize the elusive *s-cis*-conformer. We also want to explore the interaction of hydroxycarbenes with near-infrared (NIR) light. Hence, we choose dihydroxycarbene ($HO-\ddot{C}-OH$, **1c**), a high energy isomer of formic acid (**2c**) for which the generation of a higher-lying conformer with NIR light was already reported, to generate the missing *s-cis,s-cis*-conformer, a possible intermediate in the direct reaction of CO_2 and H_2 .^[13,14] As the observation of tunneling reactions in matrix isolation experiments becomes more frequent, we wanted to implement a simplified approach for predicting QMT half-lives using the Wentzel-Kramers-Brillouin (WKB) method in this thesis. But first we explore the chemistry of carbenes in general.

1.1 Carbenes in chemistry

IUPAC defines carbenes and their derivatives as an electronically neutral species with a divalent carbon atom of the type $:CR_2$.^[15] Carbenes have either one divalent or two monovalent substituents. With only six electrons at the divalent center, carbenes have an inherent electron deficiency as all atoms in the molecule try to achieve an octet of electrons (noble gas configuration). The divalent carbon center uses two electrons

for bonding, leaving two unbound electrons in the valence shell. The two-electron spins $s\left(\pm\frac{1}{2}\right)$ can be combined in a parallel or anti-parallel manner. Hence, carbenes exist in a triplet state ($S = 1$) or a singlet state ground state ($S = 0$). As the total spin operator projected onto the z-axis (\widehat{S}_z^2) has an eigenvalue of $\widehat{S}_z^2 = 2S + 1$, where S is the total net spin of the system, the result is one quantum state for the singlet and three for the triplet, hence the name. According to Hund rule,^[16-18] carbenes have a triplet ground state if the frontier orbitals are nearly equal in energy (degenerate), otherwise a carbene has a singlet ground state. Only one electron configuration is possible for the triplet state. For the singlet state, three electron configurations can be imagined (Figure 1). Hence, the computational description of (singlet) carbenes is a non-trivial task, especially for carbenes with a triplet ground state and a minor singlet-triplet splitting like methylene (**5**), the simplest conceivable carbene.

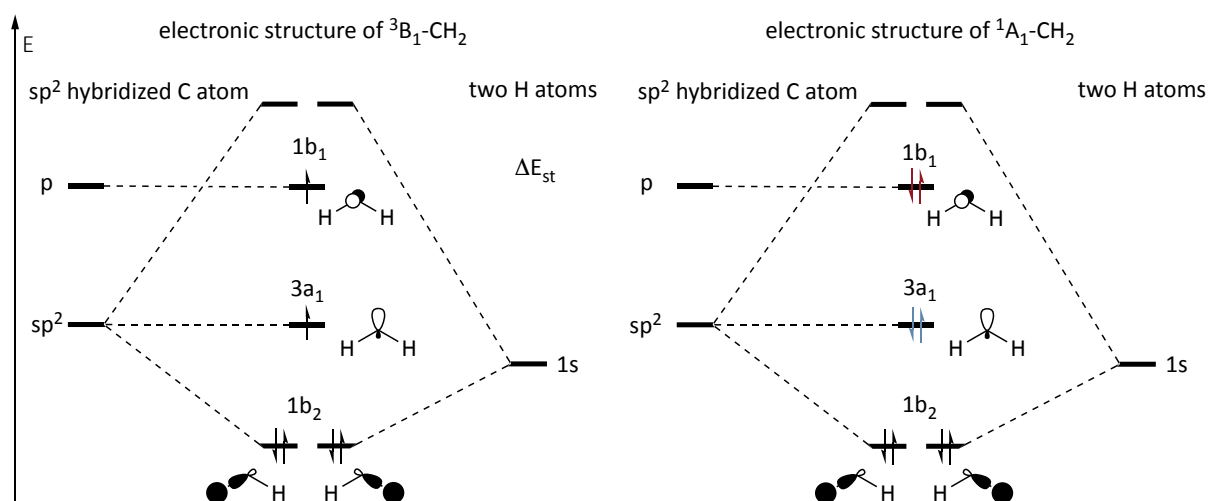


Figure 1. Qualitative electronic structure of bent methylene (**5**) demonstrating the triplet state (left) and the singlet state (right), where blue denotes the first 1A_1 state and red the second 1A_1 state. The asymmetrical singlet state ${}^1B_1(1b_2)^2(3a_1)^1(1b_1)^1$ is not shown as it is equal to the triplet state with a flipped electron.

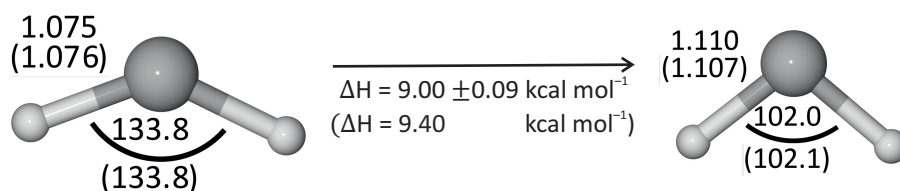


Figure 2. Experimental structure of methylene (**5**) and computed values in parentheses obtained at the AE-CCSD(T)/aug-cc-pCVQZ level of theory with zero-point energy (ZPVE) correction from second-order vibrational perturbation theory (VPT2).

Nef^[19-21] and Butlerow^[22] were the first to try the isolation of methylene (**5**). Unknown to them, their efforts were doomed to fail as the dimerization and reactions of **5** are rapid. Hence, it took 135 years after the first suggestion till Herzberg recorded a gas phase spectrum of methylene (**5**) *via* rotational-vibrational spectroscopy.^[23,24] Initially, he assumed a linear geometry, which contradicted the computational geometry.^[25] Reevaluating Herzberg's spectroscopic constants, Bender and Schaefer obtained a bent ground state in agreement with the results from high-level computations.^[26] The bent ground state is accepted today and presents a neat example for the synergy of theory and experiment. Generally, the discovery of new carbenes benefits greatly from computations (*vide infra*). Lineberger *et al.* accurately determined the singlet state (Figure 2) and found a singlet-triplet splitting of $\Delta E_{st} = 9.00 \pm 0.09 \text{ kcal mol}^{-1}$,^[27,28] which agrees well with the computations from Harrison in 1971

($\Delta E_{st} = 11.3 \text{ kcal mol}^{-1}$).^[29] Employing a state-of-the-art method, we obtained an energy difference of $9.40 \text{ kcal mol}^{-1}$. Therefore, we can assume that singlet carbenes have a bond angle close to 105° , comparable to water. Triplet carbenes have a bond angle around 135° , which is close to NO_2 .^[30] A decade after Herzberg's study, Venkateswarlu measured an emission spectrum of $:\text{CF}_2$ (**6**) in the gas phase.^[31] Like **5**, **6** has a bent ground state, but with a smaller angle around 108° and a $\Delta E_{st} = -54 \pm 3 \text{ kcal mol}^{-1}$. Hence, **6** is a typical singlet carbene and demonstrates the effect of energetically close π -electrons next to the carbene center. Substituents with π -donation capability interact with the $1b_1$ orbital, which decreases in energy, raising the energy gap towards $3a_1$. Hence, the singlet state becomes more stable and favorable. The reactivity of singlet carbenes is more predictable than of triplet carbenes, which react analog to biradicals. Application of difluorocarbene includes the production of polytetrafluoroethylene (PTFE), which we use as a coating on anti-stick frying pans.^[32]

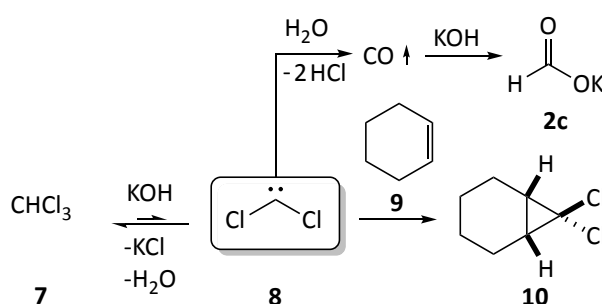


Figure 3. Top: Observation by Geuther in 1862 when treating chloroform **7** with alcoholic KOH solution. The product ratio depends on the concentration of the alcoholic KOH solution. High dilution enhances the formation of CO. Middle: Usage of dichlorocarbene (**8**) as a powerful cyclopropanation agent by Doering and Hoffmann.

After Nef and Butlerow, Geuther proposed a carbene as a reactive intermediate. Upon treatment of chloroform (**7**) with an alcoholic KOH solution, Geuther observed the formation of CO and HCl as well as formic acid (**2c**) (Figure 3).^[33,34] Geuther's interpretation involved the complex $\text{CCl}_2 \cdot \text{HCl}$, which forms from chloroform, thus mentioning the carbene in solution as a reactive intermediate for the first time. The carbene complex can then decompose to CO and HCl in water. The nascent CO is then trapped by KOH.

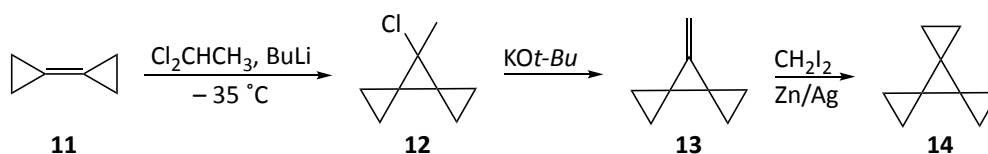


Figure 4. A simple synthesis of [3]-rotane (**14**) using a modified procedure by Doering and Hoffmann and Simmons-Smith conditions in the last step.

Doering and Hoffmann provided the first structural evidence of **8**, adding it to the olefin **9**, forming the addition product **10**.^[35] This reaction has become a standard method to achieve cyclopropanation reactions. With an increase in the electron richness of the olefin, the reaction proceeds faster, underlining the electrophilic nature of dichlorocarbene.^[36] As mentioned, methylene generated photochemically from diazomethane reacts indiscriminately with C-H bonds and double bonds.^[37] However, as an active ligand of transition metals, methylene can show similar reactivity as a singlet carbene. In a stereoselective fashion, Simmons and Smith obtained the cyclopropane moiety, which can lead to highly strained molecules like polyspirocyclopropylidenes ([3]-rotane, **14**) from **11** over **12** and **13**, pushing the limits of ring strain to the boundaries (Figure 4).^[38-40] It is worth noting that the Simmons-Smith step in this example is

quantitative in yield, underlining the high reactivity of carbenes. This could lead to a new class of polymers called polytriangulane.^[40]

In transition metal catalysis, chemists use carbenes as ligands for catalysts, *e. g.*, in metathesis.^[41] We distinguish metals with formal carbenes into Fischer and Schrock complexes named after the researchers who had the most significant impact on their characterization and chemical applicability. Fischer carbenes^[42-44] possess an electronegative but π -donating substituent resulting in a donation of electrons to the metal center. Therefore, the carbenes can be quite electrophilic, and their application lies in the functionalization of suitable nucleophiles.^[45]

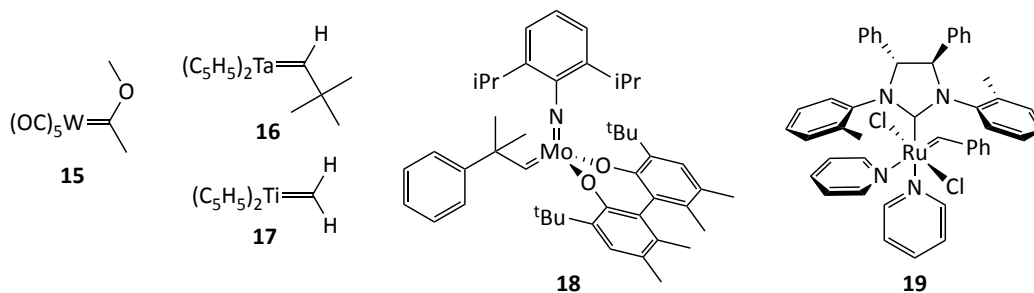


Figure 5. The first Fischer-type carbene (**15**); The first Schrock-type carbene (**16**); The active carbene in Tebbe's reagent (**17**); Schrock-Hoveyda catalyst (**18**); a chiral second-generation Grubbs catalyst (**19**).

An example of such a complex is **15** (Figure 5), which already features the core functional group of hydroxycarbenes. Schrock carbenes do not bear a heteroatom at the carbene center and are therefore unable to donate electrons to the metal.^[46] Schrock carbenes are stabilized by electron donation from the metal into the carbene center, making them rather nucleophilic, *e. g.*, **16**. In a Wittig^[47]-analogous reaction, Tebbe's reagent (**17**) takes the role of a phosphonium ylide,^[48] but the most prominent application of Schrock carbenes lies in the (stereoselective) functionalization of olefins referred to as metathesis. With **18**, the first air-stable Schrock-Hoveyda type catalyst for metathesis became accessible, followed by Grubbs's first stereoselective catalyst (**19**), allowing the synthesis of complex natural products.^[49-51] Therefore, it was no surprise that the scientific community recognized the breakthrough by awarding Chauvin, Grubbs, and Schrock with the Nobel prize.^[52] As metals are expensive, the question arises if carbenes can be utilized directly as an organocatalyst.

Wanzlick and Schikora had the idea of supplementing a carbene center with electron density from nitrogen—undoubtedly the best π -electron donor—in a constrained geometry. Hence, they predicted to generate **20** from **21** but could only isolate the dimer **22** (Figure 6).^[53] As indirect structural evidence for **20**, they added an electrophile to a heated solution of **22** and isolated the addition product **23**. We refer to the equilibrium related to the formation of **20** from **22** as the Wanzlick equilibrium. The existence of the Wanzlick equilibrium was debated, as Lemal *et al.* and Winberg *et al.* could not observe the cross-coupled dimer of two carbenes (**25**) originating from a heated solution of the dimers of **20** and **24** at first, which they later revised by adjusting the reaction conditions.^[54,55] The pioneering work of Wanzlick motivated the scientific community to present a carbene stable under ambient conditions to use in synthesis. Bertrand *et al.* introduced bulky substituents to suppress dimerization and isolate the first carbene stable for weeks under ambient conditions (**26**) (Figure 6).^[56] Arduengo *et al.* further suppressed dimerization and bimolecular reactivity synthesizing **27**, an indefinitely stable carbene at ambient conditions. The discovered

N-heterocyclic carbenes (NHCs) opened new possibilities in various fields of chemistry. NHCs can directly catalyze *Umpolung* reactions, annulations, oxidative acylation and are used in base catalysis.^[57] Today, chemical supply companies provide precursors of carbenes like Enders's carbene **28** commercially, which yields the free carbene *via* thermolysis.^[58]

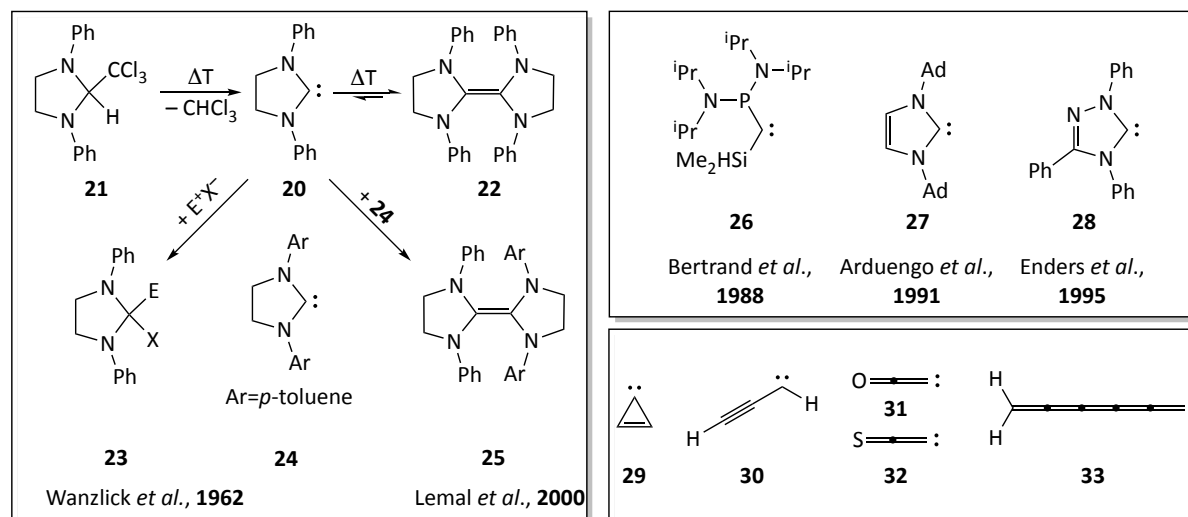


Figure 6. Left: The Wanzlick equilibrium and its experimental verification. Top-right: The history of stable carbenes. Bottom-right: Carbenes detected in space other than methylene (5)

In biochemical reactions NHC-like motives are used as coenzymes, namely thiamin (vitamin B₁), a thiazolium salt participating in, *e.g.*, glycolysis. Thiamin decarboxylates pyruvate to form the acetyl-CoA or acts in the transketolase reaction.^[59] Deprotonation of thiamine leads to the formation of a free carbene which can participate in *Umpolung* reactions, such as benzoin condensation.^[60,61] The important intermediate in the benzoin reaction is the Breslow intermediate, a formal dimer of hydroxycarbenes and the 2,3-dihydrothiazol-2-ylidene.^[62-64] The existence of the Breslow intermediate was unconfirmed until recently when Berkessel *et al.* could isolate and characterize this intriguing intermediate by reducing its nucleophilicity through electron-withdrawing groups like CF₃.^[65,66]

Astronomers also detected carbenes in space, where many highly reactive carbenes are persistent enough to be detected due to the high dilution and low temperature. As carbenes resemble potential precursors of biologically relevant molecules, astronomers search for them actively. They use rotational-vibrational emission signals to identify molecules. Hence, carbenes are prevalent molecules for detection because they usually possess a high dipole moment compared to their viable products.^[67] Astronomers identified a number of carbenes, namely 5,^[68] cyclopropylidene (**29**),^[69] propargylene (**30**),^[69,70] oxoethenylidene (**31**),^[71] thiooxaethenylidene (**32**)^[72] and hexapentenylidene (**33**).^[73]

1.2 Characterization of highly reactive carbenes

But how can we spectroscopically identify highly reactive carbenes like those detected in space? The Wanzlick equilibrium taught us to suppress the dimerization process and reactions with other electrophiles for their successful isolation, as highly reactive carbenes usually have small barriers for intermolecular reactions. The necessity of low temperature and high dilution led to the development of the matrix isolation technique where we mix the reactive intermediate/precursor with host atoms/molecules and trap it

(usually at 3-15 K). Like raisins in a cake, we separate the reactive intermediate/precursor from other molecules. We typically generate the intermediate by high vacuum flash pyrolysis (HVFP) or photolysis of the precursor. At temperatures around 3–15 K, intermediates cannot surpass potential energy barriers ($> 3 \text{ kcal mol}^{-1}$) and are therefore unable to transform into a more stable product. By trapping the intermediate ideally in a single cage of inert host atoms/molecules, one suppresses dimerization. Among the spectroscopic methods, infrared (IR) and ultraviolet-visible (UV-Vis) spectroscopy have been the methods of choice to identify intermediates, especially since individual bands are narrow compared to film/powder measurements. In addition, the computational prediction of harmonic IR- and UV-Vis spectra of the unknown compound(s) is nowadays a rather trivial task with sufficient accuracy. Nevertheless, the prediction of anharmonic spectra, which generally are closer to the experiment, is still an ongoing challenge. Astronomers use spectroscopic identification as a basis to look for carbenes in the microwave spectra. Other methods include electron spin paramagnetic resonance spectroscopy (EPR), nuclear magnetic resonance spectroscopy (NMR), and fluorescence spectroscopy.

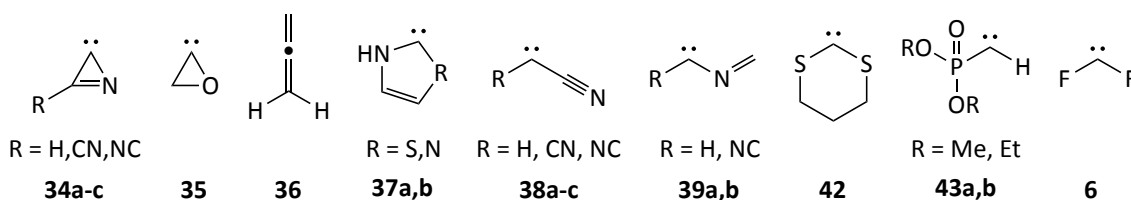


Figure 7. A selection of highly reactive carbenes that Maier and Schreiner *et al.* characterized using the matrix isolation technique

At the JLU Giessen, Maier and Schreiner *et al.* isolated many carbenes using matrix isolation (Figure 7). Among them are 3-membered cyclic carbenes such as cyclopropenyliidene (**29**),^[74] azacyclopropenyliidenes (**34**),^[75] and oxiranyliidene (**35**).^[76] Also, the list includes basic alkenyl carbenes like propadienyliidene (vinylidenecarbene, **36**),^[77] propargylene (**30**).^[70] In addition hetero-substituted carbenes with nitrogen, silicon, sulfur, and phosphorus namely 2,3-dihydrothiazol-2-ylidene (**37a**),^[78] 2,3-dihydroimidazol-2-ylidene (**37b**),^[79] several of different substituted cyano- (**38a,b**) and isocyanocarbenes (**38c,39**),^[75,80] 1,1-dichlorosilaethylidene ($\text{Cl}_2\text{H-Si-}\ddot{\text{C}}\text{-H}$, **40**),^[81] silaethylidene ($\text{H}_3\text{Si-}\ddot{\text{C}}\text{-H}$, **41**),^[82] [1,3]dithian-2-ylidene (**42**),^[83] several alkyl phosphonatocarbenes ($\text{R} = \text{Me}$, **43a**; $\text{R} = \text{Et}$, **43b**),^[84] and difluorocarbene (**6**) was isolated. In addition, Schreiner *et al.* generated a whole new family of hydroxycarbenes, which could play a role in the prebiotic formation of sugars in the gas phase in space in the absence of a strong base.^[2,85,86] Through the isolation of hydroxymethylene and its rapid disappearance under cryogenic conditions, QMT and hydroxycarbenes are closely tied together.

1.3 Quantum mechanical tunneling (QMT)

Quantum mechanical tunneling allows small particles such as electrons and atoms to penetrate and eventually pass through a barrier without sufficient energy to surmount it, which contradicts our mechanistic understanding according to which the barrier should reflect the particle. For accurate prediction of rates, it is imperative to take QMT into account, especially at lower temperatures when thermal energy is relatively low and almost all molecules are in their ground state.

The theory of quantum mechanical tunneling is closely linked to the discovery of radioactivity through the intricate research by Becquerel, and Curie *et aliae*.^[87-90] Kohlrausch could verify the decay empirically as exponential and dependent on the initial concentration.^[91] He coined the idea of half-life, *i.e.*, the time interval after which half of the initial particles have vanished. Much like the black body radiation, the researchers could not understand the phenomenon based on established physics. With the emergence of quantum mechanics, Hund already predicted in 1927 that the wave-like properties of matter should make QMT possible for light particles like electrons, hydrogen atoms, hydride ions, and protons, especially when the de Broglie wavelength shows the same order of magnitude as the width of the penetrated barrier.^[16-18,92] Gamow derived a general mathematical solution for QMT, and Gurney and Condon applied Gamow's results to a model of nuclear potential and derived a relationship between the half-life of the particle and the energy of emission.^[93,94] Gurney and Condon's solution agrees well with Kohlrausch's empirically derived function. Hence, the scientific community accepted the establishment of QMT as an effect observed in the quantum mechanical world exclusively, which is a direct consequence of the uncertainty principle derived by Heisenberg.^[95] In chemistry, Wigner mentioned tunneling for the first time.^[96] As Wigner and Eyring realized the implications of tunneling while formulating TST, they recommended not to use TST if tunneling from the ground state drives the reaction.^[8] Tunneling manifests itself in experiments through sizeable kinetic isotope effects (KIE) and temperature independence at low temperatures in the Arrhenius plot. Today we know many examples involving tunneling, including heavy atom tunneling.^[6,97]

Nevertheless, chemists widely accept TST theory and its classic implications for the explanation of product ratio at different temperatures owing to the work of Evans and Polanyi^[9] and Woodward and Bear.^[10] Their work led to the well-established concept of thermodynamic *vs.* kinetic control, which has its foundation on the (computed) kinetic rates from TST only involving the partition functions of the transition state and its energy on the potential energy surface (PES). Per definition, the thermodynamic product forms at high temperatures as the system can equilibrate freely, whereas the kinetic product forms at low temperatures over the barrier with the smallest activation energy. For reactions that mostly obey the classic mechanical rules, Wigner implemented a correction of rates using a probability function that accounts for QMT.^[96] At temperatures close to 0 K at which slow particles start to contribute significantly to the speed of a reaction, QMT is usually the only driving force, and hence not only the height but also the width of the barrier is essential for reaction rates. QMT can not only lead to the breakdown of concepts based on TST (*vide infra*) but makes the computational prediction of stability based on barrier heights impossible. Hence, Wentzel, Kramers, and Brillouin (WKB) developed a method to predict tunneling rates.

To find a general solution for slowly varying potential, WKB provided the basis for calculating tunneling rates, although it applies to many other problems with a general varying potential. As usual, we start with the Schrödinger equation in the one-dimensional case

$$\psi''(x) + Q(x)\psi(x) = 0,$$

where primes indicate derivatives with respect to x and

$$Q(x) = \frac{2m}{\hbar^2}(E - V(x)) = \frac{1}{\hbar^2}p(x)^2.$$

vanishes. With the help of these solutions, we derive the transmission probability $T(E)$. The transmission probability correlates only with the integral of the barrier, which is proportional to the width and height. As the numerical result of an integral is an accumulating quantity, width is more important than height for relatively small barriers. Theoretically, WKB is only applicable to the one-dimensional case. However, Fukui introduced the intrinsic reaction coordinate (IRC) formalism to project the total motion of atoms into a single coordinate (usually the mass of the moving particles is included),^[100] making WKB a multi-dimensional approach. Most quantum chemistry programs implement the IRC algorithm. We can also combine WKB with newer methods such as the string method or nudged elastic band for reaction path optimization.^[101,102]

Hence, it seems easy to implement this theory, but there are technical challenges. First, the potential $V(x)$ needs to be fitted to evaluate the integral between w_1 and w_2 , numerically. As we can employ different numeric integration schemes, the results are often difficult to reproduce as the numerical value of the penetration integral (σ , Figure 8) is very sensitive towards change (exponential relation). The second challenge is the correction of $V(x)$ with the zero-point vibrational energy along the path, which motivated us to implement a graphical user interface (GUI) (*vide infra*). Remarkably, WKB yields excellent half-lives compared to experiments on deep tunneling usually encountered in matrix isolation experiments, depending on the quantum mechanical (QM) method.^[1,11,103]

We can call WKB the zeroth-order approximation for tunneling as it should always lead to the lowest transmission coefficient. It takes the minimum energy path without any consideration of the momentum that the particle has gained. Usually, a predicted half-life is higher than the experiment. Of course, the modes perpendicular to the reaction path couple to the particle's motion, which results in a centrifugal effect on the path, effectively shifting it and causing a slight curvature. Small curvature causes the particle to "cut the corner". The method that includes such properties is called canonical variational transition state theory (CVT) with small curvature tunneling (SCT) correction.^[104] CVT assumes that the transition state is not a single minimum but divides the surface between the reactants and the products. Compared to the WKB method, the half-life should always be equal to CVT/SCT if the curvature is slight and lower if the curvature is high. Another approach completely ignores the total energy of the system and only maximizes the transmission coefficient. The large curvature tunneling (LCT) method approximates the tunneling path by a straight line.^[104-107] The path is not limited to the ground state and the molecule can tunnel into an excited state region if the reaction is highly exergonic, known as nonadiabatic LCT. Heavy elements like chlorine show LCT as the effective mass is higher.^[108]

A relatively new approach is the instanton theory. Instanton theory uses a discrete Feynman path integral to estimate the kinetic rate below a reaction-specific crossover temperature at which the path collapses to the TS.^[109] The resulting instanton (a "pseudo-particle") is a PES in multiple dimensions minimized for the total action. Usually, instanton theory uses discrete points starting from the TS and spreads the path as the temperature lowers. The lower the temperature, the more geometries must be computed.

Additionally, more points accumulate at the end of the path, which we have to attenuate.^[110] The optimization approach is similar to the NEB method but results in a higher computational demand for low temperatures. The results are usually in excellent agreement with the experimental half-lives.^[111] The

obtained half-lives can be lower or equal than the WKB results but are generally harder to compute. Optimized path lengths can also be obtained easily for individual atoms as they do not depend on the minimum energy path in contrast to the other methods mentioned above.

As discussed above, carbenes can either have a singlet or a triplet ground state. Carbenes with a small singlet-triplet gap are difficult to describe theoretically, especially the singlet state (*vide supra*). The singlet state consists of at least three electronic configurations, and we should not use simple single-reference methods. If the carbene has a heteroatom such as N or O, the ground state is a singlet, like hydroxycarbenes. Nevertheless, we need to compute the Potential Energy Surface (PES) transition states with unknown electronic properties. As it turned out, the state-of-the-art Coupled-Cluster (CC) method with Single, Double, and perturbative Triple excitation CCSD(T)^[112-116] works comparatively well for carbenes, as they can handle moderate multireference character through the triple excitations, as long as a single configuration primarily defines the reference wavefunction.^[117] Applied to the problematic methylene, CCSD(T) yields outstanding accuracy (*vide supra*). Newer developments such as the Domain-based Local Pair Natural Orbital (DLPNO) approximation reduces the computational cost, making CCSD(T) the method of choice.^[118] For neither DLPNO-CCSD(T) nor CCSD(T), IRC algorithms are available yet. Hence, many authors use Density-Functional Theory (DFT) to compute WKB rates. They prefer hybrid DFT methods like B3-LYP^[119-121], and M06-2X^[122,123], and the new B2PLYP^[124]. When combined with a large basis set, DFT usually results in half-lives within the same order of magnitude compared to the experiment (*vide infra*).

1.4 [1,2]H-tunneling in hydroxycarbenes

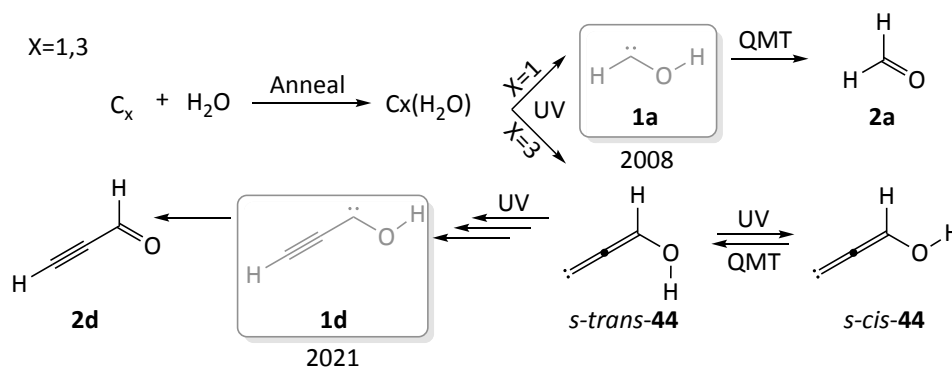


Figure 9. Potential generation of hydroxycarbenes in space by reaction of carbon clusters with water under UV radiation. Ortman *et al.* claimed to have found **1d**. Vala *et al.* reinvestigated the system and could only detect **44** after in accordance with computations from Pulay *et alia*. Schreiner *et al.* isolated formaldehyde **2a** by using C₁. The hydroxycarbenes **1a** and **1d** still remained elusive until 2008/2021.

In 1952, Miller and Urey executed an experiment in the course of which they mixed ammonia, hydrogen, methane, and water vapor in the gas phase—which they thought was the prebiotic atmosphere of earth—and introduced energy in the form of an electric discharge, resulting in the formation of molecular species such as amino acids and sugars.^[125] As they also found formaldehyde in the mixture, the involvement of hydroxycarbenes in sugar formation as high-energy conformers of the latter seemed likely and is comparable to Butlerow's research on the formose reaction decades earlier, in which two electrophiles seemingly form a dimer.^[126] Although the scientific community debates the conclusions drawn from the experiment, the discovery sparked the interest in the evolution of prebiotic chemistry and especially the isolation of hydroxycarbenes as potential nucleophiles in sugar formation.

In 1990, Ortman *et al.* allegedly isolated the first "free" hydroxycarbene **1d** by irradiating a carbon complex (C_3) and water—one of the simplest building blocks for sugar—with UV-Vis light under matrix isolation conditions.^[127] After irradiation, the authors claimed that **1d** formed. Further irradiation led to the aldehyde **2c**. Computational studies by Pulay *et al.* revealed that **44** seemed to be the more plausible cause of the new IR-Bands and Vala *et al.* could later demonstrate the formation of **44** experimentally.^[128,129] Reisenauer and Schreiner reinvestigated the reaction with singlet/triplet carbon, but they did not find the postulated hydroxymethylene (**1a**), only the aldehyde. They attributed this to the instability of **1a** towards UV irradiation.^[130] They also concluded that triplet carbon cannot insert into the O–H bond. Only the singlet carbon is reactive.

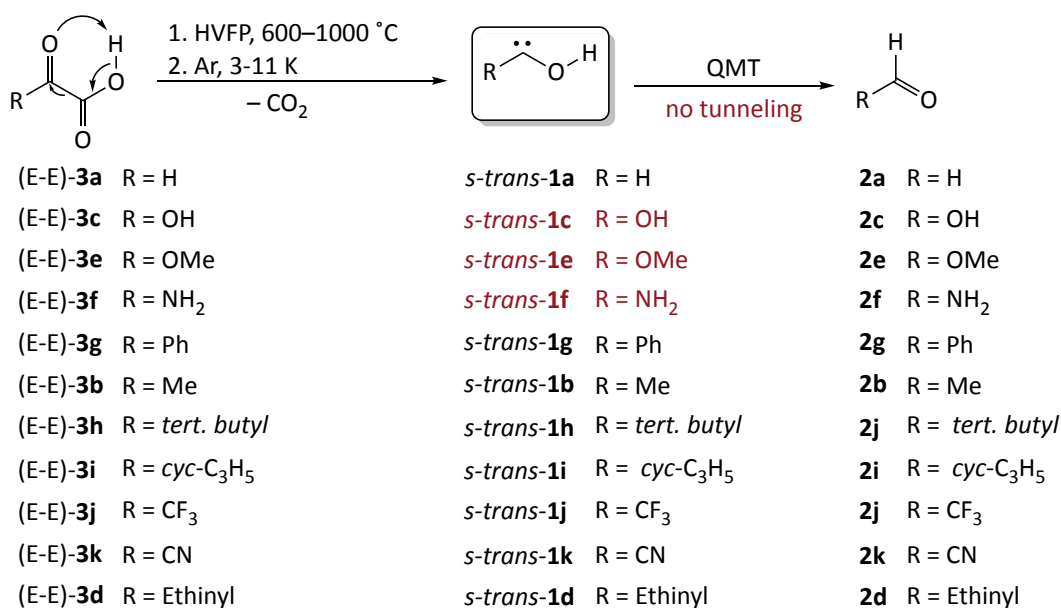


Figure 10. Generation of hydroxycarbenes (**1**) by HVFP of α -ketocarboxylic acids (**3**) or oxalic acid (**3c**) at temperatures between 600–1000 °C in chronological order. The pyrolysis products were trapped in a solid argon matrix at 3–12 K. Note that in some cases, acid esters were used as precursors to generate the ketocarboxylic acids *in situ*. *Black*: Hydroxycarbenes undergo a [1,2]H-shift to the corresponding aldehyde **2** or formic acid (**2c**). *Red*: Hydroxycarbenes that do not undergo a [1,2]H-shift. *Note*: We listed the hydroxycarbenes in chronological order of spectroscopic detection.

Therefore, Reisenauer and Schreiner *et al.* used a different precursor that forms **1a** by thermal means. Indeed, two years later, **1a** could be isolated by HVFP (Figure 10).^[1] In the pyrolysate of glyoxylic acid trapped on a cold window with Ar at 11 K, Reisenauer found **1a** besides formaldehyde (**2a**) and CO₂ using UV- and IR-spectroscopy. As initially proposed, the signals of **1a** disappeared while the concentration of **2a** concomitantly increased upon UV-irradiation, making the formation of **2a** from C₁ and water feasible. Surprisingly, the peaks of **1a** decreased in the dark within two hours with first-order kinetic. High-level computations (AE-CCSD(T)/cc-pVTZ) revealed a reaction barrier of around 30 kcal mol⁻¹, making it impossible to traverse the barrier with the thermal energy available at 11 K by classical means. Moreover, the OH-deuterated species *d*₁-**1a** did not transform to the aldehyde *d*₁-**2a**, and the reaction does not show a significant temperature dependence. Logically, QMT is the only effect that explains the result as it only depends on the barrier's width (including mass) and height (*vide supra*) but not the temperature. Theoretical investigations using the WKB method revealed a narrow barrier for which the computed half-life matches the experimental half-life. Similarly, Reisenauer and Schreiner could isolate dihydroxycarbene (**1c**) and methoxyhydroxycarbene (**1e**) by thermal extrusion of CO₂ from oxalic acid (**3c**)

and oxalic acid monomethyl ester (**3e**),^[131] as well as aminohydroxycarbene (**1f**).^[12] However, **1c**, **1e**, **1f** do not undergo tunneling.

Schreiner *et al.* generated phenylhydroxycarbene (**1g**) to investigate the effect of π -donation into the divalent carbene center.^[132] Despite the π -donation, **1g** has a shorter half-life and a slightly smaller adiabatic singlet-triplet gap than parent hydroxymethylene, indicating that the σ -withdrawing effect of the phenyl group overwrites the π -interaction (**1a**). For σ -donating groups, like methylhydroxycarbene^[11] (**1b**) and *tert* butyl-hydroxycarbene^[133] (**1h**), Schreiner *et al.* measured a shorter half-life compared to **1a**. In contrast, the cyclopropyl group (**1i**)^[134] showed a prolonged half-life compared to **1a** due to π -donation. From this deduction, it is unclear what the half-life of a hydroxycarbene with a captodative substitution would be ($R=CF_3$, *vide infra*).

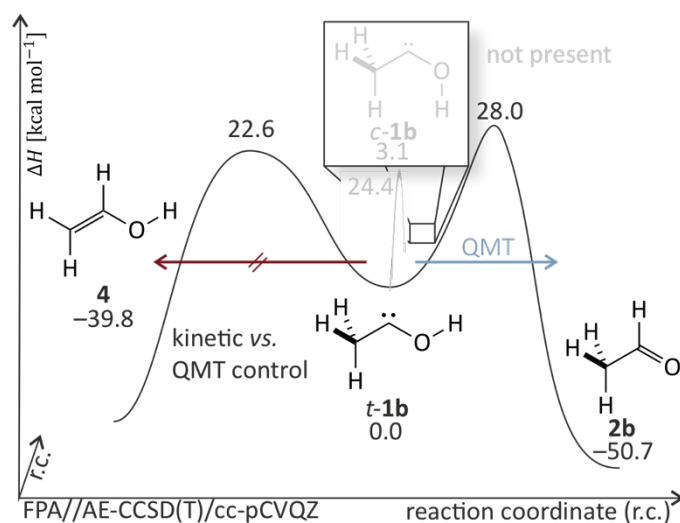


Figure 11. The reactivity of methylhydroxycarbene **1b** is governed by the tunneling process through the higher but narrower barrier yielding acetaldehyde (**2b**). The classic kinetic vs. thermodynamic control based on reaction barrier heights is invalidated.

For **1b**, two [1,2]H-shifts can occur. The [1,2]H-shift of the O-H hydrogen forms **2b** and the [1,2]H-shift of the methyl H forms **4**. Schreiner *et al.* observed only the reaction to **2b** as in all hydroxycarbenes (Figure 11). As it turned out, the QMT process proceeds *via* the higher activation barrier (28.0 vs. 22.6 kcal mol⁻¹) despite the cryogenic temperature. Following the reaction paradigm of kinetic vs. thermodynamic control deduced by Woodward and Baer (*vide supra*), this is a clear violation. QMT controls the reaction, hence the term *tunneling control*. Consequently, researchers found several more examples of *tunneling control*, like **1h**,^[133] **1i**,^[134] noradamantyl methyl carbene^[135]—for which the formation of vinyl noradamantane is preferred over the ring expansion—2,2a,5,7b-tetrahydro-1*H*-cyclobuta[*e*]indene derivatives^[136]—for which the [1,5]H-shift is preferred over the 6 π -cycloreversion ($R = H$ or CH_2), and *tert*-butylchlorocarbene— for which the C-H insertion is preferred over the [1,2]methyl-shift.^[137]

Hence, the results motivated us to use the same method as in Figure 10 to generate trifluoromethylhydroxycarbene (**1j**). Fluorine substitution has a tremendous effect on conformer distribution in molecules. Carbon-fluorine bonds exhibit a very low lying σ_{C-F}^* -orbital, which can accept electrons from a nearby σ_{C-H} -orbital, leading to a stabilization, which manifests itself, *e. g.*, in the fluorine *gauche* effect.^[138] In 1,2-difluoroethane, the *gauche* conformation is around 1 kcal mol⁻¹ more stable than the *anti*-conformation.^[139] Catalyst designers use the *gauche* effect to drive the molecular pre-organization

in asymmetric catalysis and increase the selectivity.^[138] Therefore, they are incorporated in several organocatalytic compounds on the aryl ring, *e. g.*, the most efficient thiourea catalysts in a Diels-Alder reaction (this group), among others.^[140,141] Additionally, we hoped to generate the unobserved *s-cis*-conformer of hydroxycarbenes, which could be stabilized by an O-H...F-C interaction, although the effect could be relatively small.^[142-144] As the *s-cis*-conformer cannot undergo an [1,2]H-shift, we could switch off the tunneling reaction. But how does one generate a higher-lying conformer under matrix isolation conditions?

1.5 Generation of conformers in matrix isolation studies

The simplest way to generate higher-lying conformers of a trapped species is through thermal annealing of the matrix and subsequent cooling, which only works if the barriers are within 1-3 kcal mol⁻¹.^[145] Another way to generate conformers through thermal means is provided by equilibration in the gas phase and subsequent rapid freezing of the equilibrium on a matrix window. This strategy is excellent when preparing carbenes. We usually used HFVP at high temperatures to generate the carbene from suitable precursors (Figure 10), and the nascent carbene could then equilibrate to form different conformers. Schreiner *et al.* already applied this strategy to observe two different conformers of dihydroxycarbene (**1c**). After pyrolysis of oxalic acid (**3c**) and subsequent trapping on a cold window, Reisenauer and Schreiner could identify two distinct conformers of **1c**, namely the *s-trans,s-trans*-conformer (*tt-1c*), and the *s-cis,s-trans*-conformer (*ct-1c*), which nearly have the same energy ($\Delta H = 0.1$ kcal mol⁻¹) separated by a barrier of approximately 17.5 kcal mol⁻¹ (results from CCSD(T)/cc-pVTZ level of theory).^[131]

The third possible conformer with an *s-cis,s-cis*-configuration (*cc-1c*), which is higher in energy ($\Delta H = 6.7$ kcal mol⁻¹) could not be observed as expected by the Boltzmann distribution. Irradiation with UV-light produced thermodynamically more stable reaction products and no other conformers. Schreiner *et al.* observed similar behavior for **1e**. Nevertheless, there are examples from other groups, which used UV-Vis light to generate conformers of carbenes. Selected examples include phenoxychlorocarbene (**44**),^[146] methylmethoxycarbene (**45**),^[147] fluoromethoxycarbene (**46**),^[148] 2-naphthylphenylcarbene (**47**).^[149,150] Another option with lower energy is (N)IR light.

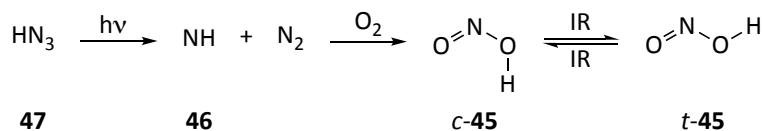


Figure 12. The generation of nitrous acid **45** conducted by Baldeschwieler and Pimentel. The energy difference of *c-45* and *t-45* is $\Delta H_{t-c} = 0.6$ kcal mol⁻¹

Heteronuclear diatomic molecules are prototypic to study the interaction of matter with (N)IR light, as they have only one vibrational mode. For a single excited molecule, energy can be dissipated by emission (fluorescence) or through non-radiative processes. Non-radiative processes depend on the concentration of the guest in the matrix host. If the concentration is low, energy can only dissipate by host-guest interactions, releasing the energy into the delocalized lattice vibrations (phonons). For diatomic molecules, this process is slow and increases with vibrational excitation level as the energy spacing gets smaller.^[151,152] At high concentrations, long-range dipole-dipole interactions between the guest molecules

are plausible, in addition to radiative processes. Excited species can transfer their vibrational energy towards other molecules, which is known as Förster-type resonance energy transfer (FRET).^[153,154] FRET could be observed between the OD and OH radical at high concentrations.^[154] Dubost *et al.* excited NO to vibrational levels as high as $v=27$ through FRET, resulting in electronic excitation of the low lying quartet state, which resulted in chemiluminescent dissociation.^[155]

For polyatomic molecules, there are a lot more decay channels. As the mode's energy spacing is smaller than in diatomic molecules, polyatomic molecules can dissipate energy into the environment (phonons in matrix isolation) much easier. Additionally, intramolecular vibrational energy transfer (IVT)—which is very fast (10^{-12} - 10^{-9} s)—distributes energy to all modes in a molecule. The first example of IR-induced processes in matrix isolation dates to Baldeschwieler and Pimentel. In 1960, they described the IR-induced transformation in nitrous acid (HONO, **45**) generated by oxidation of **46**—made by irradiation of **47**—with oxygen.^[156] Upon prolonged IR irradiation from the spectrometer, they observed a photo equilibration of *trans*- to *cis*-**45**. Through annealing, Baldeschwieler and Pimentel could not trigger an equilibration process. Curiously, d_1 -HONO did not undergo isomerization, and $^{18}\text{O}_2$ -**45** equilibrated only very slowly.

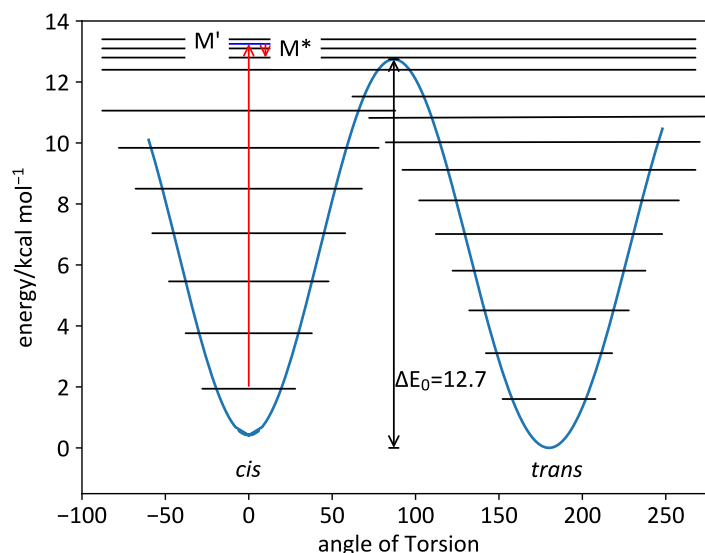


Figure 13. Proposed mechanism of NIR excitation for the transformation of *c*-**45** to *t*-**45**. We performed the computations at the B3LYP/def2-TZVP level of theory. As Hall, we did not assume the possibility of tunneling.

Further studies from Hall^[157] and Pimentel revealed that the transformation occurred within a specific wavelength range by filtering the IR light carefully. Hall estimated the barrier to be 9.7 ± 0.7 kcal mol⁻¹. Additionally, he could enable the transformation of d_1 -**45**, but it was ten times slower than in **45**. As deuterium redshifts, the fundamental bands of **45**, only overtones and combination bands are available for excitation with sufficient energy to enable the transformation. Hence, the absorption coefficients are smaller for d_1 -**45** than for **45**.

Mechanistically, Hall excluded the direct excitation of the torsional mode, as the overtone/combination band absorption is negligible. Therefore, the process must proceed IVT. Excitation of the OH-stretch vibration of **45** (M' , Figure 13) eventually leads to high excitation of the torsional motion *via* IVT (M^*). As the excitation is higher than the torsional barrier, the system can easily equilibrate between the *c*-**45** and *t*-**45** potentials. Through cooling *via* energy dissipation, *e. g.*, into the host phonons, the energy of the

molecule falls below the torsional barrier, eventually stabilizing one of the two conformers. Dihydroxycarbene(**1c**) is a similar system to **45**.

As it turns out, IR-induced transformations in the matrix are common. The list includes the rotamerization of the OH-group in alcohols,^[158-163] acids,^[13,164-172] ketocarboxylic acids,^[173-175] squaric acid,^[176] or attached to ring systems.^[177-182] In addition, isomerization around C-C single bonds,^[183,184] and formyl groups^[185] were reported. Researchers also use IR light for conformational analysis of biologically relevant molecules like amino acids,^[186-191] sugars,^[192] and others,^[193]. Khriachtchev *et al.* reported the rotamerization of an O-H-group in the HOCO radical, which is very similar to dihydroxycarbene (**1c**), thus further motivating us to find the elusive *s-cis,s-cis*-conformer by NIR excitation.^[194]

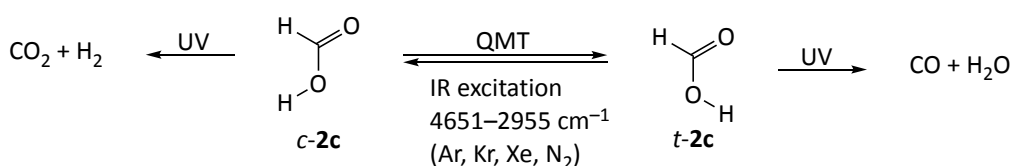


Figure 14. The conformer-selective reaction of formic acid (**2c**) was conducted at 8 K in solid argon. The barrier between the *t*-**2c** and *c*-**2c** is estimated to amount to $3810 \pm 100 \text{ cm}^{-1}$.

Although the scientific community has known the method of IR excitation since 1963, the higher energy conformer of the simplest organic acid *c*-**2c** was unidentified until 1997.^[13] Schaefer and Kong *et al.* estimated the barrier for interconversion at $\sim 4500 \text{ cm}^{-1}$,^[195,196] a target that NIR excitation could reach by excitation into the second overtone of the OH-vibration ($2\nu_{\text{OH}}$). In the paper "A tribute to Markku Räsänen",^[197] Khriachtchev wrote:

'Markku had suggested that problem to a young student as an "easy experiment" that could be accomplished in few weeks. It took seven years before cis-formic acid was finally observed in a matrix! Since then, it has become a common joke to ask Markku if he has any short, easy experiments in mind. Of course, the reason for earlier failures became clear when the fast-tunneling reaction from the unstable cis form to the trans form was observed. Any method that did not include active pumping of the cis to trans form was doomed to fail.'

This demonstrates that we must be aware of very fast QMT when dealing with higher energy conformers and low mass particles like hydrogen atoms.

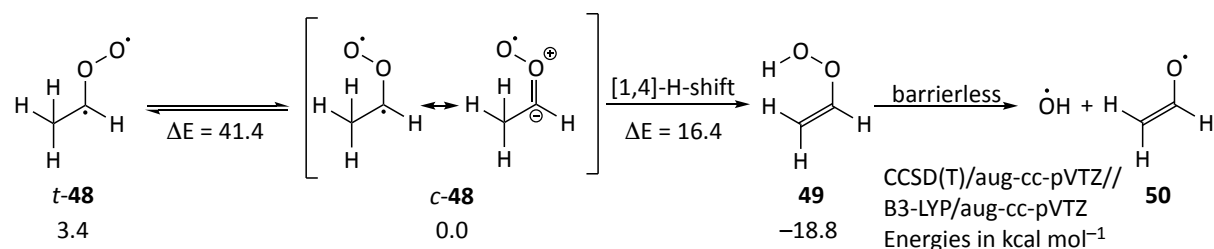


Figure 15. The Criegee intermediate **48** was generated by photoionization of 1,1-diodoethane through supersonic expansion in the gas phase. Intermediate **48** can undergo a [1,4]H-shift to generate **49**, which dissociates to the OH-radical and **50**. The OH-radicals can be probed via Light-Induced Fluorescence (LIF). The IR-excitation energy can be as low as 2850 cm^{-1} ($10.0 \text{ kcal mol}^{-1}$).

The discovery of *c*-**2c** was the start of several studies on the influence of the host material on the QMT rate,^[198,199] the UV irradiation of *c*-**2c**,^[200] or the quantum yield dependence on IR energy (Figure 14).^[201] Concerning the IR/UV irradiation, Räsänen *et al.* observed conformer-specific reactions when irradiating

the matrix with IR light (Figure 14). The *c*-**2c** preferably forms CO₂ and H₂ and whereas the *t*-**2c** yields CO and H₂O. Hence, they controlled the product ratio by IR irradiation.

In a separate study, Räsänen *et al.* showed that the interconversion upon IR radiation below the torsional barrier is feasible. As they lowered the energy of the incident light, the quantum yield dropped significantly but was not zero even below the computed torsional TS, making it the first example of torsional excited state tunneling or 'IR-pumped' tunneling. They stated—supported by computations of the vibrational state functions—that the vibrational states in both conformers must match each other at the top of the barrier; otherwise, the transformation does not occur. As [1,2]H-shift in **1c** is highly exothermic, we would expect a high density of states on the product side, making the coupling to the product **2c** likely. The question arises: Are there barriers that we can surpass by (N)IR activation to form a new product?

Indeed, Lester *et al.* addressed this question. They observed the formation of *c*-**48** from 1,1,-diiodoethane. After IR-irradiation **49**, which dissociates quickly into **50** and OH-radicals.^[202,203] They measured an IR-action spectrum by probing OH-radical formation using light-induced fluorescence. Surprisingly, OH-radicals can still be observed well below the computed reaction barrier of 16.4 kcal mol⁻¹, leading to the conclusion that tunneling must be involved. Repeating the experiment with the deuterated species, Lester *et al.* could not observe a [1,4]H-shift between 6000–2850 cm⁻¹. At ca. 6000 cm⁻¹, an isotope effect of approx. ten can be determined. Additionally, the group observed lower reaction rates when moving to smaller IR excitation energies in line with the concept of pumped tunneling.

1.6 Our experimental insights concerning conformer chemistry in hydroxycarbenes

We were able to generate **1j** by the route established in this group (Figure 10). However, the main product after pyrolysis was not **1j** but CO and HF besides CO₂, which results from the elimination of HF from **1j** (*vide infra*). Another product was trifluoromethyl acetic acid, which, according to our computations, probably results from decarbonylation of **3j** in the gas phase. As for the other hydroxycarbenes, the *s*-*cis*-conformer (*c*-**1j**) was not present after pyrolysis despite the slight energy separation of 0.8 kcal mol⁻¹ to the *s*-*trans*-conformer (*t*-**1j**) and a barrier for thermal interconversion of 26.4 kcal mol⁻¹.

Due to the barrier height for interconversion between *t*-**1j** and *c*-**1j**, NIR-light cannot be used to interconvert the conformers and tunneling seems probable for the absence of *c*-**1j** absence. Therefore, we were surprised to find *c*-**1j** after irradiation with 465 nm besides the primary photoproduct **2j**. The *c*-**1j** conformer is stable and does not undergo any transformation. As *t*-**1j** is unstable at 10 K in an argon matrix and undergoes a [1,2]H-shift *via* QMT to **2j**, the presence of *c*-**1j** has consequences for the reaction system. We could completely shut down the tunneling reaction through UV-Vis irradiation and make **1j** indefinitely stable at 3 K. Hence, we termed this behavior "conformer-specific QMT" (Figure 16). Compared to **1b**, the formation of the vinyl alcohol (**51**) is not kinetically favored as it involves an [1,2]F-shift compared to an [1,2]H-shift which increases the barrier significantly (22.6 vs. 47.5 kcal mol⁻¹, Figure 16). Hence, tunneling control does not play a role for **1j**. Additionally, the *c*-**1j** conformer has a very short H-F-distance of just 1.907 Å, which results in significant bonding interaction according to our atoms in molecules (AIM) analysis.^[204]

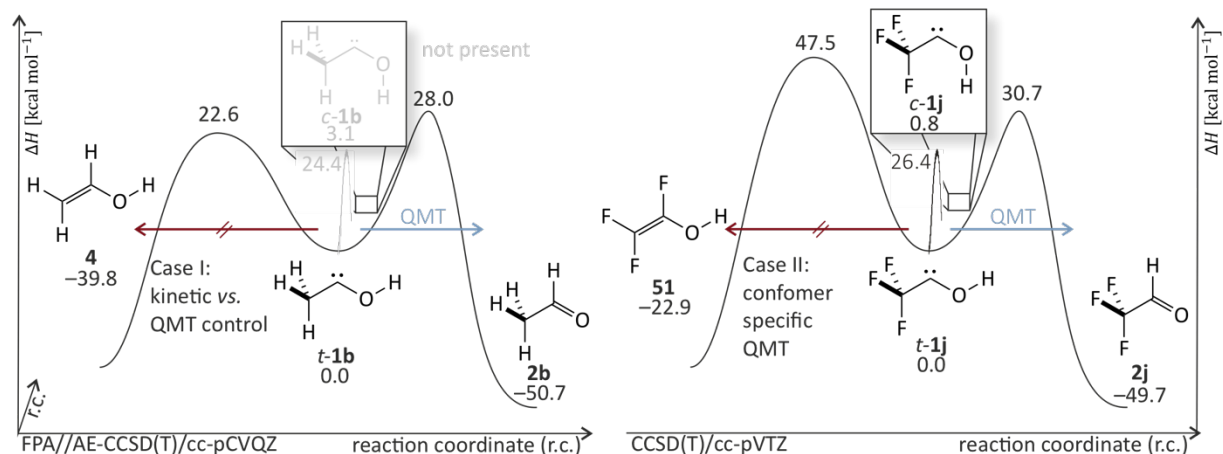


Figure 16. Case I: The reactivity of methylhydroxycarbene **1b** is governed by the tunneling process through the higher but narrower activation barrier yielding acetaldehyde (**2b**). Case II: The reactivity of trifluoromethylhydroxycarbene (**1j**) is governed by the [1,2]H-shift to trifluoro acetaldehyde **2j**, which is the kinetic and thermodynamic product based on the energetic landscape. The *s-cis*-conformer (**c-1j**) does not undergo QMT. Hence, this constitutes the first example of conformer-specific QMT. The *s-cis*-conformer can be generated by irradiation (*vide infra*)

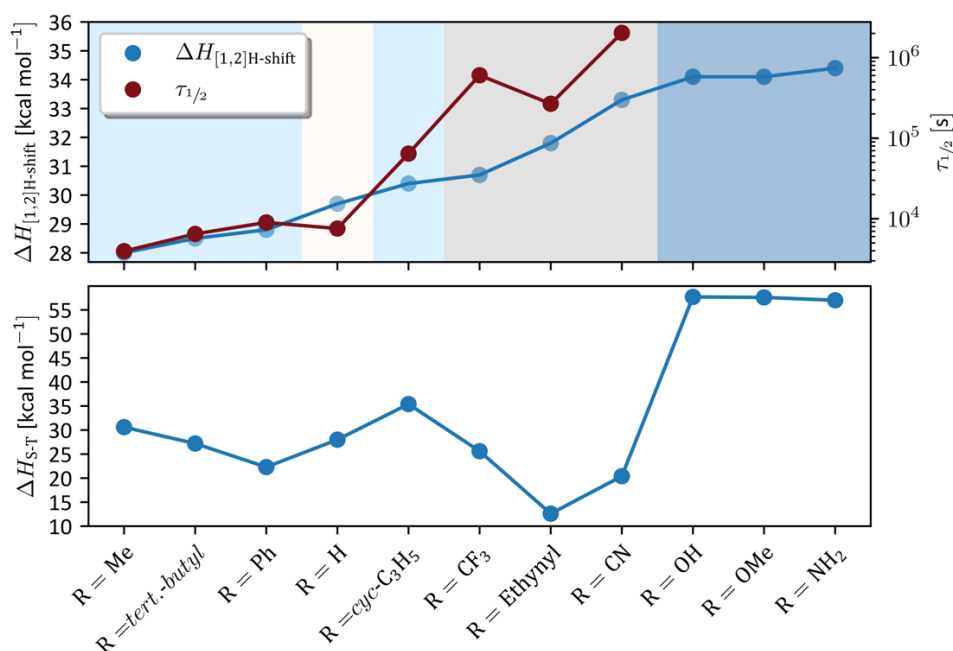


Figure 17. Top: The barrier height for the [1,2]H-shift to the aldehyde and the experimental half-life vs. the substituent is shown, sorted from the lowest to the highest activation barrier. The data is directly taken from the respective publications (usually CCSD(T) with a triple ζ -basis set). If the data was not available (e.g., aminohydroxycarbene), we used the CCSD(T)/cc-pVTZ//M06-2X/def2QZVP level of theory. Colors: Light blue: electron donation (push-push interaction), Light yellow: No interaction, Grey: Captodative effect (push-pull interaction), and Blue: Heteroatom substitution (strong π -push-push interaction) Bottom: The adiabatic singlet-triplet gap. The data was taken from the respective publications

Compared to other hydroxycarbenes, the tunneling half-life is significantly longer (7 days, Figure 17). We argue that the captodative interaction of substituents with the carbene center is responsible for the increase in half-life. The captodative substitution leads to a higher and broader barrier, and therefore a longer half-life. In terms of QMT, the push-pull substitution stabilizes hydroxycarbenes, which our group also observed for cyanohydroxycarbene (**1k**). Substitution patterns that provide electron density to the carbene center through either the +M or +I-effect (push-push) destabilize the carbene relative to **1a**. An increasing barrier height can rationalize the trend for push-push substitution. For the push-pull systems, the barrier width is important, which is highly dependent on the substituents. The barrier width is not a value that someone retrieves by intuition and stresses the importance of WKB computations for such systems. Curiously, **1d**

recently published definitely demonstrate the barrier width effect of push-pull systems (it contains less heavier atoms that have to move).^[205]

The adiabatic singlet-triplet gap, which should give a rough estimate of the electron density at the carbene center due to the destabilizing effects on the triplet geometry, does not follow the trend of barrier heights and half-lives. The +I-effect only increases the electron density only slightly. On the contrary, the -I-effect decreases the electron density. For phenylhydroxycarbene, the -I-effect must be stronger than the +M-effect. The cyclopropyl group provides a strong +M-effect. As expected, the double hetero substituted hydroxycarbenes show the most elevated ΔH_{S-T} . As expected, electron withdrawing groups in push-pull carbenes reduce the electron density at the carbene center

The results on trifluoromethylhydroxycarbene motivated us to dig deeper into the conformational isomerization of hydroxycarbenes. Dihydroxycarbene (**1c**) seemed the best choice as a benchmark system as the yields after pyrolysis is high. Additionally, it does not undergo tunneling. Dihydroxycarbene is the best-investigated hydroxycarbene to date, as it is a fundamental intermediate on the $[H_2CO_2]$ hypersurface and may play a role in the direct reaction of H_2 with CO_2 . Hence, Feller *et al.* computed the potential energy surface as early as 1979 with a detailed study on the decomposition of **1c**.^[206,207]

Dihydroxycarbene has three rotamers depending on the two dihedral angles $\delta_{H-O-C-O}$, which can be 180° (*s-cis*, *c*) or 0° (*s-trans*, *t*). In 1994, Wesdemiotis *et al.* indirectly detected dihydroxycarbene for the first time by neutralization/reionization mass spectrometry. In 2008, the spectroscopic identification followed by this group through pyrolysis of oxalic acid (*vide supra*).^[131] Since then, Douberly *et al.* isolated dihydroxycarbene in helium nanodroplets.^[208] McCarthy *et al.* could determine the exact structure of the *cc-1c* in the gas phase. They used the direct reaction of CO_2 and H_2 induced by an electric spark. The important conformer in this reaction, the *cc-1c*, however, remained illusive.

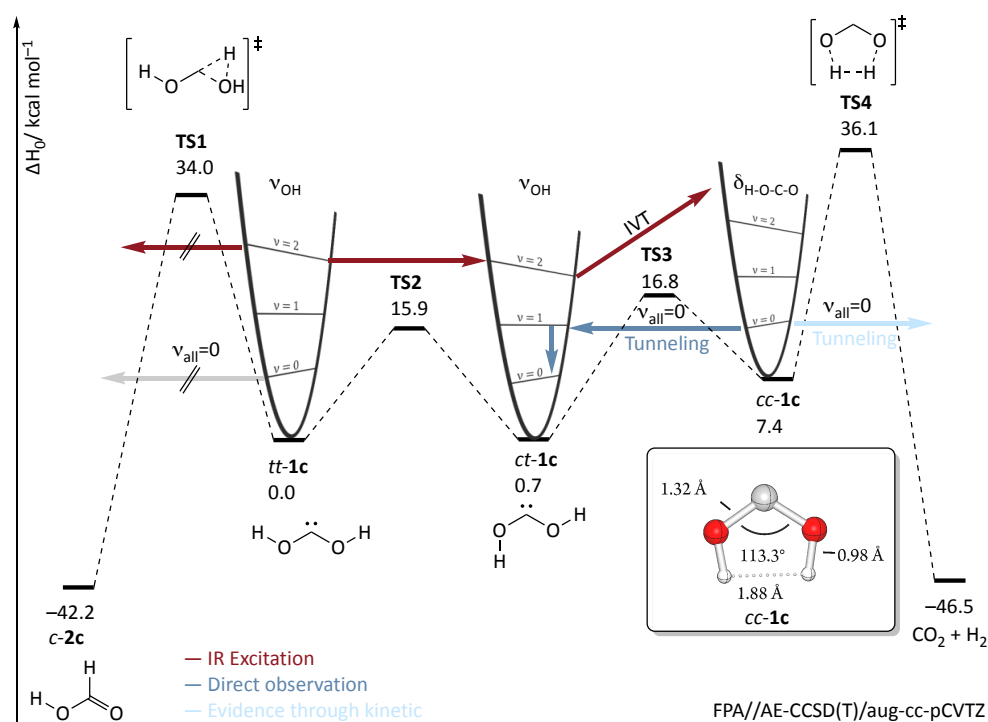


Figure 18. Potential energy surface around dihydroxycarbene **1c** (color code: carbon: grey, oxygen: red, hydrogen: white) at the FPA//AE-CCSD(T)/cc-pCVTZ + ZPVE level of theory.

Two of them (*tt-1c* and *ct-1c*) are very close in energy. The *tt-1c* and *ct-1c* separate a barrier that we anticipated to overcome by (N)IR irradiation (Figure 18). The third conformer, *cc-1c*, is slightly higher in energy but reachable *via* a comparable reaction barrier and could be overcome by (N)IR-irradiation. Hitherto, nobody detected the *cc-1c* conformer spectroscopically. The detection of *ct-1c* following an electric spark ignition of H₂ and CO₂ made us curious to generate *cc-1c* for the first time.

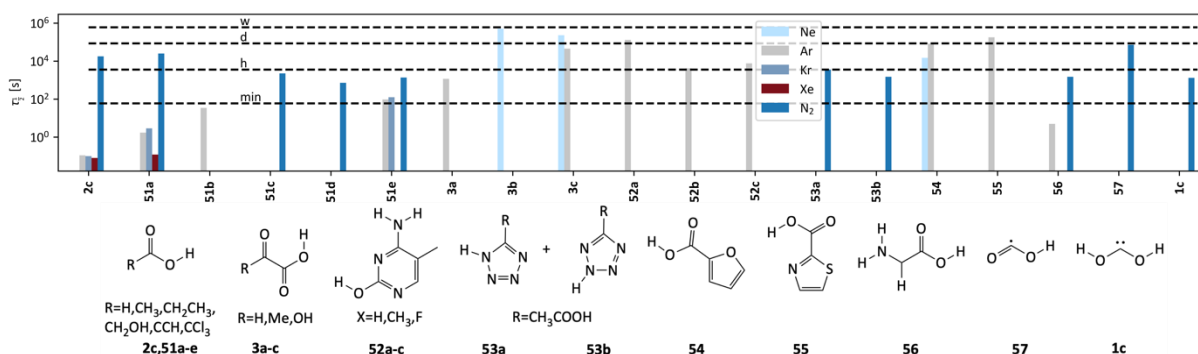


Figure 19. The tunneling half-life of the reaction from the higher energy conformer to the lower energy conformer isolated in a cryogenic matrix at temperatures between 3–12 K and different matrix host materials. For **3a** and **3c** the average values were taken.

Khriachtchev *et al.* found that N₂ stabilizes *s-cis*-conformer of formic acid.^[199] Using N₂, through conformer selective NIR excitation in the O-H overtone region, we could observe new peaks belonging to *cc-1c* based on high-level computations (*vide infra*) after conformer-selective NIR excitation into the O-H overtone region. Analogous to *s-2c*, the energetically high lying conformer is not stable and undergoes tunneling to *ct-1c* within 22 minutes at 3 K. Through sophisticated kinetic analysis, we could determine that not all the *cc-1c* molecules tunnel back to the *ct-1c* conformer, but a small amount of an unknown product must form. Through computations, we concluded that the second product forms due to the decomposition of *cc-1c* to CO₂ and H₂. Sadly, we could not confirm this experimentally due to the high concentration of CO₂ after pyrolysis and the IR inactivity of H₂. Attempts to break symmetry in **1c** through selective deuteration of one hydroxy group have yet remained unsuccessful. Contrary to the case of formic acid and **48**, we could not enable the [1,2]H-shift through (N)IR light. Later, our group confirmed this for cyanohydroxycarbene, where prolonged NIR irradiation did not lead to a faster tunneling rate.^[209]

Compared to other cases of conformational interconversions that were induced by (N)IR irradiation in cryogenic matrices, dihydroxycarbene exhibits a comparable half-life (Figure 19) of tunneling in the reverse reaction.^[167,171-172,178-179,188-190,194,198,210,211] Also, from the relative half-lives for **2c** and **51a**, we are certain that N₂ stabilizes *cc-1c* and hence it is not observable in a noble gas matrix environment.

1.7 Our contributions to the computational determination of tunneling half-lives

During the work on this thesis, it became clear how crucial deep tunneling is under matrix isolation conditions. Hence, we turned our attention to computing the tunneling half-lives straightforwardly. First, we solved the problem of generating the necessary data. Second, we created a GUI to import that data and calculate the tunneling half-lives, called TUNNEX (*vide infra*). The tools are designed for experimental chemists with some experience in computations of IRCs, and WKB provides the foundation as it only needs a one-dimensional profile. We hope that other groups find this tool helpful. We also hope to use TUNNEX to

simplify the input of more sophisticated methods like CVT/SCT and instanton and provide a more user-friendly approach for tunneling computations in matrix isolation conditions without invoking the command line.

1.8 Concluding remarks

Only with the power of modern computational chemistry, this thesis became possible. We published a program for computing tunneling half-lives by simply using WKB. We hope that this program can lead to the discovery of more intriguing tunneling reactions establishing QMT as a fascinating facet in chemistry and as a common kinetic phenomenon for chemical reactions. We are confident that we delivered the basis for a continuous effort to make the computation of accurate rates in the deep tunneling regime a simple task. We would like to add features like a GUI for Polyrate input, temperature-dependent rates, and a GUI for managing tunneling computations on servers.

Trifluoromethylhydroxycarbene is the first example of conformer-specific tunneling. The *s-trans*-conformer undergoes QMT while the *s-cis*-conformer displays no reactivity. Conformer-specific tunneling can affect selectivity in chemical reactions tremendously as only one conformer is stable and engages in intermolecular interactions. The well-known Curtin-Hammett principle is not applicable in the case of trifluoromethylhydroxycarbene as the *s-trans*-conformer cannot be replenished from the *s-cis*-conformer but as in the case of methylhydroxycarbene, one should always be vigilant for the violation of principles derived from TST if deep tunneling is involved. Further investigations should concentrate on the effect of sp_x ($x=1,2$) substituted carbenes and hetero atoms with similar electronegativities, such as sulfur.

With the discovery of the *s-cis,s-cis*-conformer of dihydroxycarbene, we found one of the last intermediates on the $[CH_2O_2]$ hypersurface. The *s-cis,s-cis*-conformer could be an important intermediate in the reaction of CO_2 with H_2 . Dihydroxycarbene can be seen as the reactive form of formic acid, enabling further investigation on the reactivity of CO_2 and H_2 . Additionally, we have found an indication of tunneling to CO_2 and H_2 , effectively lowering the reaction barrier. Hence, we argue that *cc-1c* is involved in the direct reaction of CO_2 and H_2 . As carbenes are good nucleophiles, longer carbon chains can be formed under the right conditions. We should further investigate the existence of *s-cis,s-cis*-dihydroxycarbene from the direct reaction of CO_2 and H_2 by means of rotational-vibrational spectroscopy. Furthermore, we should investigate the (N)IR excitation of the methoxyhydroxycarbene, where the unknown *s-cis,s-cis*-conformer may form methane and CO.

As tunneling was considered mostly a mathematical construct, I want to close this thesis as it has begun with a quotation from Albert Einstein:

„Insofern sich die Sätze der Mathematik auf die Wirklichkeit beziehen, sind sie nicht sicher, und insofern sie sicher sind, beziehen sie sich nicht auf die Wirklichkeit.“

Albert Einstein (1879–1955)

1.9 References

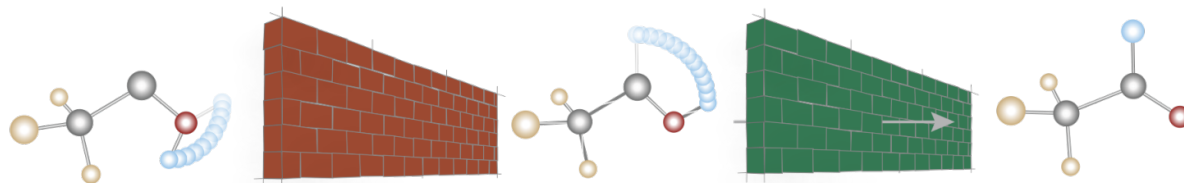
- [1] Schreiner, P. R.; Reisenauer, H. P.; Pickard, F. C., IV; Simmonett, A. C.; Allen, W. D.; Mátyus, E.; Császár, A. G. *Nature* **2008**, *453*, 906–909.
- [2] Eckhardt, A. K.; Linden, M. M.; Wende, R. C.; Bernhardt, B.; Schreiner, P. R. *Nat Chem* **2018**, *10*, 1141–1147.
- [3] The Nobel Prize in Physics 1986. NobelPrize.org. Nobel Prize Outreach AB **2021**. Fri. 13 Aug 2021 <<https://www.nobelprize.org/prizes/physics/1986/summary/>>
- [4] Marcus, R. A. *J Chem Phys* **1956**, *24*, 966–978.
- [5] Marcus, R. A. *J Chem Phys* **1956**, *24*, 979–989.
- [6] Bell, R. P.; Roy, R. J. L. *Phys Today* **1982**, *35*, 85–86.
- [7] Refer to reference 4–11 in: Ref [12]
- [8] Eyring, H. *J Chem Phys* **1935**, *3*, 107–115.
- [9] Evans, M. G.; Polanyi, M. *Trans Faraday Soc* **1935**, *31*, 875–894.
- [10] Woodward, R. B.; Baer, H. *J Am Chem Soc* **1944**, *66*, 645–649.
- [11] Schreiner, P. R.; Reisenauer, H. P.; Ley, D.; Gerbig, D.; Wu, C.-H.; Allen, W. D. *Science* **2011**, *332*, 1300–1303.
- [12] Schreiner, P. R. *J Am Chem Soc* **2017**, *139*, 15276–15283.
- [13] Pettersson, M.; Lundell, J.; Khriachtchev, L.; Räsänen, M. *J Am Chem Soc* **1997**, *119*, 11715–11716.
- [14] Womack, C. C.; Crabtree, K. N.; McCaslin, L.; Martinez, O.; Field, R. W.; Stanton, J. F.; McCarthy, M. C. *Angew Chem Int Ed* **2014**, *53*, 4089–4092.
- [15] McNaught, A. D.; Wilkinson, A., Eds. IUPAC. Compendium of Chemical Terminology, 2nd ed. (the "Gold Book"). Blackwell Scientific Publications, Oxford (1997), 1997.
- [16] Hund, F. *Z Phys* **1927**, *40*, 742–764.
- [17] Hund, F. *Z Phys* **1927**, *42*, 93–120.
- [18] Hund, F. *Z Phys* **1927**, *43*, 805–826.
- [19] Nef, J. U. *Liebigs Ann* **1892**, *270*, 267–335.
- [20] Nef, J. U. *Liebigs Ann* **1894**, *280*, 291–342.
- [21] Nef, J. U. *Liebigs Ann* **1895**, *287*, 265–359.
- [22] Butlerow, A. *Liebigs Ann* **1861**, *120*, 356–356.
- [23] Herzberg, G. *Proc Roy Soc A* **1961**, *262*, 291–317.
- [24] Herzberg, G.; Shoosmith, J. *Nature* **1959**, *183*, 1801–1802.
- [25] Foster, J. M.; Boys, S. F. *Rev Mod Phys* **1960**, *32*, 305–307.
- [26] Bender, C. F.; Schaefer, H. F., III. *J Am Chem Soc* **1970**, *92*, 4984–4985.
- [27] Leopold, D. G.; Murray, K. K.; Miller, A. E. S.; Lineberger, W. C. *J Chem Phys* **1985**, *83*, 4849–4865.
- [28] Bunker, P. R.; Jensen, P. *J Chem Phys* **1983**, *79*, 1224–1228.
- [29] Harrison, J. F. *J Am Chem Soc* **1971**, *93*, 4112–4119.
- [30] Ritchie, R. K.; Walsh, A. D.; Warsop, P. A.; Linnett, J. W. *Proc Roy Soc A* **1962**, *266*, 257–271.
- [31] Venkateswarlu, P. *Phys Rev* **1950**, *77*, 676–680.
- [32] Brahms, D. L. S.; Dailey, W. P. *Chem Rev* **1996**, *96*, 1585–1632.
- [33] Geuther, A. *Liebigs Ann* **1862**, *123*, 113–121.
- [34] Geuther, A. *Liebigs Ann* **1862**, *123*, 121–122.
- [35] Doering, W. E.; Hoffmann, A. K. *J Am Chem Soc* **1954**, *76*, 6162–6165.
- [36] Doering, W. E.; Henderson, A. J. *J Am Chem Soc* **1958**, *80*, 5274–5277.
- [37] Doering, W. E.; Buttery, R. G.; Laughlin, R. G.; Chaudhuri, N. *J Am Chem Soc* **1956**, *78*, 3224–3224.
- [38] Erden, I. *Synth Commun* **1986**, *16*, 117–121.
- [39] De Meijere, A.; Kozhushkov, S. I.; Fokin, A. A.; Emme, I.; Redlich, S.; Schreiner, P. R. *Pure Appl Chem* **2003**, *75*, 549–562.
- [40] Allen, W. D.; Quanz, H.; Schreiner, P. R. *J Chem Theory Comput* **2016**, *12*, 4707–4716.
- [41] Vougioukalakis, G. C.; Grubbs, R. H. *Chem Rev* **2010**, *110*, 1746–1787.
- [42] Fischer, E. O.; Maasbol, A. *Angew Chem Int Ed* **1964**, *3*, 580–581.
- [43] Fischer, E. O.; Maasböl, A. *Chem Ber* **1967**, *100*, 2445–2456.
- [44] Fischer, E. O.; Weiß, K.; Kreiter, C. G. *Chem Ber* **1974**, *107*, 3554–3561.
- [45] Dötze, K. H.; Stendel, J. *Chem Rev* **2009**, *109*, 3227–3274.
- [46] Schrock, R. R. *J Am Chem Soc* **1974**, *96*, 6796–6797.
- [47] Wittig, G.; Schöllkopf, U. *Chem Ber* **1954**, *87*, 1318–1330.
- [48] Tebbe, F. N.; Parshall, G. W.; Reddy, G. S. *J Am Chem Soc* **1978**, *100*, 3611–3613.
- [49] Fu, G. C.; Grubbs, R. H. *J Am Chem Soc* **1992**, *114*, 7324–7325.
- [50] Scholl, M.; Ding, S.; Lee, C. W.; Grubbs, R. H. *Org Lett* **1999**, *1*, 953–956.
- [51] Khan, R. K. M.; O'Brien, R. V.; Torker, S.; Li, B.; Hoveyda, A. H. *J Am Chem Soc* **2012**, *134*, 12774–12779.
- [52] Grubbs, R. H. *Angew Chem Int Ed* **2006**, *45*, 3760–3765.
- [53] Wanzlick, H.-W.; Schikora, E. *Angew Chem* **1960**, *72*, 494–494.
- [54] Lemal, D. M.; Lovald, R. A.; Kawano, K. I. *J Am Chem Soc* **1964**, *86*, 2518–2519.
- [55] Winberg, H. E.; Carnahan, J. E.; Coffman, D. D.; Brown, M. *J Am Chem Soc* **1965**, *87*, 2055–2056.
- [56] Igau, A.; Grutzmacher, H.; Bacciredo, A.; Bertrand, G. *J Am Chem Soc* **1988**, *110*, 6463–6466.
- [57] Flanigan, D. M.; Romanov-Michailidis, F.; White, N. A.; Rovis, T. *Chem Rev* **2015**, *115*, 9307–9387.
- [58] Enders, D.; Breuer, K.; Raabe, G.; Runsink, J.; Teles, J. H.; Melder, J.-P.; Ebel, K.; Brode, S. *Angew Chem Int Ed* **1995**, *34*, 1021–1023.
- [59] Lonsdale, D. *Evid-Based Complementary Altern Med* **2006**, *3*, 349513.
- [60] Lapworth, A. *J Chem Soc, trans* **1903**, *83*, 995–1005.
- [61] Mizuhara, S.; Tamura, R.; Arata, H. *Proc Jpn Ac* **1951**, *27*, 302–308.
- [62] Breslow, R. *J Am Chem Soc* **1957**, *79*, 1762–1763.
- [63] Breslow, R. *J Am Chem Soc* **1958**, *80*, 3719–3726.
- [64] Breslow, R.; McNelis, E. *J Am Chem Soc* **1959**, *81*, 3080–3082.
- [65] Berkessel, A.; Yatham, V. R.; Elfert, S.; Neudörfl, J.-M. *Angew Chem Int Ed* **2013**, *52*, 11158–11162.
- [66] Paul, M.; Sudkaow, P.; Wessels, A.; Schlörner, N. E.; Neudörfl, J. M.; Berkessel, A. *Angew Chem Int Ed* **2018**, *57*, 8310–8315.
- [67] Thaddeus, P.; Gottlieb, C. A.; Mollaaghababa, R.; Vrtilek, J. M. *J Chem, Faraday Trans* **1993**, *89*, 2125.
- [68] Hollis, J. M.; Jewell, P. R.; Lovas, F. J. *Astrophys J* **1995**, *438*, 259–264.

- [69] Thaddeus, P.; Vrtilik, J.; Gottlieb, C. *Astrophys J* **1985**, *299*, L63–L66.
- [70] Maier, G.; Reisenauer, H. P.; Schwab, W.; Čársky, P.; Špirko, V.; Hess, B. A.; Schaad, L. J. *J Chem Phys* **1989**, *91*, 4763–4773.
- [71] Ohishi, M.; Suzuki, H.; Ishikawa, S.-I.; Yamada, C.; Kanamori, H.; Irvine, W. M.; Brown, R. D.; Godfrey, P. D.; Kaifu, N. *Astrophys J* **1991**, *380*, L39–L42.
- [72] Saito, S.; Kawaguchi, K.; Yamamoto, S.; Ohishi, M.; Suzuki, H.; Kaifu, N. *Astrophys J* **1987**, *317*, L115–L118.
- [73] Fosse, D.; Cernicharo, J.; Gerin, M.; Cox, P. *Astrophys J* **2001**, *552*, 168–174.
- [74] Reisenauer, H. P.; Maier, G. N.; Riemann, A.; Hoffmann, R. W. *Angew Chem Int Ed* **1984**, *23*, 641–641.
- [75] Maier, G.; Reisenauer, H. P.; Rademacher, K. *Chem Eur J* **1998**, *4*, 1957–1963.
- [76] Maier, G.; Reisenauer, H. P.; Cibulka, M. *Angew Chem Int Ed* **1999**, *38*, 105–108.
- [77] Maier, G.; Reisenauer, H. P.; Schwab, W.; Čársky, P.; Hess, B. A.; Schaad, L. J. *J Am Chem Soc* **1987**, *109*, 5183–5188.
- [78] Maier, G.; Endres, J.; Reisenauer, H. P. *Angew Chem Int Ed* **1997**, *36*, 1709–1712.
- [79] Maier, G.; Endres, J. *Eur J Org Chem* **1998**, *1998*, 1517–1520.
- [80] Maier, G.; Reisenauer, H. P.; Hans, Ruppel, R. *Eur J Org Chem* **2003**, *2003*, 2695–2701.
- [81] Schreiner, P. R.; Reisenauer, H. P.; Allen, W. D.; Sattelmeyer, K. W. *Org Lett* **2004**, *6*, 1163–1166.
- [82] Schreiner, P. R.; Reisenauer, H. P.; Sattelmeyer, K. W.; Allen, W. D. *J Am Chem Soc* **2005**, *127*, 12156–12157.
- [83] Schreiner, P. R.; Reisenauer, H. P.; Romanski, J.; Mlostoń, G. *Angew Chem* **2006**, *118*, 4093–4096.
- [84] Nemirowski, A.; Reisenauer, H. P.; Romanski, J.; Mlostoń, G.; Schreiner, P. R. *J Phys Chem A* **2008**, *112*, 13244–13248.
- [85] Halfen, D. T.; Apponi, A. J.; Woolf, N.; Polt, R.; Ziurys, L. M. *Astrophys J* **2006**, *639*, 237–245.
- [86] Snyder, L. E.; Buhl, D.; Zuckerman, B.; Palmer, P. *Phys Rev Lett* **1969**, *22*, 679–681.
- [87] Becquerel, H. *C R Acad Sci* **1896**, *122*, 420–421.
- [88] Becquerel, A. *C R Acad Sci* **1896**, *122*, 689–694.
- [89] Curie, P.; Skłodowska-Curie, M. *C R Acad Sci* **1898**, *127*, 175–178.
- [90] Curie, P. *C R Acad Sci* **1898**, *127*, 1215–1217.
- [91] Kohlrausch, K. W. F. *Handbuch der Experimentalphysik: Radioaktivität*; Akad. Verl.-Ges.: Leipzig, **1928**.
- [92] Louis de Broglie. *Recherches sur la théorie des Quanta. Physique [physics]. Migration - université en cours d'affectation, 1924*. Français. tel-00006807
- [93] Gamow, G. *Z Phys* **1928**, *51*, 204–212.
- [94] Gurney, R. W.; Condon, E. U. *Phys Rev* **1929**, *33*, 127–140.
- [95] Heisenberg, W. *Z Phys* **1927**, *43*, 172–198.
- [96] Wigner, E. P. *Z Phys Chem* **1932**, *19*, 203–216.
- [97] Eckhardt, A. K.; Gerbig, D.; Schreiner, P. R. *J Phys Chem A* **2018**, *122*, 1488–1495.
- [98] Jeffreys, H. *Proc London Math Soc* **1925**, *s2-23*, 428–436.
- [99] Riccati, J. *Actorum Erud Suppl* **1724**, *8*, 66–73.
- [100] Fukui, K. *J Phys Chem* **1970**, *74*, 4161–4163.
- [101] Henkelman, G.; Uberuaga, B. P.; Jónsson, H. *J Chem Phys* **2000**, *113*, 9901–9904.
- [102] Peters, B.; Heyden, A.; Bell, A. T.; Chakraborty, A. *J Chem Phys* **2004**, *120*, 7877–7886.
- [103] Mardiyukov, A.; Quanz, H.; Schreiner, P. R. *Nat Chem* **2017**, *9*, 71–76.
- [104] Truhlar, D. G.; Isaacson, A. D.; Garrett, B. C. *Generalized transition state theory*; CRC Press: Boca Raton, FL, 1985.
- [105] Garrett, B. C.; Joseph, T.; Truong, T. N.; Truhlar, D. G. *Chem Phys* **1989**, *136*, 271–293.
- [106] Lu, D.-H.; Truong, T. N.; Melissas, V. S.; Lynch, G. C.; Liu, Y.-P.; Garrett, B. C.; Steckler, R.; Isaacson, A. D.; Rai, S. N.; Hancock, G. C.; Lauderdale, J. G.; Joseph, T.; Truhlar, D. G. *Comput Phys Commun* **1992**, *71*, 235–262.
- [107] Liu, Y. P.; Lu, D. H.; Gonzalez-Lafont, A.; Truhlar, D. G.; Garrett, B. C. *J Am Chem Soc* **1993**, *115*, 7806–7817.
- [108] Fernández-Ramos, A.; Truhlar, D. G.; Corchado, J. C.; Espinosa-García, J. *J Phys Chem A* **2002**, *106*, 4957–4960.
- [109] Rommel, J. B.; Goumans, T. P. M.; Kästner, J. *J Chem Theory Comput* **2011**, *7*, 690–698.
- [110] Rommel, J. B.; Kästner, J. *J Chem Phys* **2011**, *134*, 184107.
- [111] Kästner, J. *Chem Eur J* **2013**, *19*, 8207–8212.
- [112] Čížek, J. *J Chem Phys* **1966**, *45*, 4256–4266.
- [113] Purvis, G. D., III; Bartlett, R. J. *J Chem Phys* **1982**, *76*, 1910–1918.
- [114] Pople, J. A.; Head-Gordon, M.; Raghavachari, K. *J Chem Phys* **1987**, *87*, 5968–5975.
- [115] Harding, M. E.; Metzroth, T.; Gauss, J.; Auer, A. A. *J Chem Theory Comput* **2008**, *4*, 64–74.
- [116] Matthews, D. A.; Cheng, L.; Harding, M. E.; Lipparini, F.; Stopkowitz, S.; Jagau, T.-C.; Szalay, P. G.; Gauss, J.; Stanton, J. F. *J Chem Phys* **2020**, *152*, 214108.
- [117] Stanton, J. F. *Chem Phys Lett* **1997**, *281*, 130–134.
- [118] Riplinger, C.; Neese, F. *J Chem Phys* **2013**, *138*, 034106.
- [119] Becke, A. D. *Phys Rev A* **1988**, *38*, 3098–3100.
- [120] Lee, C.; Yang, W.; Parr, R. G. *Phys Rev B* **1988**, *37*, 785–789.
- [121] Becke, A. D. *J Chem Phys* **1993**, *98*, 5648–5652.
- [122] Zhao, Y.; Truhlar, D. G. *Theor Chem Acc* **2008**, *120*, 215–241.
- [123] Zhao, Y.; Truhlar, D. G. *Acc Chem Res* **2008**, *41*, 157–167.
- [124] Grimme, S. *J Chem Phys* **2006**, *124*, 034108.
- [125] Miller, S. L.; Urey, H. C. *Science* **1959**, *130*, 245–251.
- [126] Butlerow, A. *Liebigs Ann* **1861**, *120*, 295–298.
- [127] Ortman, B. J.; Hauge, R. H.; Margrave, J. L.; Kafafi, Z. H. *J Phys Chem* **1990**, *94*, 7973–7977.
- [128] Liu, R.; Zhou, X.; Pulay, P. *J Phys Chem* **1992**, *96*, 5748–5752.
- [129] Szczepanski, J.; Ekern, S.; Vala, M. *J Phys Chem* **1995**, *99*, 8002–8012.
- [130] Schreiner, P. R.; Reisenauer, H. P. *ChemPhysChem* **2006**, *7*, 880–885.
- [131] Schreiner, P. R.; Reisenauer, H. P. *Angew Chem Int Ed* **2008**, *47*, 7071–7074.
- [132] Gerbig, D.; Reisenauer, H. P.; Wu, C.-H.; Ley, D.; Allen, W. D.; Schreiner, P. R. *J Am Chem Soc* **2010**, *132*, 7273–7275.
- [133] Ley, D.; Gerbig, D.; Schreiner, P. R. *Chem Sci* **2013**, *4*, 677–684.
- [134] Ley, D.; Gerbig, D.; Wagner, J. P.; Reisenauer, H. P.; Schreiner, P. R. *J Am Chem Soc* **2011**, *133*, 13614–13621.
- [135] Kozuch, S.; Zhang, X.; Hrovat, D. A.; Borden, W. T. *J Am Chem Soc* **2013**, *135*, 17274–17277.
- [136] Karmakar, S.; Datta, A. *J Org Chem* **2017**, *82*, 1558–1566.
- [137] Zuev, P. S.; Sheridan, R. S. *J Am Chem Soc* **1994**, *116*, 4123–4124.
- [138] Zimmer, L. E.; Sparr, C.; Gilmour, R. *Angew Chem Int Ed* **2011**, *50*, 11860–11871.
- [139] Wolfe, S. *Acc Chem Res* **1972**, *5*, 102–111.
- [140] Wittkopp, A.; Schreiner, P. R. *Chem Eur J* **2003**, *9*, 407–414.

- [141] Lippert, K. M.; Hof, K.; Gerbig, D.; Ley, D.; Hausmann, H.; Guenther, S.; Schreiner, P. R. *Eur J Org Chem* **2012**, *2012*, 5919–5927.
- [142] Dunitz, J. D. *ChemBioChem* **2004**, *5*, 614–621.
- [143] Dunitz, J. D.; Taylor, R. *Chem Eur J* **1997**, *3*, 89–98.
- [144] Howard, J. A. K.; Hoy, V. J.; O'Hagan, D.; Smith, G. T. *Tetrahedron Lett* **1996**, *52*, 12613–12622.
- [145] Vidya, V.; Sankaran, K.; Viswanathan, K. S. *Chem Phys Lett* **1996**, *258*, 113–117.
- [146] Kesselmayer, M. A.; Sheridan, R. S. *J Am Chem Soc* **1986**, *108*, 844–845.
- [147] Sheridan, R. S.; Moss, R. A.; Wilk, B. K.; Shen, S.; Wlostowski, M.; Kesselmayer, M. A.; Subramanian, R.; Kmiecik-Lawrynowicz, G.; Krogh-Jespersen, K. *J Am Chem Soc* **1988**, *110*, 7563–7564.
- [148] Du, X. M.; Fan, H.; Goodman, J. L.; Kesselmayer, M. A.; Krogh-Jespersen, K.; Lavilla, J. A.; Moss, R. A.; Shen, S.; Sheridan, R. S. *J Am Chem Soc* **1990**, *112*, 1920–1926.
- [149] Maloney, V.; Platz, M. S. *J Phys Org Chem* **1990**, *3*, 135–138.
- [150] Roth, H. D.; Platz, M. S. *J Phys Org Chem* **1996**, *9*, 252–254.
- [151] Dubost, H. *J Low Temp Phys* **1998**, *111*, 615–628.
- [152] E. Bondybey, V.; Räsänen, M.; Lammers, A. *Annu Rep Prog Chem, Sect C: Phys Chem* **1999**, *95*, 331–372.
- [153] Förster, T. *Ann Phys* **1948**, *437*, 55–75.
- [154] Brus, L. E.; Bondybey, V. E. *J Chem Phys* **1975**, *63*, 786–793.
- [155] Hadj Bachir, I.; Charneau, R.; Dubost, H. *Chem Phys* **1993**, *177*, 675–692.
- [156] Baldeschwieler, J. D.; Pimentel, G. C. *J Chem Phys* **1960**, *33*, 1008–1015.
- [157] Hall, R. T.; Pimentel, G. C. *J Chem Phys* **1963**, *38*, 1889–1897.
- [158] Homanen, L.; Murto, J. *Chem Phys Lett* **1982**, *85*, 322–324.
- [159] Hoffman, W. F.; Shirk, J. S. *Chem Phys* **1983**, *78*, 331–338.
- [160] Räsänen, M.; Aspiala, A.; Homanen, L.; Murto, J. *J Mol Struct* **1983**, *96*, 81–100.
- [161] Räsänen, M.; Aspiala, A.; Murto, J. *J Chem Phys* **1983**, *79*, 107–116.
- [162] Hoffman, W. F.; Shirk, J. S. *J Mol Struct* **1987**, *157*, 275–287.
- [163] Shirk, J. S.; Marquardt, C. L. *J Chem Phys* **1990**, *92*, 7234–7240.
- [164] Maçôas, E. M. S.; Fausto, R.; Lundell, J.; Pettersson, M.; Khriachtchev, L.; Räsänen, M. *J Phys Chem A* **2001**, *105*, 3922–3933.
- [165] Maçôas, E. M. S.; Khriachtchev, L.; Pettersson, M.; Fausto, R.; Räsänen, M. *J Am Chem Soc* **2003**, *125*, 16188–16189.
- [166] Reva, I. D.; Jarmelo, S.; Lapinski, L.; Fausto, R. *J Phys Chem A* **2004**, *108*, 6982–6989.
- [167] Maçôas, E. M. S.; Khriachtchev, L.; Pettersson, M.; Fausto, R.; Räsänen, M. *J Phys Chem A* **2005**, *109*, 3617–3625.
- [168] Puletti, F.; Mallocci, G.; Mulas, G.; Cecchi-Pestellini, C. *Mon Not R Astron Soc* **2010**, *402*, 1667–1674.
- [169] Lopes, S.; Domanskaya, A. V.; Fausto, R.; Räsänen, M.; Khriachtchev, L. *J Chem Phys* **2010**, *133*, 144507.
- [170] Järvinen, T.; Lundell, J.; Dopieralski, P. *Theor Chem Acc* **2018**, *137*, 100–108.
- [171] Apóstolo, R. F. G.; Bento, R. R. F.; Fausto, R. *Croat Chem Acta* **2015**, *88*, 377–386.
- [172] Apóstolo, R. F. G.; Bazsó, G.; Ogruc-Ildiz, G.; Tarczay, G.; Fausto, R. *J Chem Phys* **2018**, *148*, 044303.
- [173] Maçôas, E. M. S.; Fausto, R.; Pettersson, M.; Khriachtchev, L.; Räsänen, M. *J Phys Chem A* **2000**, *104*, 6956–6961.
- [174] Fausto, R.; Maçôas, E. M. S. *J Mol Struct* **2001**, *563-564*, 27–40.
- [175] Lopes, S.; Nikitin, T.; Fausto, R. *J Phys Chem A* **2019**, *123*, 1581–1593.
- [176] Lapinski, L.; Reva, I.; Rostkowska, H.; Halasa, A.; Fausto, R.; Nowak, M. J. *J Phys Chem A* **2013**, *117*, 5251–5259.
- [177] Lapinski, L.; Nowak, M. J.; Reva, I.; Rostkowska, H.; Fausto, R. *Phys Chem Chem Phys* **2010**, *12*, 9615–9618.
- [178] Reva, I.; Nowak, M. J.; Lapinski, L.; Fausto, R. *J Chem Phys* **2012**, *136*, 064511.
- [179] Lapinski, L.; Reva, I.; Rostkowska, H.; Fausto, R.; Nowak, M. J. *J Phys Chem B* **2014**, *118*, 2831–2841.
- [180] Halasa, A.; Lapinski, L.; Reva, I.; Rostkowska, H.; Fausto, R.; Nowak, M. J. *J Am Chem Soc* **2015**, *119*, 1037–1047.
- [181] Justino, L. L. G.; Reva, I.; Fausto, R. *J Chem Phys* **2016**, *145*, 014304.
- [182] Lopes Jesus, A. J.; Reva, I.; Araujo-Andrade, C.; Fausto, R. *J Am Chem Soc* **2015**, *137*, 14240–14243.
- [183] Sander, S.; Willner, H.; Khriachtchev, L.; Pettersson, M.; Räsänen, M.; Varetti, E. L. *J Mol Spectrosc* **2000**, *203*, 145–150.
- [184] Olbert-Majkut, A.; Reva, I. D.; Fausto, R. *Chem Phys Lett* **2008**, *456*, 127–134.
- [185] Lopes Jesus, A. J.; Nunes, C. M.; Fausto, R.; Reva, I. *Chem Comm* **2018**, *54*, 4778–4781.
- [186] Stepanian, S. G.; Reva, I. D.; Radchenko, E. D.; Rosado, M. T. S.; Duarte, M. L. T. S.; Fausto, R.; Adamowicz, L. *J Phys Chem A* **1998**, *102*, 1041–1054.
- [187] Bazsó, G.; Magyarfalvi, G.; Tarczay, G. *J Mol Struct* **2012**, *1025*, 33–42.
- [188] Bazsó, G.; Najbauer, E. E.; Magyarfalvi, G.; Tarczay, G. *J Phys Chem A* **2013**, *117*, 1952–1962.
- [189] Nunes, C. M.; Lapinski, L.; Fausto, R.; Reva, I. *J Chem Phys* **2013**, *138*, 125101.
- [190] Najbauer, E. E.; Bazsó, G.; Góbi, S.; Magyarfalvi, G.; Tarczay, G. *J Phys Chem B* **2014**, *118*, 2093–2103.
- [191] Borba, A.; Gómez-Zavaglia, A.; Fausto, R. *J Chem Phys* **2014**, *141*, 154306.
- [192] Duvernay, F.; Butscher, T.; Chiavassa, T.; Coussan, S. *Chem Phys* **2017**, *496*, 9–14.
- [193] Rostkowska, H.; Lapinski, L.; Kozankiewicz, B.; Nowak, M. J. *J Phys Chem A* **2012**, *116*, 9863–9871.
- [194] Ryazantsev, S. V.; Feldman, V. I.; Khriachtchev, L. *J Am Chem Soc* **2017**, *139*, 9551–9557.
- [195] Goddard, J. D.; Yamaguchi, Y.; Schaefer, H. F. *J Chem Phys* **1992**, *96*, 1158–1166.
- [196] Su, H.; He, Y.; Kong, F.; Fang, W.; Liu, R. *J Chem Phys* **2000**, *113*, 1891–1897.
- [197] Khriachtchev, L.; Pettersson, M.; Gerber, R. B. *J Phys Chem A* **2015**, *119*, 2187–2190.
- [198] Pettersson, M. *J Chem Phys* **2002**, *117*, 9095–9098.
- [199] Marushkevich, K.; Räsänen, M.; Khriachtchev, L. *J Phys Chem A* **2010**, *114*, 10584–10589.
- [200] Khriachtchev, L.; Maçôas, E. M. S.; Pettersson, M.; Räsänen, M. *J Am Chem Soc* **2002**, *124*, 10994–10995.
- [201] Pettersson, M.; Maçôas, E. M. S.; Khriachtchev, L.; Fausto, R.; Räsänen, M. *J Am Chem Soc* **2003**, *125*, 4058–4059.
- [202] Barber, V. P.; Pandit, S.; Esposito, V. J.; McCoy, A. B.; Lester, M. I. *J Phys Chem A* **2019**, *123*, 2559–2569.
- [203] Fang, Y.; Liu, F.; Barber, V. P.; Klippenstein, S. J.; McCoy, A. B.; Lester, M. I. *J Chem Phys* **2016**, *145*, 234308.
- [204] Bader, R. F. W. *Acc Chem Res* **1985**, *18*, 9–15.
- [205] Bernhardt, B.; Ruth, M.; Eckhardt, A. K.; Schreiner, P. R. *J Am Chem Soc* **2021**, *143*, 3741–3746.
- [206] Feller, D.; Borden, W. T.; Davidson, E. R. *J Chem Phys* **1979**, *71*, 4987–4992.
- [207] Feller, D.; Borden, W. T.; Davidson, E. R. *J Comput Chem* **1980**, *1*, 158–166.
- [208] Broderick, B. M.; McCaslin, L.; Moradi, C. P.; Stanton, J. F.; Douberly, G. E. *J Chem Phys* **2015**, *142*, 144309–144316.
- [209] Eckhardt, A. K.; Erb, F. R.; Schreiner, P. R. *Chem Sci* **2019**, *10*, 802–808.
- [210] Maçôas, E. M. S.; Khriachtchev, L.; Pettersson, M.; Fausto, R.; Räsänen, M. *J Chem Phys* **2004**, *121*, 1331–1338.
- [211] Olbert-Majkut, A.; Lundell, J.; Wierzejewska, M. *J Phys Chem A* **2014**, *118*, 350–357.

2 Publications

2.1 Conformer-specific hydrogen atom tunnelling in trifluoromethylhydroxycarbene



Abstract: Conformational control of organic reactions is at the heart of the biomolecular sciences. To achieve a particular reactivity, one of many conformers may be selected, for instance, by a (bio)catalyst, as the geometrically most suited and appropriately reactive species. The equilibration of energetically close-lying conformers is typically assumed to be facile and less energetically taxing than the reaction under consideration itself: this is termed the 'Curtin–Hammett principle'. Here, we show that the *trans* conformer of trifluoromethylhydroxycarbene preferentially rearranges through a facile quantum-mechanical hydrogen tunnelling pathway, while its *cis* conformer is entirely unreactive. Hence, this presents the first example of a conformer-specific hydrogen tunnelling reaction. The Curtin–Hammett principle is not applicable, due to the high barrier between the two conformers.

Reference

Artur Mardyukov, Henrik Quanz and Peter R. Schreiner Conformer-specific hydrogen atom tunnelling in trifluoromethylhydroxycarbene. *Nat Chem* **2017**, 9, 71–76 (doi:10.1038/nchem.2609)

Underline denotes first author.

Reproduced with permission

© 2017, Springer Nature
Springer-Verlag GmbH, Heidelberg,
Zweigniederlassung der Springer-Verlag GmbH, Berlin
Tiergartenstraße 17
D-69121 Heidelberg
Germany

Conformer-specific hydrogen atom tunnelling in trifluoromethylhydroxycarbene

Artur Mardyukov, Henrik Quanz and Peter R. Schreiner*

Conformational control of organic reactions is at the heart of the biomolecular sciences. To achieve a particular reactivity, one of many conformers may be selected, for instance, by a (bio)catalyst, as the geometrically most suited and appropriately reactive species. The equilibration of energetically close-lying conformers is typically assumed to be facile and less energetically taxing than the reaction under consideration itself: this is termed the 'Curtin-Hammett principle'. Here, we show that the *trans* conformer of trifluoromethylhydroxycarbene preferentially rearranges through a facile quantum-mechanical hydrogen tunnelling pathway, while its *cis* conformer is entirely unreactive. Hence, this presents the first example of a conformer-specific hydrogen tunnelling reaction. The Curtin-Hammett principle is not applicable, due to the high barrier between the two conformers.

Conformationally controlled reactions play a crucial role in the selectivity and function of chemical reactions^{1,2} and biologically active molecules³. Conformers can be interconverted via hindered rotation about single bonds, and the low energy barriers associated with these rotamerizations lead to rapid equilibration, even at low temperatures. Conformational specificity has been demonstrated in the gas phase and in low-temperature matrix-isolation experiments^{4,5}. For example, conformer-dependent reactions have been reported for the dissociation of iodopropane radical cation conformers that produce different products⁶. In another study, the photodissociation channels of the *trans* and *cis* conformers of formic acid in solid argon matrices were shown to give different product distributions: the *trans* rotamer predominantly dissociates into H₂O and CO, and the *cis* rotamer undergoes photodissociation to H₂ and CO₂ (ref. 7). In parallel, *cis* formic acid also converts back to the more stable *trans* isomer with a half-life of only a few minutes via quantum mechanical tunnelling (QMT). These studies beautifully demonstrate the possibility of reaction control via narrowband infrared radiation.

Experimental evidence of QMT of hydrogen atoms is a widely observed phenomenon in chemistry^{8–10} and biology^{11–13}. Conformer-specific tunnelling, on the other hand, has, at least to the best of our knowledge, only been reported for a single case. Such specificity was demonstrated for the preferential carbon atom tunnelling of *exo*-1-methylcyclobutylfluorocarbene, with the *endo* isomer remaining unchanged under identical conditions¹⁴.

Recently, we have shown that hydroxycarbenes (R–C–OH) undergo facile tunnelling reactions, even at temperatures as low as 10 K in noble gas matrices⁸, eventually leading to the new reactivity paradigm of tunnelling control¹⁵. Here, we present the preparation and study of novel trifluoromethylhydroxycarbene (**1**, Fig. 1), which allowed the first observation of the *cis* and *trans* conformers of a hydroxycarbene. Thus far, previous studies only yielded the corresponding *trans* hydroxycarbene conformer, because it is the conformer that preferentially forms in the decarboxylation of the respective precursor. Photochemical conformer equilibration was not possible as this also triggered the tunnelling isomerizations. Hence, **1** is the first hydroxycarbene to allow the photochemical preparation and spectroscopic identification of a hydroxycarbene *cis* isomer (**1c**). As only the *trans* conformer (**1t**) shows the typical [1,2]hydrogen tunnelling ([1,2]H-tunnelling) shift to

trifluoroacetaldehyde (**2**), while **1c** remains unchanged, we present the first example of a conformer-specific H-tunnelling reaction.

Our initial idea was to study the effect of CF₃ substitution on the H-tunnelling half-life, which is strongly affected by the electronic properties of the atoms adjacent to the carbene centre¹⁶. For instance, π donors extend the half-lives and thereby allow control of the tunnelling process on the basis of stereoelectronic effects and straightforward structure–activity relationships. As the CF₃ group in **1** is σ -electron-withdrawing, we expected reactivity significantly different from the parent methylhydroxycarbene (**8**)¹⁵. With respect to the QMT behaviour, one would expect that σ -electron withdrawal increases the electron deficiency at the carbene carbon, leading to a shorter half-life, while hyperconjugative stabilization through one of the C–F bonds should diminish the driving force for QMT and therefore increase the half-life. As we demonstrate here, the CF₃ group stabilizes **1c** sufficiently for it to be prepared photochemically and so that it remains unchanged during the tunnelling isomerization of **1t** to **2**.

Result and discussion

Following our established route to hydroxycarbenes, commercially available 3,3,3-trifluoro-2-oxopropanoic acid (**3**) was chosen as the thermal precursor for the generation and matrix-isolation of **1** at 10 K through thermally allowed CO₂ extrusion using flash vacuum pyrolysis (FVP) at 900 °C in an argon gas flow at less than 1 × 10^{−3} mbar total pressure^{8,15,17}. The infrared spectrum of the FVP products of **3** (Supplementary Fig. 1) shows several new absorptions in the C=O stretching region between 1,850 and 1,650 cm^{−1}, next to some unreacted starting material and the usual impurities (for example, H₂O) often found in FVP matrix-isolation experiments. The target carbene **1t** is present in minor amounts but can be identified on the basis of matching the observed and the unscaled (harmonic) computed vibrational bands computed at the coupled-cluster singles and doubles as well as the perturbatively included triple excitations level of theory (CCSD(T)/cc-pVTZ; for details see Supplementary Sections 3–7 and Supplementary Table 1). Additionally, selective photolysis of **1t** (Fig. 2), gives infrared difference spectra that match the computed data very well. The infrared spectrum of the matrix-isolated pyrolysis mixture contained a significant amount of CO and HF, and the most prominent bands at 1,221 and 1,102 cm^{−1} were attributed to difluorocarbene **4**, which most probably derives from the gas-phase

Institute of Organic Chemistry, Justus-Liebig University, Heinrich-Buff-Ring 17, 35392 Giessen, Germany. *e-mail: prs@uni-giessen.de

NATURE CHEMISTRY | ADVANCE ONLINE PUBLICATION | www.nature.com/naturechemistry

1

© 2016 Macmillan Publishers Limited, part of Springer Nature. All rights reserved.

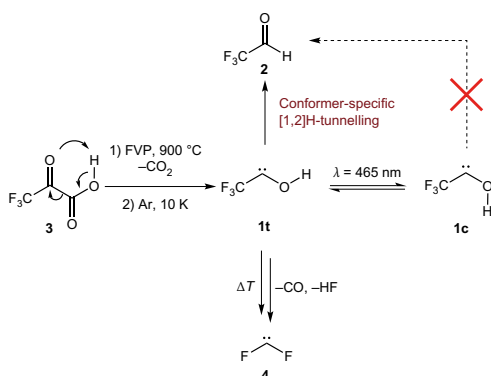


Figure 1 | Schematic presentation of the thermal generation of *trans*-trifluoromethylhydroxycarbene (**1t**) from 3,3,3-trifluoro-2-oxopropanoic acid (**3**) and subsequent reactions. Thermal extrusion of CO₂ via an allowed six-electron/five-centre electrocyclic process yields the title compound **1t**. Difluorocarbene (**4**), CO and HF also form under the FVP conditions through decomposition of **1t**. Conformer-specific tunnelling rearranges **1t** to **2** via a [1,2]H shift. The *cis*-isomer **1c** can be populated through irradiation but does not undergo tunnelling isomerization to **2**.

decomposition of **1**, involving HF elimination from **1c**, which gives intermediate difluoroketene **5**, which loses CO to yield **4** (Supplementary Fig. 1). We also observed other less intense signals at 1,818, 1,250, 1,207, 1,186, 1,131 and 776 cm⁻¹ that can be assigned to trifluoroacetic acid **6**, formed by gas-phase decarbonylation. The infrared spectra of the pyrolysis mixture of **3** also showed a small amount of **2**, the [1,2]H shift product of **1t**.

Prolonged irradiation of the pyrolysis products in argon at 465 nm results in complete bleaching of the infrared bands of **1t** and the formation of new bands at 1,782, 1,383, 1,304, 1,193, 1,172, 833 and 705 cm⁻¹ (Fig. 2d), which were assigned to 2,2,2-trifluoroacetaldehyde **2** formed via a [1,2]H migration. Photoproduct **2** was

identified by comparison of its experimental and computed infrared spectra (Fig. 2e). The assignments are also supported by isotope labelling experiments using *O*-deuterated acid *d*-**3**, yielding the corresponding deuterated carbene *d*-**1t** as well as *d*-**1c** and *d*-**2** upon irradiation of *d*-**1t** at 465 nm (Supplementary Fig. 2).

Carbene **1t** was unambiguously identified in the matrix by the excellent matching of the experimental and unscaled CCSD(T)/cc-pVTZ computed infrared absorptions (Fig. 2a,b); this conformer is 0.8 kcal mol⁻¹ more stable than **1c** at this level (*vide infra*). In line with our earlier studies on other hydroxycarbenes, there are no indications for the formation of **1c** directly from pyrolysis. Indeed, a *cis* conformer has never been observed for any hydroxycarbene. The ultraviolet/visible (UV-vis) absorption maximum of **1t** computed with time-dependent density functional theory (TD-DFT) at TD-M06-2X/cc-pVTZ predicts a weak transition at λ_{max} = 415 nm. Visible-light irradiation (λ = 465 nm) of the FVP mixture results in a rapid decrease of all infrared bands attributed to **1t**, with the other bands remaining unaffected. The infrared difference spectrum of **1t** after 30 s irradiation at λ = 465 nm shows two sets of bands, one appearing (pointing upward) and another disappearing (pointing downward) during irradiation of the matrix (Fig. 2b). The bands disappearing clearly correspond to **1t**, as is evident from a comparison between the CCSD(T)/cc-pVTZ computed and experimental infrared spectra. From the decay kinetics of these bands during photolysis, the most intense band at 1,175 cm⁻¹ is assigned to the C–F stretching mode of **1t**. The strong band at 3,506 cm⁻¹ is attributed to the OH stretching ν(O–H) mode of **1t**. An additional set of bands at 1,396, 1,299, 1,238, 830 and 670 cm⁻¹ were also assigned to **1t** (Supplementary Table 1). All characteristic infrared frequencies for **1t** nicely match the computed unscaled harmonic vibrational frequencies at CCSD(T)/cc-pVTZ. The experimentally observed UV-vis spectrum of the pyrolysis mixture revealed a strong absorption pattern at 225–270 nm (Supplementary Fig. 3). The absorption bands display a resolved vibrational structure that belongs to difluorocarbene **4**, in perfect match with the literature spectra. Unfortunately, due to the low extinction coefficient, the UV-vis transitions of **1t** could not be detected (for time-dependent DFT-computed spectra see Supplementary Fig. 4).

At least two distinct species formed simultaneously during photolysis. The comparison with the computed infrared spectrum indicates that most of the appearing bands correspond to **1c**. In

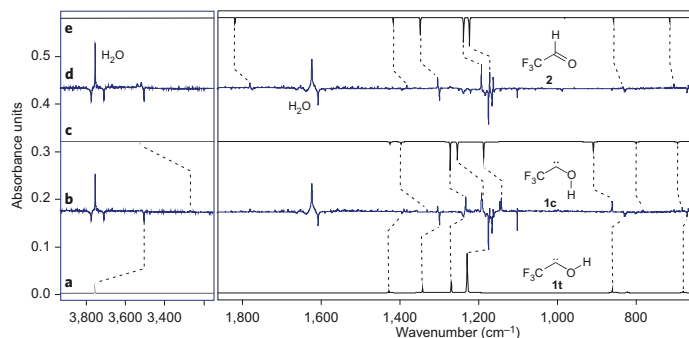


Figure 2 | Comparison of experimentally measured and computed infrared spectra for the key compounds in the observed tunnelling isomerization. **a**, Infrared spectrum of **1t** computed at CCSD(T)/cc-pVTZ (harmonic, unscaled). Simulated bandwidth = 1 cm⁻¹. **b**, Infrared difference spectra showing the photochemistry of **1t** after 30 s of irradiation with λ = 465 nm in argon at 10 K. Downward bands assigned to **1t** disappear, while upward bands assigned to **1c** appear after irradiation. **c**, Infrared spectrum of **1c** computed at the CCSD(T)/cc-pVTZ level of theory. **d**, Infrared difference spectra showing the photochemistry of **1t** after 300 s of irradiation with λ = 465 nm in argon at 10 K. Bands pointing downwards assigned to **1t** disappear, and bands pointing upwards assigned to **2** appear after irradiation. **e**, Infrared spectrum of **2** computed at CCSD(T)/cc-pVTZ (unscaled). As there are no significant absorptions in the 1,850–3,200 cm⁻¹ regime for **1** and **2**, this part is not depicted (for full spectra see Supplementary Fig. 1).

2

NATURE CHEMISTRY | ADVANCE ONLINE PUBLICATION | www.nature.com/naturechemistry

© 2016 Macmillan Publishers Limited, part of Springer Nature. All rights reserved.

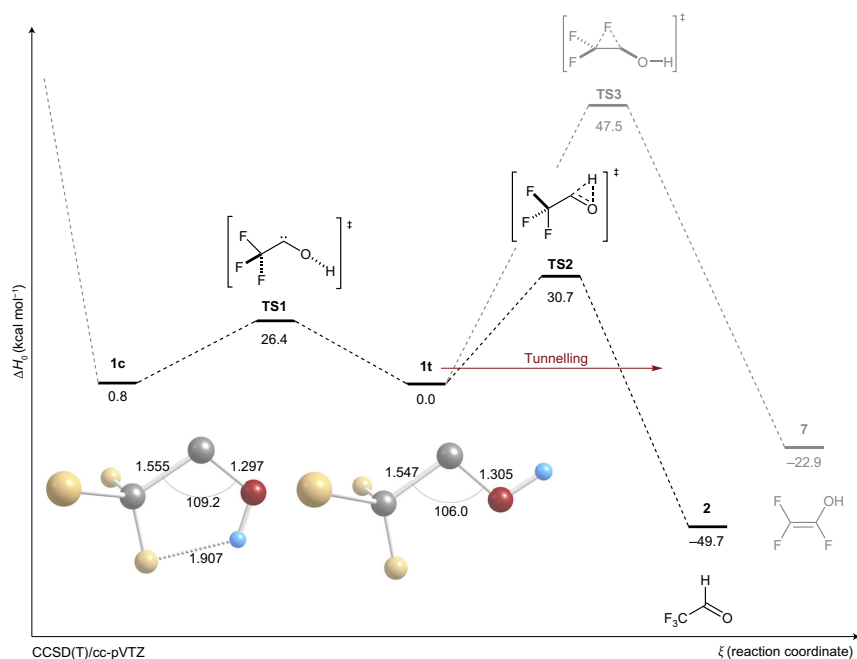


Figure 3 | Depiction of the computed potential energy surface (ΔH_0) of ground-state singlet **1t** for its unimolecular reactions at CCSD(T)/cc-pVTZ.

Colour code: yellow, fluorine; grey, carbon; red, oxygen; light blue, hydrogen. The grey pathway for the rearrangement to trifluoro enol **7** is energetically unfeasible but is shown for completeness. Tunnelling of **1t** to **2** depletes the concentration of **1t**. This cannot be replenished through rotamerization of **1c** owing to the higher barrier (via **TS1**), which cannot be overcome at the experimental temperature of 10 K. Hence, a Curtin–Hammett situation is not given and this principle does not apply. Selected bond lengths are in Å, bond angles are in degrees. Dagger symbols represent transition state.

particular, the signals at 3,269, 1,436, 1,331, 1,233, 1,191, 1,146, 861 and 683 cm⁻¹ increase in intensity after irradiation and were assigned to **1c** (Fig. 2b and Supplementary Table 1). The photochemical conversion of **1t** to **1c** and **2** is rapid; irradiation for 10, 20, 30 and 60 s showed that 30 s are sufficient for complete conversion of **1t**. A comparison of the computed and experimental infrared frequencies of the two rotamers of **1** allowed their unambiguous identification. Remarkably, in the case of **1t**, the O–H stretching vibration mode appears at 3,506 cm⁻¹, whereas **1c** shows a weak absorption at 3,269 cm⁻¹. The experimentally frequency shift between the two isomers is calculated to be -237 cm⁻¹, in excellent agreement with the computed frequency shift of -238 cm⁻¹ (Supplementary Table 2). This shift is smaller than the corresponding frequency shift in parent **8** (321 cm⁻¹) but much larger than the experimentally found 22 cm⁻¹ shift between the *trans* and *gauche* conformers of 1,1,1-trifluoroethanol¹⁸, which is the hydrogenated congener of **1**. One may suspect that these large infrared frequency shifts of the *cis* and *trans* conformers arise from the carbene lone pair donation into the periplanar C–O, C–F and C–H bonds in **1c** and **8c**. The $lp(C) \rightarrow \sigma^*(OH)$ interaction can be recognized in both *cis* carbenes: a second-order perturbation natural bond orbital (NBO)¹⁹ analysis at the M06-2X/cc-pVDZ level of theory gives 7.8 and 10.2 kcal mol⁻¹ for **1c** and **8c**, respectively. The $lp(C) \rightarrow \sigma^*(CF)$ (7.2 kcal mol⁻¹) and $lp(C) \rightarrow \sigma^*(CH)$ (7.8 kcal mol⁻¹) interactions in **1c** and **8c**, respectively, are about equally large. All of these interaction terms are rather small, and their differences are too small to draw firm conclusions. A quantum theory of atoms in molecules (QTAIM) analysis²⁰ reveals both a bond critical point between the

in-plane fluorine and hydrogen atoms and a ring critical point (Supplementary Fig. 9). Furthermore, the C–F stretching absorption in **1t** (1,175 cm⁻¹) is slightly lower than that of **1c** (1,191 cm⁻¹), again in agreement with the computed value, which gives a shift difference of $\Delta\nu = 24$ cm⁻¹ (Supplementary Tables 1 and 2). Hence, it is likely that conformer **1c** benefits from weak internal H...F bonding, as is also evident from the CCSD(T)/cc-pVTZ structure (Fig. 2), which gives an H...F bond distance in **1c** of 1.907 Å, which is even shorter than the shortest H...F distance (2.01 Å) found in the crystal structure of HOC(CF₃)₂(4-Si(*i*-Pr)₃-2,6-C₆H₂(CF₃)₂) (ref. 21). A balanced (homodesmotic) equation (Supplementary Fig. 6) gives a stabilization of **1c** over **8c** of ~2 kcal mol⁻¹.

Carbene **1** has large singlet–triplet energy separation of $\Delta E_{ST} = -26.8$ kcal mol⁻¹ at CCSD(T)/cc-pVTZ, underlining its singlet ground-state nature, similar to other hydroxycarbenes (note that there is only one C₁ triplet conformer). Thermolysis of **3** under FVP conditions at 900 °C is strongly dominated by entropy, a situation that preferentially leads to difluorocarbene **4** as well as HF and CO as the major products trapped from the pyrolysis mixture (for a complete CCSD(T)/cc-pVTZ-computed potential energy hypersurface (PES), see Supplementary Fig. 7). However, **1** forms in sufficiently significant amounts to allow its characterization and study of its reactivity. The key parts of the PES are depicted in Fig. 3. Carbene **1t** is only 0.8 kcal mol⁻¹ more stable than **1c**, which is a significantly smaller energy difference than for the parent methylhydroxycarbene (**8t** is 3.1 kcal mol⁻¹ more stable than **8c** at CCSD(T)/CBS), probably due to the intramolecular H...F interaction, which may be estimated through this

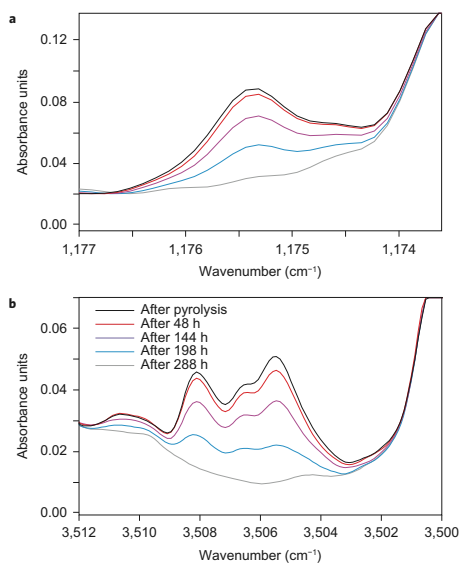


Figure 4 | Time evolution of a selection of infrared bands for the disappearance of **1t.** **a, b**, The band around $3,506\text{ cm}^{-1}$ corresponds to the O–H stretching absorption (**b**), while the signals at $1,175\text{ cm}^{-1}$ are composed of C–F stretching and O–H wagging bands (**a**). The spectra were recorded over the course of nearly 300 h in an argon matrix at 10 K and demonstrate the facile QMT process for the isomerization of **1t** to **2**.

conformer pair energy difference to be $\sim 2\text{ kcal mol}^{-1}$, in line with our homodesmotic evaluation (Supplementary Fig. 6). The transition structure **TS1** for the rotamerization of **1t** to **1c** is associated with a sizeable barrier of $26.4\text{ kcal mol}^{-1}$; is also 2 kcal mol^{-1} above that for the **8t** \rightarrow **8c** conversion ($24.4\text{ kcal mol}^{-1}$).

Apart from the reactions depicted in Fig. 3 and discussed in detail below, **1c** can undergo a mildly exothermic ($-3.1\text{ kcal mol}^{-1}$) concerted HF extrusion to difluoroketene (**5**) that requires $27.2\text{ kcal mol}^{-1}$ activation. Subsequent CO extrusion to difluorocarbene (**4**) is accompanied by a surprisingly low activation barrier of only $10.0\text{ kcal mol}^{-1}$ via **TS5** (Supplementary Fig. 7). The fact that we did not observe characteristic peaks for **1c** directly after FVP suggests that the energy is sufficient in the pyrolysis zone for **1t** to undergo all of these reactions to give **4** as the major product. The experimentally not observed formation of the enol 1,2,2-trifluoroethen-1-ol (**7**) either from **1t** or **1c** is energetically excluded as it requires activation energies of $\sim 48\text{ kcal mol}^{-1}$, which is far too high to be surmounted at the temperature of our FVP experiments. Finally, the pyrolysis of starting material **3** at $900\text{ }^\circ\text{C}$ also yielded infrared signals that were clearly identifiable as trifluoroacetic acid (**6**), which is the decarbonylation product of **3**; computations on this part of the PES of **6** are summarized in Supplementary Fig. 8.

Conformer-dependent QMT. Carbene **1t** is metastable under matrix-isolation conditions as it slowly rearranges to **2** through a [1,2]H-shift, even at temperatures as low as 3 K, despite a considerable barrier for this process of $\sim 31\text{ kcal mol}^{-1}$. The decay kinetics were monitored using the intense O–H and C–F stretching absorptions of **1t** at $3,605$ and $1,175\text{ cm}^{-1}$ (Fig. 4). We determine an experimental half-life of **1t** of $144 \pm 11\text{ h}$, which is largely independent of the temperature of the matrix in the

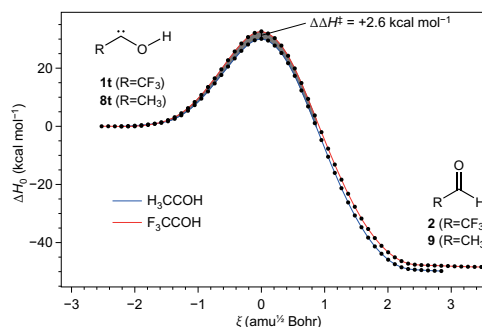


Figure 5 | Comparison of the intrinsic reaction coordinates of **1t and **8t** for rearrangement to their corresponding aldehydes.** Although the differences in the path curvatures are small (computed at the M06-2X/cc-pVTZ level of theory), the slightly wider and higher barrier for the rearrangement of **1t** results in a significantly longer half life of **1t** ($\sim 144\text{ h}$) versus parent **8t** ($\sim 1\text{ h}$).

measured 3–20 K temperature interval (for changes in the infrared spectra over time at 20 K, see Supplementary Fig. 5). This is highly indicative of a QMT process, as is typical for the majority of hydroxycarbenes²². As found for other hydroxycarbenes, O-deuteration (*d*-**1t**) completely suppresses the rearrangement to *d*-**2**, and no spectral changes were observed for at least 30 days. This provides additional solid evidence that the observed phenomenon is indeed a tunnelling process that very sensitively depends on the mass of the tunnelling particle (as well as on barrier height and width).

To confirm our experimental observations, we computed the tunnelling half-lives of **1t** and *d*-**1t** using the Wentzel–Kramers–Brillouin (WKB) formalism, which has been shown to deliver excellent agreement between experiment and theory^{8,15,23}. Kästner has demonstrated that our one-dimensional WKB treatment for determining the tunnelling half-lives of hydroxycarbenes agrees well with a more elaborate instanton approach²⁴. The WKB calculations at the (M06-2X/6-311++G(d,p)) level of theory yield a [1,2]H-tunnelling half-life for **1t** of 172 h, in excellent agreement with the experimental value. The computed half-life of *d*-**1t** is on the order of 10^6 years. Unsurprisingly, we could not locate a transition structure for the direct conversion of **1c** to **2**, implying that the QMT ‘escape’ path to **2** is blocked, leading to entrapment of **1c** in a rather deep minimum of the PES. As a consequence, tunnelling arises specifically from the **1t** conformer only. The Curtin–Hammett principle does not apply as the barrier between the two conformers is large relative to the adjacent reaction barriers^{25,26}.

Competing QMT processes may be envisaged for the reaction of **1t** or **1c** to **7** via a [1,2]F-shift, that is, F-tunnelling, or for the HF extrusion from **1c** to **5**. However, apart from the fact that an element heavier than hydrogen is involved, which would significantly slow QMT, the barriers are wider in all cases and much higher than for **1t** \rightarrow **7**. As a consequence, these reactions were not observed. As QMT of **1t** is relatively slow, we also investigated whether **1c** would undergo conformational tunnelling back to **1t**; this would be a conformational QMT process that is very common to carboxylic acids through C–OH bond rotation^{27–29}. The tunnelling half-lives for such conformational tunnelling of carboxylic acids are in the range of 10^{-3} s to several minutes^{30–36}. After photochemical generation of **1c**, no spectral changes were observed in an argon matrix at 10 K over a period of at least 24 h, making **1c** kinetically stable under matrix-isolation conditions. Accordingly, our WKB computations yield a half-life for the

rotamerization of **1c** to **1t** of 1,190 years, owing to the high (26.4 kcal mol⁻¹) and wide barrier as compared to the much smaller barriers typically encountered for carboxylic acid rotational isomerizations (2–13 kcal mol⁻¹)^{27,37–41}.

The long QMT half-life for **1t** of 144 h must be related to the stereoelectronic effect of the CF₃ group on the carbene carbon (note that the half-life of parent methylhydroxycarbene **8** is only 1.1 h)¹⁵. As σ -electron withdrawal would increase the electron deficiency in **1t**, one may argue that it may be the $\sigma_{C-F} \rightarrow C(p)$ or $lp(C) \rightarrow \sigma_{C-F}^*$ hyperconjugation interactions⁴² that are responsible for this effect. However, our NBO analysis (*vide supra*) does not reveal particularly large contributions from such interactions, as they are quite comparable to those in parent **8t**. The intrinsic reaction paths associated with the rearrangement of hydroxycarbenes **1t** and **8t** are qualitatively the same, and they differ quantitatively only very little (Fig. 5), with the barrier for **1t** being 2.6 kcal mol⁻¹ higher and also wider.

This alone is probably sufficient to rationalize the large differences in half-lives, even though it is quite remarkable just how sensitive QMT is to the fine details of a PES. From a chemical viewpoint it is instructive to consider the atomic NBO charges of **1t** and **8t**, because they are quite different. Although the methyl-group carbon in **8t** bears a $-0.8e$ charge, the CF₃ carbon shows just the opposite ($+0.9e$). The carbene carbons are similarly charged ($+0.3e$ in **8t** and $+0.2e$ in **1t**), implying that **1t** is unexpectedly somewhat less electron-deficient than **8t**, leading to a longer tunnelling half-life.

Another important aspect may be the differential sensitivity of the conformers to the host material^{35,37,43–49} and also to different matrix sites³⁰. The effect of noncovalent interactions on H-tunnelling processes was investigated primarily for conformational changes in carboxylic acids. For instance, the parent formic acid displays two conformers that differ by the orientation of the OH group with respect to the carbonyl oxygen⁵⁰. The higher-energy *E*-conformer can be prepared selectively through vibrational excitation of the *Z*-conformer in inert host materials, including noble gases, N₂ and para-hydrogen^{43,51}. *Z*- to *E*-conformer re-equilibration occurs through H-tunnelling rotamerizations.

Conclusions

Here, we present the first example of a conformer-specific [1,2]H-tunnelling process. This was demonstrated through the generation of a novel hydroxycarbene, namely trifluoromethylhydroxycarbene (**1**), whose *trans* (**1t**) and *cis* (**1c**, generated photochemically from **1t**) conformers behave very differently. The study presents the first preparation of a hydroxycarbene *cis* conformer (**1c**), prepared from photoisomerization of the *trans* form **1t**. While **1t** undergoes a [1,2]H-tunnelling shift at 10 K in solid Ar with a half-life of 144 ± 11 h (172 h, theoretical), **1c** remains unchanged over the same length of time. The intramolecular hydrogen bonding in **1c** is not responsible for this specificity as **1c** has about the same thermodynamic stability as **1t**. Rather, there does not seem to be a direct tunnelling path for **1c** to the aldehyde product (**2**). Owing to the large (26.4 kcal mol⁻¹ at CCSD(T)/cc-pVTZ) and wide barrier for the interconversion of **1c** to **1t**, the latter cannot effectively be replenished, and the Curtin–Hammett principle does not apply.

Methods

Matrix apparatus design. For the matrix isolation studies we used an APD Cryogenics HC-2 cryostat with a closed-cycle refrigerator system, equipped with an inner CsI window for infrared measurements. Spectra were recorded with a Bruker IFS 55 Fourier transform infrared spectrometer with a spectral range of 4,500–400 cm⁻¹ and a resolution of 0.7 cm⁻¹. For the combination of high-vacuum flash pyrolysis with matrix isolation, we employed a small, home-built, water-cooled oven, which was directly connected to the vacuum shroud of the cryostat. The pyrolysis zone consisted of an empty quartz tube with an inner diameter of 8 mm, which was resistively heated over a length of 50 mm by a coaxial wire. The temperature was monitored with a NiCr–Ni thermocouple. 3,3,3-Trifluoro-2-

oxopropanoic acid (received from Rare Chemicals Building Blocks) was evaporated at 20–24 °C from a storage bulb into the quartz pyrolysis tube. At a distance of ~50 mm, all pyrolysis products were co-condensed with a large excess of argon (typically 60–120 mbar from a 2,000 ml storage bulb) on the surface of the matrix window at 11 K (or at 20 K, see the Supplementary Information). Several experiments with pyrolysis temperatures ranging from 600 to 960 °C were performed to determine the optimal pyrolysis conditions. A high-pressure mercury lamp (HBO 200, Osram) with a monochromator (Bausch & Lomb) was used for irradiation.

Computations. All coupled cluster computations were carried out with the CFOUR⁵² program package. The structures were pre-optimized at the B3LYP/cc-pVTZ level using the Gaussian09 program package⁵³. All computed harmonic vibrational frequencies are unscaled. For more details, see Supplementary Information. Details on the WKB tunnelling computation are provided in the Supplementary Information.

Received 18 April 2016; accepted 9 September 2016;
published online 19 September 2016

References

- Assion, A. *et al.* Control of chemical reactions by feedback-optimized phase-shaped femtosecond laser pulses. *Science* **282**, 919–922 (1998).
- Kim, M. H., Shen, L., Tao, H., Martinez, T. J. & Suits, A. G. Conformationally controlled chemistry: excited-state dynamics dictate ground-state reaction. *Science* **315**, 1561–1565 (2007).
- Choi, K.-W., Ahn, D.-S., Lee, J.-H. & Kim, S. K. A highly conformationally specific α - and β -Ala⁺ decarboxylation pathway. *Chem. Commun.* 1041–1043 (2007).
- Zuev, P. S., Sheridan, R. S., Sauer, R. R., Moss, R. A. & Chu, G. Conformational product control in the low-temperature photochemistry of cyclopropylcarbenes. *Org. Lett.* **8**, 4963–4966 (2006).
- Khriachtchev, L. *et al.* Conformation-dependent chemical reaction of formic acid with an oxygen atom. *J. Phys. Chem. A* **113**, 8143–8146 (2009).
- Park, S. T., Kim, S. K. & Kim, M. S. Observation of conformation-specific pathways in the photodissociation of 1-iodopropane ions. *Nature* **415**, 306–308 (2002).
- Khriachtchev, L., Pettersson, M. & Räsänen, M. Conformational memory in photodissociation of formic acid. *J. Am. Chem. Soc.* **124**, 10994–10995 (2002).
- Ley, D., Gerbig, D. & Schreiner, P. R. Tunnelling control of chemical reactions—the organic chemist's perspective. *Org. Biomol. Chem.* **10**, 3781–3790 (2012).
- Kästner, J. Theory and simulation of atom tunneling in chemical reactions. *WIREs Comput. Mol. Sci.* **4**, 158–168 (2014).
- Borden, W. T. Reactions that involve tunneling by carbon and the role that calculations have played in their study. *WIREs Comput. Mol. Sci.* **6**, 20–46 (2016).
- Kohen, A., Cannio, R., Bartolucci, S. & Klinman, J. P. Enzyme dynamics and hydrogen tunnelling in a thermophilic alcohol dehydrogenase. *Nature* **399**, 496–499 (1999).
- Masgrau, L. *et al.* Atomic description of an enzyme reaction dominated by proton tunneling. *Science* **312**, 237–241 (2006).
- Layfield, J. P. & Hammes-Schiffer, S. Hydrogen tunneling in enzymes and biomimetic models. *Chem. Rev.* **114**, 3466–3494 (2014).
- Zuev, P. S. *et al.* Carbon tunneling from a single quantum state. *Science* **299**, 867–870 (2003).
- Schreiner, P. R. *et al.* Methylhydroxycarbene: tunneling control of a chemical reaction. *Science* **332**, 1300–1303 (2011).
- Ley, D., Gerbig, D., Wagner, J. P., Reisenauer, H. P. & Schreiner, P. R. Cyclopropylhydroxycarbene. *J. Am. Chem. Soc.* **133**, 13614–13621 (2011).
- Schreiner, P. R. *et al.* Capture of hydroxymethylene and its fast disappearance through tunnelling. *Nature* **453**, 906–909 (2008).
- Krueger, P. J. & Mettee, H. D. Spectroscopic studies of alcohols III. Fundamental OH stretching bands of 2,2-di- and 2,2,2-tri-haloethanols. *Can. J. Chem.* **42**, 340–346 (1964).
- Glendenning, E. D., Landis, C. R. & Weinhold, F. Natural bond orbital methods. *WIREs Comput. Mol. Sci.* **2**, 1–42 (2012).
- Bader, R. F. W. Atoms in molecules. *Acc. Chem. Res.* **18**, 9–15 (1985).
- Barbarich, T. J., Rithner, C. D., Miller, S. M., Anderson, O. P. & Strauss, S. H. Significant inter- and intramolecular O–H...F–C hydrogen bonding. *J. Am. Chem. Soc.* **121**, 4280–4281 (1999).
- Razavy, M. *Quantum Theory of Tunneling* (World Scientific, 2003).
- Ley, D., Gerbig, D. & Schreiner, P. R. Tunneling control of chemical reactions: C–H insertion versus H-tunneling in *tert*-butylhydroxycarbene. *Chem. Sci.* **4**, 677–684 (2013).
- Kästner, J. Path length determines the tunneling decay of substituted carbenes. *Chem. Eur. J.* **19**, 8207–8212 (2013).
- Seeman, J. I. Effect of conformational change on reactivity in organic chemistry. Evaluations, applications, and extensions of Curtin–Hammett/Winsten–Holness kinetics. *Chem. Rev.* **83**, 83–134 (1983).
- Oki, M. Reactivity of conformational isomers. *Acc. Chem. Res.* **17**, 154–159 (1984).

27. Amiri, S., Reisenauer, H. P. & Schreiner, P. R. Electronic effects on atom tunneling: conformational isomerization of monomeric *para*-substituted benzoic acid derivatives. *J. Am. Chem. Soc.* **132**, 15902–15904 (2010).
28. Pettersson, M., Maçõas, E. M. S., Khriachtchev, L., Fausto, R. & Räsänen, M. Conformational isomerization of formic acid by vibrational excitation at energies below the torsional barrier. *J. Am. Chem. Soc.* **125**, 4058–4059 (2003).
29. Reva, I., Nunes, C. M., Biczysko, M. & Fausto, R. Conformational switching in pyruvic acid isolated in Ar and N₂ matrices: spectroscopic analysis, anharmonic simulation, and tunneling. *J. Phys. Chem. A* **119**, 2614–2627 (2015).
30. Schreiner, P. R. *et al.* Domino tunneling. *J. Am. Chem. Soc.* **137**, 7828–7834 (2015).
31. Halasa, A. *et al.* Three conformers of 2-furoic acid: structure changes induced with near-IR laser light. *J. Am. Chem. Soc.* **119**, 1037–1047 (2015).
32. Domanskaya, A., Marushkevich, K., Khriachtchev, L. & Räsänen, M. Spectroscopic study of *cis*-to-*trans* tunneling reaction of HCOOD in rare gas matrices. *J. Chem. Phys.* **130**, 154509 (2009).
33. Mackenzie, R. B., Dewberry, C. T. & Leopold, K. R. The formic acid–nitric acid complex: microwave spectrum, structure, and proton transfer. *J. Phys. Chem. A* **118**, 7975–7985 (2014).
34. Tsuge, M. & Khriachtchev, L. Tunneling isomerization of small carboxylic acids and their complexes in solid matrices: a computational insight. *J. Chem. Phys. A* **119**, 2628–2635 (2015).
35. Maçõas, E. M. S., Khriachtchev, L., Pettersson, M., Fausto, R. & Räsänen, M. Rotational isomerism of acetic acid isolated in rare-gas matrices: effect of medium and isotopic substitution on IR-induced isomerization quantum yield and *cis*→*trans* tunneling rate. *J. Chem. Phys.* **121**, 1331–1338 (2004).
36. Maçõas, E. M. S. *et al.* Infrared-induced conformational interconversion in carboxylic acids isolated in low-temperature rare-gas matrices. *Vib. Spectrosc.* **34**, 73–82 (2004).
37. Pettersson, M. *et al.* *Cis*→*trans* conversion of formic acid by dissipative tunneling in solid rare gases: influence of environment on the tunneling rate. *J. Chem. Phys.* **117**, 9095–9098 (2002).
38. Bazsó, G., Góbi, S. & Tarczay, G. Near-infrared radiation induced conformational change and hydrogen atom tunneling of 2-chloropropionic acid in low-temperature Ar matrix. *J. Phys. Chem. A* **116**, 4823–4832 (2012).
39. Bazsó, G., Magyarfalvi, G. & Tarczay, G. Tunneling lifetime of the *ttc/Vjp* conformer of glycine in low-temperature matrices. *J. Phys. Chem. A* **116**, 10539–10547 (2012).
40. Bazsó, G., Najbauer, E. E., Magyarfalvi, G. & Tarczay, G. Near-infrared laser induced conformational change of alanine in low-temperature matrices and the tunneling lifetime of its conformer VI. *J. Phys. Chem. A* **117**, 1952–1962 (2013).
41. Gerbig, D. & Schreiner, P. R. Hydrogen-tunneling in biologically relevant small molecules: the rotamerizations of α -ketocarboxylic acids. *J. Phys. Chem. B* **119**, 693–703 (2015).
42. Alabugin, I. V., Gilmore, K. M. & Peterson, P. W. Hyperconjugation. *WIREs Comput. Mol. Sci.* **1**, 109–141 (2011).
43. Lopes, S., Domanskaya, A. V., Fausto, R., Räsänen, M. & Khriachtchev, L. Formic and acetic acids in a nitrogen matrix: enhanced stability of the higher-energy conformer. *J. Chem. Phys.* **133**, 144507 (2010).
44. Marushkevich, K., Khriachtchev, L., Lundell, J., Domanskaya, A. & Räsänen, M. Matrix isolation and *ab initio* study of *Trans-Trans* and *Trans-Cis* dimers of formic acid. *J. Chem. Phys. A* **114**, 3495–3502 (2010).
45. Marushkevich, K., Khriachtchev, L., Lundell, J. & Räsänen, M. *cis*-*trans* formic acid dimer: experimental observation and improved stability against proton tunneling. *J. Am. Chem. Soc.* **128**, 12060–12061 (2006).
46. Marushkevich, K., Khriachtchev, L. & Räsänen, M. Hydrogen bonding between formic acid and water: complete stabilization of the intrinsically unstable conformer. *J. Phys. Chem. A* **111**, 2040–2042 (2007).
47. Marushkevich, K., Khriachtchev, L. & Räsänen, M. High-energy conformer of formic acid in solid neon: giant difference between the proton tunneling rates of *cis* monomer and *trans*-*cis* dimer. *J. Chem. Phys.* **126**, 241102 (2007).
48. Marushkevich, K., Räsänen, M. & Khriachtchev, L. Interaction of formic acid with nitrogen: stabilization of the higher-energy conformer. *J. Phys. Chem. A* **114**, 10584–10589 (2010).
49. Tsuge, M., Marushkevich, K., Räsänen, M. & Khriachtchev, L. Infrared characterization of the HCOOH–CO₂ complexes in solid argon: stabilization of the higher-energy conformer of formic acid. *J. Phys. Chem. A* **116**, 5305–5311 (2012).
50. Pettersson, M., Lundell, J., Khriachtchev, L. & Räsänen, M. IR spectrum of the other rotamer of formic acid, *cis*-HCOOH. *J. Am. Chem. Soc.* **119**, 11715–11716 (1997).
51. Marushkevich, K., Khriachtchev, L. & Räsänen, M. High-energy conformer of formic acid in solid hydrogen: conformational change promoted by host excitation. *Phys. Chem. Chem. Phys.* **9**, 5748–5751 (2007).
52. CFOUR (Coupled-Cluster Techniques for Computational Chemistry) quantum chemical program package www.cfour.de/.
53. Gaussian09, Revision B.02 (Gaussian, 2009).

Acknowledgements

This work was supported by the Deutsche Forschungsgemeinschaft. The authors thank I. Alabugin and G. dos Passos Gomes (FSU Tallahassee) for discussions.

Author contributions

A.M. and P.R.S. conceived the experiments. A.M. performed the experiments and all data analysis. A.M. and H.Q. carried out all computations. All authors co-wrote the manuscript.

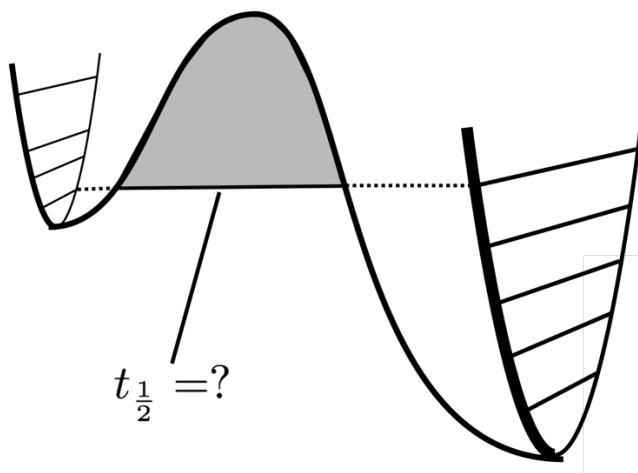
Additional information

Supplementary information is available in the online version of the paper. Reprints and permissions information is available online at www.nature.com/reprints. Correspondence and requests for materials should be addressed to P.R.S.

Competing financial interests

The authors declare no competing financial interests.

2.2 TUNNEX: An easy-to-use Wentzel-Kramers-Brillouin (WKB) implementation to compute tunneling half-lives



Tunneling in experiments (TUNNEX) is a free open-source program with an easy-to-use graphical user interface to simplify the process of Wentzel-Kramers-Brillouin (WKB) computations. TUNNEX aims at experimental chemists with basic knowledge of computational chemistry, and it offers the computation of tunneling half-lives, visualization of data, and exporting of graphs. It also provides a helper tool for executing the zero-point vibrational energy correction along the path. The program also enables computing high-level single points along the intrinsic reaction path. TUNNEX is available at <https://github.com/prs-group/TUNNEX>. As the WKB approximation usually overestimates tunneling half-lives, it can be used to screen tunneling processes before proceeding with elaborate kinetic experiments or higher-level tunneling computations such as instanton theory and small curvature tunneling approaches.

Reference

Henrik Quanz and Peter R. Schreiner TUNNEX: An easy-to-use Wentzel-Kramers-Brillouin (WKB) implementation to compute tunneling half-lives. *J Comput Chem*, **2018**, *40*, 543–547, (doi:10.1002/jcc.25711)

Reproduced with permission

License number: 5134671065328

© 2018, John Wiley and Sons, Inc.

111 River Street, MS 4-02

Hoboken, New Jersey, 07030-5774

United States of America



TUNNEX: An Easy-to-Use Wentzel-Kramers-Brillouin (WKB) Implementation to Compute Tunneling Half-Lives

Henrik Quanz and Peter R. Schreiner *

Tunneling in experiments (TUNNEX) is a free open-source program with an easy-to-use graphical user interface to simplify the process of Wentzel-Kramers-Brillouin (WKB) computations. TUNNEX aims at experimental chemists with basic knowledge of computational chemistry, and it offers the computation of tunneling half-lives, visualization of data, and exporting of graphs. It also provides a helper tool for executing the zero-point vibrational energy correction along the path. The program also enables computing high-level single points along the

intrinsic reaction path. TUNNEX is available at <https://github.com/prs-group/TUNNEX>. As the WKB approximation usually overestimates tunneling half-lives, it can be used to screen tunneling processes before proceeding with elaborate kinetic experiments or higher-level tunneling computations such as instanton theory and small curvature tunneling approaches. © 2018 Wiley Periodicals, Inc.

DOI:10.1002/jcc.25711

Introduction

Recent experimental findings^[1–5] imply that selectivity based on thermodynamic versus kinetic control is undermined by quantum mechanical tunneling (QMT) that can override this classic concept. The concept of a product that forms despite a high barrier that cannot be overcome (within finite time) at a given (low) temperature was termed “tunneling control,”^[5] and can be considered as the third paradigm of chemical reactivity next to kinetic and thermodynamic control.^[6] The first such example was reported only in 2011 with the hydrogen tunneling via a [1,2]H-shift of methylhydroxycarbene ($\text{H}_3\text{C}-\text{C}-\text{OH}$) to acetaldehyde ($\text{H}_3\text{C}-\text{CHO}$) through the *higher* barrier relative to the competing reaction of $\text{H}_3\text{C}-\text{C}-\text{OH}$ rearranging to vinyl alcohol ($\text{H}_2\text{C}=\text{CH}-\text{OH}$), the kinetic product.^[5] Despite the low temperature of the experiment (ca. 10 K in solid argon), facile tunneling with a half-life (τ) of only about 1 h entirely dominates the reactivity. Recent examples demonstrate^[7] that tunneling is not relevant to cryogenic temperatures, but also for reactions under ambient conditions.^[11]

Currently, the major challenge is to predict if tunneling control or simply tunneling will play a role for a particular reaction. Experimentally, QMT may reveal itself by higher than expected reaction rates, no or only little temperature dependence of the reaction rate, a large kinetic isotope effect, and a nonlinear Arrhenius plot. Still, there are no general predictive guidelines regarding the occurrence and relative importance of tunneling, and predictions currently solely rely on elaborate computations; these are often undertaken only after the (experimental) fact. These QMT computations involve calculating the intrinsic reaction path (IRP) connecting starting material and product, a projection of the reactive vibrational mode (and correction of the path) in 3N–7 dimensions (one mode is removed as a translational degree of freedom along the IRP toward the transition structure that has one imaginary frequency), determination of the attempt energy for the tunneling particle through the barrier at the zero-point vibrational energy (ZPVE) level, and finally

calculating the penetration integral. After some simple operations, this leads to τ .

Computing the IRP is a simple task and is available in many common quantum mechanical (QM) programs; even the computation of IRPs involving whole enzymes is nowadays possible.^[8] There are many comprehensive tools available to compute rates with tunneling corrections such as Polyrate,^[9] MultiWell,^[10–12] and Chemshell/DL-find^[13–15] as well as others, but they sometimes lack the simplicity of a simple graphical user interface (GUI) that would make them readily accessible for non-theoreticians (i.e., experimental chemists more likely to encounter unusually high reaction rates). The freely available GUI program presented here caters to this group.

Wentzel-Kramers-Brillouin (WKB)^[16–18] theory is often used together with mathematical scripts for the tasks described above. This somewhat cumbersome mix of approaches and tools motivated us to develop the TUNNEX (TUNNeling in EXperiments) program to simplify tunneling computations and to allow routine predictions of half-lives. In turn, we expect that experimentalists familiar with common QM software will employ TUNNEX to assess the possibility of QMT in their reactions. TUNNEX is designed to guide the user through the WKB computations by visualization of the energetic profile of the IRP and asking for the necessary parameter(s). TUNNEX aims at using data from QM/MM programs and currently works with simple text input file (txt) which will be extended in the near future.

TUNNEX is written mainly in C++ and makes use of the comprehensive Qt library to ensure a native look and feel on every supported platform. The source code is available for free,

H. Quanz, P. R. Schreiner
Institute of Organic Chemistry, Justus Liebig University Giessen, Heinrich-Buff-Ring 17, Giessen 35392, Germany
E-mail: prs@uni-giessen.de

This paper is dedicated to the memory of our colleague Keiji Morokuma.

© 2018 Wiley Periodicals, Inc.

making it easy to add new plugins and functionalities to the program.

General Features of TUNNEX

WKB theory

WKB theory attempts to solve the Schrödinger equation in the form of

$$\frac{d^2\psi(x)}{dx^2} + Q(x)\psi(x) = 0 \quad (1)$$

where

$$Q(x) = \frac{2m}{\hbar^2} (E - V(x)) \quad (2)$$

by transferring it to a Riccati differential equation for which solutions are known. This is done by substituting ψ with

$$\psi(x) = \exp\left(\int \frac{i}{\hbar} y(x) dx\right) \quad (3)$$

The resulting Riccati equation is then given by

$$\frac{i\hbar}{2m} \frac{dy(x)}{dx} - \frac{1}{2m} y^2(x) + E - V(x) = 0 \quad (4)$$

Because $\frac{y(x)}{dx}$ only contributes slightly with its small coefficient $\frac{\hbar}{2m}$, eq. 4 can be solved by an expansion around \hbar :

$$y = \sum_{\nu=0}^{\infty} \left(\frac{\hbar}{\nu!}\right)^{\nu} \cdot y_{\nu}(x) \quad (5)$$

Truncating the series at $\nu = 2$ in eq. 5 and only taking the terms with \hbar in 0th order yields:

$$\hbar^0 \left(E - V(x) - \frac{1}{2m} [y_0(x)]^2 \right) = 0 \quad (6)$$

which is solved to

$$y_0(x) = \pm \sqrt{2m(E - V(x))} \quad (7)$$

and from eq. 3:

$$\psi(x) = A \exp\left(\frac{i}{\hbar} \int \pm \sqrt{2m(E - V(x))} dx\right) \quad (8)$$

This is the simplest WKB solution for the Schrödinger equation for $\hbar \rightarrow 0$. Obviously, this solution shows a divergence, because it is divided by $\hbar \approx 0$. Therefore, solutions for $\hbar = 0, 1$, and 2 have to be included. The resulting transmission probability after solving the corresponding equation is then defined as:^[19]

$$T(E) = \frac{\exp(-2\sigma)}{\left(1 + \frac{1}{4} \exp(-2\sigma)\right)^2} \quad (9)$$

where $\sigma = \int_a^b \sqrt{-Q(x)} dx$.

In TUNNEX, we use the method of Miller and Good.^[20] In this method, the probability of a particle tunnel through a barrier is equal to

$$|T|^2 = \frac{1}{1 + \exp[2\theta(E)]} \quad (10)$$

in which

$$\theta(E) = \int_a^b \sqrt{2[V(x) - E]} dx \quad (11)$$

is known as the penetration integral and a and b are the turning points where a classical particle is reflected. This corresponds to the intersection of the attempt energy line with the IRP curve.

If the exponent is much larger 1, eq. 10 is reduced to

$$\ln(|T|^2) = -2 \int_{x_1}^{x_2} \sqrt{\frac{2m}{\hbar^2} [V(x) - E]} dx \quad (12)$$

which agrees with WKB's result in eq. 9 when $\sigma > 1$.

The Role of the Barrier Width

The penetration integral [eq. 11] can be rewritten to analyze the factors that contribute to the tunneling rate

$$\theta(E) = \sqrt{\frac{m}{\hbar^2}} \left(\frac{\pi}{\sqrt{8}}\right) w(E) (\sqrt{V_0 - E}) f(\alpha, \beta) \quad (13)$$

as done as in Ref.^[5]. V_0 is the potential barrier height connecting starting material and the transition state (TS), $w(E)$ the width of the barrier, and $f(\alpha, \beta)$ a dimensionless function. $f(\alpha, \beta)$ equals 1 for a truncated parabolic barrier, which coincides with the illustration of Borden et al.^[21] This leads to the conclusion that the barrier penetration integral depends on the product of three factors: the *barrier width* $w(E)$, the *activation energy* $\sqrt{V_0 - E}$, and the *mass* \sqrt{m} . Hence, the barrier width influences the penetration integral linearly whereas mass and activation energy are only considered as the square root. This means width dominates height, as noted before,^[22,23] and readily evident from the series of tunneling reactions of the hydroxycarbonyls, which all have a very similar activation energies (28–31 kcal mol⁻¹), but very different half-lives (1–144 h).^[6]

The GUI of TUNNEX

The GUI (Figure 2) was programmed using the Qt 5 libraries.^[24] The Qt-Project is open source and can be used under the GPL v3 and the LGPL v2.1 license. Qt provides an application programmable interface (API) and tools for building cross-platform applications.^[24] Currently, TUNNEX runs on Mac OS X (10.9 or higher), Windows (7 or higher) as well as on all Linux distributions offering a C++11 compiler (Fig. 1). QCustomPlot^[27] is employed for graphical depictions of the reaction paths needed for WKB, the ZPVE along the IRP, and for their combination. We prefer to use the reaction coordinate formulation of Fukui^[28,29] together with the Hessian-based predictor-corrector algorithm^[30–32] as implemented in, for example, Gaussian09 (and subsequent versions).

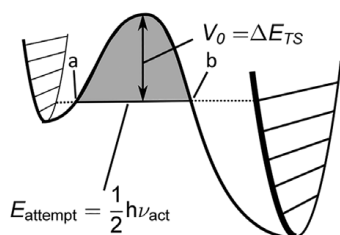


Figure 1. An illustration of the WKB approach. The black line represents the IRP ($V(x)$) and the gray area represents the integral.

Table 1. Benchmark results^[a] for tunneling half-lives of three hydrocarbenes computed at M06-2X/6-311++G(d,p).

Molecule	Without ZPVE	With ZPVE	Expt.
Methylhydroxycarbene ^[5]	1203 y	3 d	1 h
Phenylhydroxycarbene ^[25]	3401 y	5 d	3 h
Dihydroxycarbene ^[26]	6×10^6 y	353 y	— ^[b]

[a] The half-lives computed at the much more sophisticated CCSD(T) level of theory in combination with very large basis set extrapolations for methylhydroxycarbene and phenylhydroxycarbene are 1^[5] and 3 h^[28], respectively.
[b] Tunneling not observed.

To correct the IRP with the ZPVE at every single discretized gradient point, the user can choose a tab or comma separated file containing the reaction coordinate with the associated ZPVE. This file can be generated with a tool described below. The computations can also be performed without ZPVE correction resulting in half-lives that are generally much too high (Table 1). This procedure is advantageous to estimate whether a time-consuming frequency computation really is needed.

WKB also requires the attempt energy ν , that is, the frequency (in wavenumbers) corresponding to the reaction coordinate between stationary points on the potential energy surface, which turns into an imaginary frequency along the reaction path toward the TS. An easy method to identify the attempt energy is to inspect the eigenvalues of the projected Hessian matrix computations of the points near the starting material with the frequencies of the starting material side by side. The attempt frequency is then identified as the frequency of the starting material that is missing in the projected frequencies.

The algorithm employed in TUNNEX relies on the common agreement that the TS defines the zero of the reaction coordinate, with the starting material on the left (negative) and the product on the right (positive). This enables TUNNEX to take the energy and the ZPVE of the starting material straight from the IRP. In cases where the IRP does not fully connect to the starting material, the user can add the starting material energy and ZPVE manually. It is possible to save the “new” curve as a

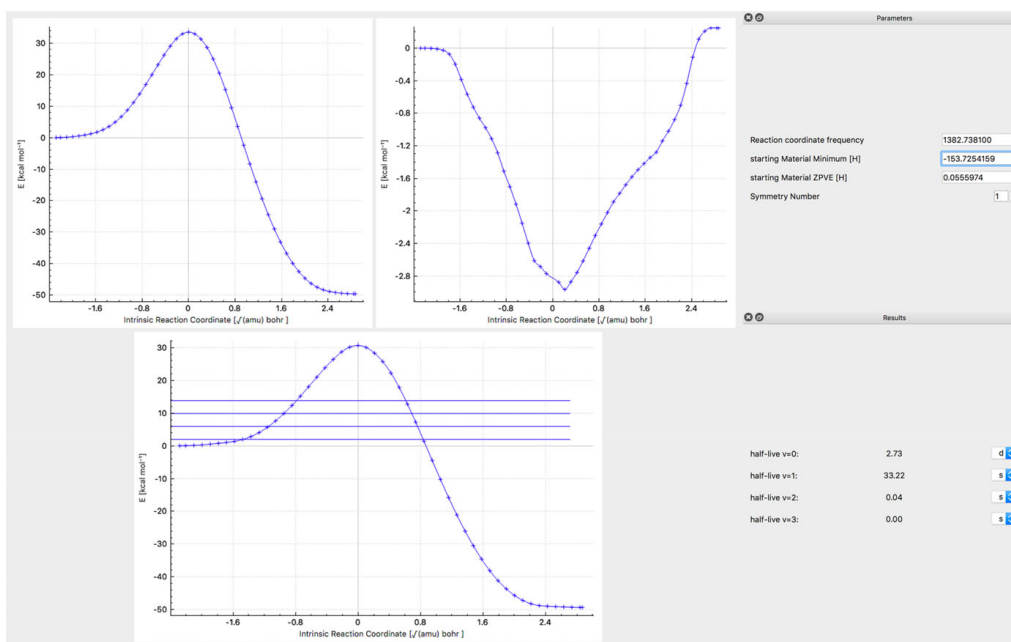


Figure 2. The GUI of TUNNEX. (Top) Display of the electronic IRP and the ZPVE curves. The combined IRP is automatically computed and displayed at the bottom. The user has to input the reactive mode and the energy of the starting material, and the tunneling half-life is computed automatically. [Color figure can be viewed at wileyonlinelibrary.com]

separate value table in a *tsv*-file. The computation can be saved into one xml file, which TUNNEX can read.

Obtaining the data

To extract data from quantum chemical programs, a small tool was written to support TUNNEX. Currently, it is possible to extract the coordinate to generate the input for the “projected frequency” (explained below) computation^[33] and to extract the energy as well as the reaction coordinate. At this time Gaussian09 and Gaussian16 are supported; other programs will follow.

The general workflow on how to compute the data is shown in Figure 3. First the TS is optimized, followed by a separate IRP computation to the product and starting material. Make_projection fuses these two computations into one single IRP. The second step requires the computation of the ZPVE, which is corrected by projecting the Hessian matrix on the tangent of the path, thus transferring one vibrational degree of freedom to a translational degree of freedom. We term the resulting computation the “projected frequencies.” Make_projection can help facilitate this otherwise work-intensive task and generates the input for the QM program. The last step includes a visual inspection of the starting material’s frequencies in order to obtain the attempt energy, which is the frequency that turns into an imaginary frequency along the IRP. Make_projection also provides a flexible interface to compute high-level single points on each point of the IRP.

Installation

The source code of Make_projection can be obtained from https://github.com/prs-group/make_projections. Make_projection needs to be compiled on the server where Gaussian is running. The compilation details and dependences are listed on the website. Make_projection guides the administrator through the configuration upon running Make_projection. The source code of TUNNEX is available at <https://github.com/prs-group/TUNNEX>. We also provide precompiled binaries for Windows, MacOS, and Linux Debian. For MacOS and Linux, a simple installer for popular packet management software will be provided in the future. Currently, auto update is not yet supported.

Algorithms. Third party libraries. TUNNEX uses the ALGLIB project library for spline interpolation.^[34] The ALGLIB project is a collection of numerical analysis tools, which comes in two different license terms (GPL and commercial). The GPL-licensed version delivers a full set of numerical functionalities but lacks the support for multithreaded applications. Due to the fact that most IRPs consist of less than 100 points, the speed of this library is sufficient and has been used for the implementation. In the case of WKB, the monotonic cubic Hermite interpolation was used.^[34] This type of spline is of the third-degree and very reliable, but lacks the accuracy of higher-order splines. Some tests with the Akima spline gave similar results.^[34] A simple cubic spline could not be used due to the instability with respect to outliers.

Root finding and integration. As shown in Figure 1, the integration starts at predefined points (a and b) located at the two

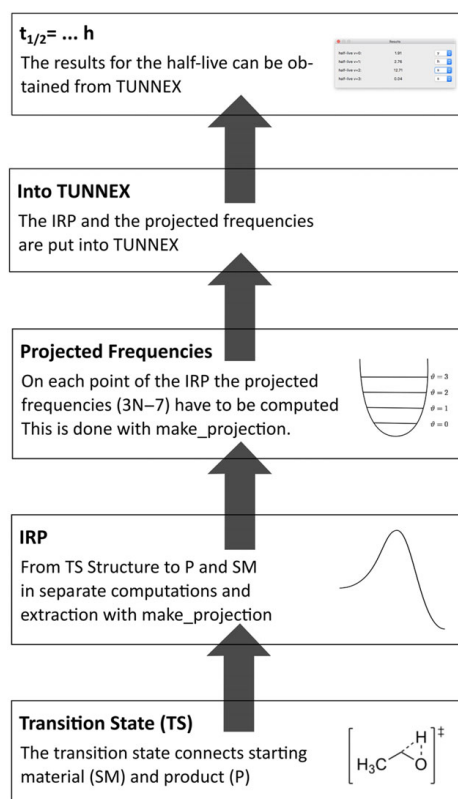


Figure 3. General workflow for WKB computations. The process starts at the bottom and continues stepwise to the top to yield the tunneling half-life. Make_projection is a helper tool to extract data from the QM computations and help facilitate the input generation of the “projected frequencies” on each point of the IRP. [Color figure can be viewed at wileyonlinelibrary.com]

intersections of the attempt energy curve and the IRP. The attempt energies are the vibrational states starting at $\nu = 0$. The energies are computed by using the attempt frequency as a reference point. Therefore, a root finding algorithm had to be included to find both intersections. This is done by bracketing of the roots between the TS and the product coordinate and vice versa for the starting material. A bisection method is then used to locate the root within an accuracy of 1×10^{-4} , which is enough for most potentials.^[35]

The integration between the obtained borders uses the so-called adaptive quadrature algorithm. This algorithm has been described by Gander and Gautschi.^[36] The basic idea behind this integration method is that one has numerical estimates of I_1 and I_2 for the integral

$$I = \int_a^b f(x) dx \quad (14)$$

Using the difference between I_1 and I_2 as an error estimate (ϵ), the answer to I would be I_1 if $I_1 - I_2 < \epsilon$. Otherwise, the integral is divided into two subintervals

$$I = \int_a^m f(x) dx + \int_m^b f(x) dx \quad (15)$$

where $m = (a + b)/2$. The subintervals are computed independently. The algorithm stops if the contribution to ϵ is sufficiently small^[4,10].

Conclusions and Outlook

We present an easy-to-use implementation of the WKB method to compute tunneling half-lives. WKB is a simple approximation that does not include corner-cutting effects like small-curvature tunneling or optimized tunneling paths as included in instanton theory. Therefore, all half-lives computed with this method are systematically too high. The advantage is its ease of use and simplicity. A drawback is the computation of the Hessian at each point of the IRP. If the generation of the IRP uses interpolated Hessians, the Hessian can be computed in parallel at each point. Another caveat of this method can be the mathematical failure for computing the projected frequency near the minima of the starting materials (division by a number nearing zero); the obtained ZPVE then is wrong. This issue is fixed by evaluating the amplitude of the gradient. If the gradient is small enough (10^{-3} Hartree Bohr⁻¹) the reactive mode is not projected. This is implemented in Gaussian16.

In the future, TUNNEX will include a ssh interface to send and receive data; the Make_projection source code will be included as well. To overcome the computation of the Hessian at each point, an interpolation algorithm will be implemented. TUNNEX should also provide an interface to generate the input for standard kinetic suites like POLYRATE. The support for more QM/MM programs will be added in the near future. Customization of the style of the plots is going to be added soon.

Acknowledgment

The authors thank Dr. D. Gerbig and A. K. Eckhardt for fruitful discussions and the Hessische Kompetenzzentrum für Hochleistungsrechner (HPC) for computational hardware support.

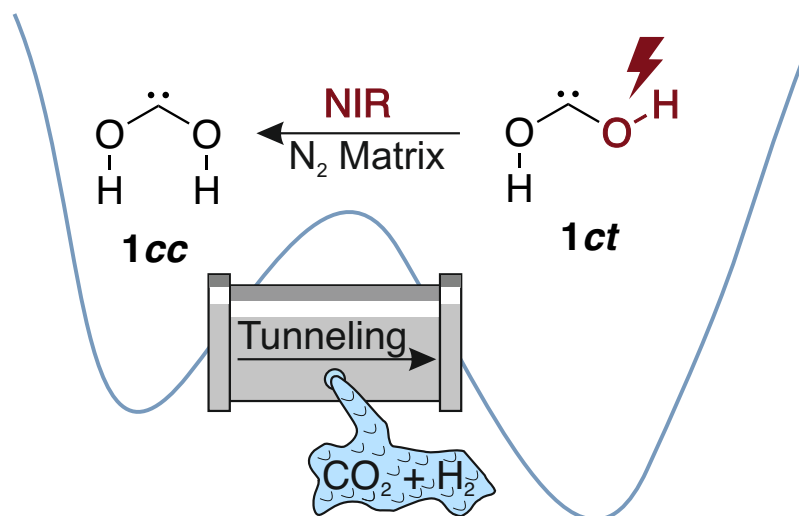
Keywords: kinetics · GUI · tunneling · tunneling control

How to cite this article: H. Quanz, P. R. Schreiner. *J. Comput. Chem.* **2018**, 9999, 1–5. DOI: 10.1002/jcc.25711

- [1] M. Schäfer, K. Peckelsen, M. Paul, J. Martens, J. Oomens, G. Berden, A. Berkessel, A. J. Meijer, *J. Am. Chem. Soc.* **2017**, 139, 5779.
- [2] A. Mardyukov, H. Quanz, P. R. Schreiner, *Nat. Chem.* **2017**, 9, 71.
- [3] D. Gerbig, P. R. Schreiner, *Angew. Chem.* **2017**, 129, 9573.
- [4] C. M. Nunes, S. N. Knezz, I. Reva, R. Fausto, R. J. McMahon, *J. Am. Chem. Soc.* **2016**, 138, 15287.
- [5] P. R. Schreiner, H. P. Reisenauer, D. Ley, D. Gerbig, C.-H. Wu, W. D. Allen, *Science* **2011**, 332, 1300.
- [6] P. R. Schreiner, *J. Am. Chem. Soc.* **2017**, 139, 15276.
- [7] A. Nandi, D. Gerbig, P. R. Schreiner, W. T. Borden, S. Kozuch, *J. Am. Chem. Soc.* **2017**, 139, 9097.
- [8] Y. Zheng, W. Thiel, *J. Org. Chem.* **2017**, 82, 13563.
- [9] J. Zheng, S. Zhang, B. J. Lynch, J. C. Corchado, Y.-Y. Chuang, P. L. Fast, W.-P. Hu, Y.-P. Liu, G. C. Lynch, K. A. Nguyen, C. F. Jackels, A. F. Ramos, B. A. Ellingson, V. S. Melissas, J. Villa, I. Rossi, E. L. Coitipo, J. Pu, T. V. Albu, Polyrate, Ver. 17b, University of Minnesota, Minneapolis, **2017**. <https://comp.chem.umn.edu/polyrate/>.
- [10] J. R. Barker, *Int. J. Chem. Kinet.* **2001**, 33, 232.
- [11] J. R. Barker, *Int. J. Chem. Kinet.* **2009**, 41, 748.
- [12] J. R. Barker, N. F. Ortiz, J. M. Preses, L. L. Lohr, A. Maranzana, P. J. Stimac, Mutiwell Ver. 2017ab, 2017. Available at <http://clasp-research.engin.umich.edu/multiwell/?url=multiwell/>
- [13] J. B. Rommel, T. P. M. Goumans, J. Kästner, *J. Chem. Theory Comput.* **2011**, 7, 690.
- [14] J. B. Rommel, J. Kästner, *J. Phys. Chem.* **2011**, 134, 184107.
- [15] J. Kästner, *WIREs Comput. Mol. Sci.* **2013**, 4, 158.
- [16] G. Wentzel, *Z. Phys.* **1926**, 38, 518.
- [17] H. A. Kramers, *Z. Phys.* **1926**, 39, 828.
- [18] L. C. R. Brillouin, *Acad. Sci.* **1926**, 183, 24.
- [19] M. Razavy, *Quantum Theory of Tunneling*, World Scientific Publishing Co. Pte. Ltd., Singapore, **2003**.
- [20] S. C. Miller, R. H. Good, *Phys. Rev.* **1953**, 91, 174.
- [21] W. T. Borden, *WIREs Comput. Mol. Sci.* **2016**, 6, 20.
- [22] B. K. Carpenter, *J. Am. Chem. Soc.* **1983**, 105, 1700.
- [23] B. K. Carpenter, *Science* **2011**, 332, 1269.
- [24] Qt Project Hosting, Qt Project. <https://www.qt.io/developers/> (accessed February 20, 2018).
- [25] D. Gerbig, H. P. Reisenauer, C.-H. Wu, D. Ley, W. D. Allen, P. R. Schreiner, *J. Am. Chem. Soc.* **2010**, 132, 7273.
- [26] P. R. Schreiner, H. P. Reisenauer, *Angew. Chem. Int. Ed.* **2008**, 47, 7071.
- [27] Emanuel Eichhammer, Qt Plotting Widget QCustomPlot. <http://www.qcustomplot.com> (accessed February 22, 2018).
- [28] K. Fukui, *Acc. Chem. Res.* **1981**, 14, 363.
- [29] K. Fukui, *J. Phys. Chem.* **1970**, 74, 4161.
- [30] H. P. Hratchian, H. B. Schlegel, *J. Chem. Theory Comput.* **2005**, 1, 61.
- [31] H. P. Hratchian, H. B. Schlegel, *J. Phys. Chem.* **2004**, 120, 9918.
- [32] R. Z. Bulirsch, J. Stoer, *Numer. Math.* **1966**, 8, 1.
- [33] A. G. Baboul, H. B. Schlegel, *J. Phys. Chem.* **1997**, 107, 9413.
- [34] ALGLIB Project, ALGLIB—numerical analysis library. <http://www.alglib.net> (accessed February 20, 2018).
- [35] W. H. Press, S. A. Teukolsky, W. T. Vetterling, B. P. Flannery, *Numerical Recipes*, 3rd ed., Cambridge University Press, New York, **2007**.
- [36] W. Gander, W. Gautschi, *BIT Numer. Math.* **2000**, 40, 84.

Received: 31 May 2018
Revised: 31 August 2018
Accepted: 21 September 2018

2.3 Identification and reactivity of *s-cis,s-cis*-dihydroxycarbene, a new [CH₂O₂] intermediate



Abstract: We report the first preparation of the *s-cis,s-cis* conformer of dihydroxycarbene (**1cc**) by means of pyrolysis of oxalic acid, isolation of the lower-energy *s-trans,s-trans* (**1tt**) and *s-cis,s-trans* (**1ct**) product conformers at cryogenic temperatures in a N₂ matrix, and subsequent narrow-band near-infrared (NIR) laser excitation to give **1cc**. Carbene **1cc** converts quickly to **1ct** via quantum-mechanical tunneling with an effective half-life of 22 min at 3 K. The potential energy surface features around **1** were pinpointed by convergent focal point analysis targeting the AE-CCSDT(Q)/CBS level of electronic structure theory. Computations of the tunneling kinetics confirm the time scale of the **1cc** → **1ct** rotamerization and suggest that direct **1cc** → H₂ + CO₂ decomposition may also be a minor pathway. The intriguing latter possibility cannot be confirmed spectroscopically, but hints of it may be present in the measured kinetic profiles.

Reference

Henrik Quanz, Bastian Bernhardt, Frederik E. Erb, Marcus A. Bartlett, Wesley D. Allen, Peter R Schreiner Identification and Reactivity of *s-cis,s-cis*-Dihydroxycarbene, a New [CH₂O₂] Intermediate. *J Am Chem Soc.* **2020**, *142*, 19457–19461. (doi:10.1021/jacs.0c09317)

Underline denotes the first author

Reprinted (adapted) with permission

© 2020, American Chemical Society
1155 16th Street NW
Washington, DC, 20036
United States of America

Identification and Reactivity of *s-cis,s-cis*-Dihydroxycarbene, a New [CH₂O₂] Intermediate

Henrik Quanz,^{||} Bastian Bernhardt,^{||} Frederik R. Erb, Marcus A. Bartlett, Wesley D. Allen,^{*} and Peter R. Schreiner^{*}



Cite This: *J. Am. Chem. Soc.* 2020, 142, 19457–19461



Read Online

ACCESS |

Metrics & More

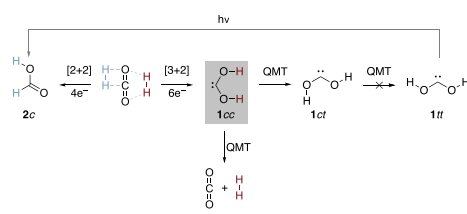
Article Recommendations

Supporting Information

ABSTRACT: We report the first preparation of the *s-cis,s-cis* conformer of dihydroxycarbene (*1cc*) by means of pyrolysis of oxalic acid, isolation of the lower-energy *s-trans,s-trans* (*1tt*) and *s-cis,s-trans* (*1ct*) product conformers at cryogenic temperatures in a N₂ matrix, and subsequent narrow-band near-infrared (NIR) laser excitation to give *1cc*. Carbene *1cc* converts quickly to *1ct* via quantum-mechanical tunneling with an effective half-life of 22 min at 3 K. The potential energy surface features around *1* were pinpointed by convergent focal point analysis targeting the AE-CCSDT(Q)/CBS level of electronic structure theory. Computations of the tunneling kinetics confirm the time scale of the *1cc* → *1ct* rotamerization and suggest that direct *1cc* → H₂ + CO₂ decomposition may also be a minor pathway. The intriguing latter possibility cannot be confirmed spectroscopically, but hints of it may be present in the measured kinetic profiles.

The fundamental chemistry of the [CH₂O₂] system is paramount to the grand challenges of energy storage and transportation as well as control of global warming. Moreover, as highly abundant molecules in space, H₂ and CO₂ may provide access to simple organic molecules in the atmosphere of prebiotic earth and extraterrestrial environments.^{1–3} Although the direct reduction of CO₂ with H₂ has a prodigious activation barrier (>80 kcal mol⁻¹), McCarthy et al.⁴ formed both *s-cis,s-trans*-dihydroxycarbene (*1ct*) (Scheme 1) and *s-*

Scheme 1. Formal Electrocyclic Reactions of H₂ + CO₂ Leading to *s-cis,s-cis*-Dihydroxycarbene (*1cc*), *s-cis*-Formic Acid (*2c*), and the Lower-Lying Rotamers of *1*



trans-formic acid (*2t*) by electric discharge of gaseous H₂ + CO₂ mixtures. This alternative route complements our original synthesis of *1ct* and *s-trans,s-trans*-dihydroxycarbene (*1tt*) based on pyrolysis of oxalic acid.⁵

The formation of *1* and subsequently *2* from H₂ + CO₂ potentially plays a role in the origin of life by trapping of H₂ from volcanic or other origins before its rapid escape into the atmosphere.⁶ As *2* is present in volcanic eruptions and black smokers,⁷ one viable route may involve *1* as a reactive intermediate. In a different vein, we have shown recently that

hydroxycarbenes react with carbonyl compounds to form sugars in the gas phase.⁸ Analogously, *1* may be a C₁ building block for amino acids through its reactions with imines.

In contrast to most hydroxycarbenes, at cryogenic temperatures *1* does not undergo a [1,2]-H shift via quantum-mechanical tunneling (QMT) to the associated carbonyl product⁹ *2* because strong oxygen lone-pair electron donation increases the accompanying barrier.⁴ Of the three possible dihydroxycarbene rotamers,¹⁰ *1tt* and *1ct* have been identified spectroscopically,^{4,5,11} but the higher-energy species *s-cis,s-cis*-dihydroxycarbene (*1cc*) has not been reported. Here we isolate and spectroscopically characterize *1cc*, document its conformational QMT to *1ct*, and explore the possibility of its direct dissociation into H₂ + CO₂ at very low temperatures.

The direct formation of *1* from H₂ and CO₂⁴ seems feasible only through the *1cc* rotamer, elevating the need to fully characterize this species. While *2c* is 44.6 kcal mol⁻¹ lower in energy than *1cc* (Figure 1), the activation barriers to form *1* and *2* from H₂ + CO₂ differ by less than 8 kcal mol⁻¹. Although the formation of *2* is formally a thermally forbidden^{12,13} four-electron [2 + 2] cycloaddition,^{14,15} it is kinetically favored in the absence of QMT over the allowed six-electron [3 + 2] reaction to give *1cc* (Scheme 1). However, the situation might change when QMT is taken into account, as this phenomenon leads to increased reaction rates, i.e., effectively lower activation barriers. The possible involvement of *1* in fundamental [CH₂O₂] chemistry has long been

Received: August 30, 2020

Published: November 9, 2020



ACS Publications

© 2020 American Chemical Society

19457

<https://dx.doi.org/10.1021/jacs.0c09317>
J. Am. Chem. Soc. 2020, 142, 19457–19461

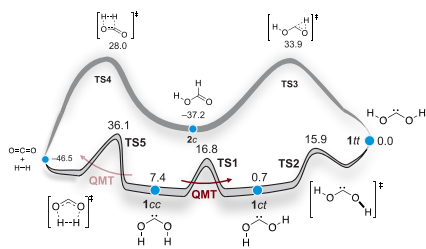
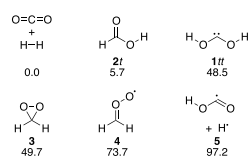


Figure 1. Pictorial presentation (not drawn to scale) of the converged FPA relative energies (ΔH_0 , in kcal mol⁻¹) of key species connected to **1**. Details of the computations are given in the SI.

Scheme 2. Relative Energies of the Experimentally Identified Species (Lowest-Energy Conformers) on the [CH₂O₂] Potential Energy Surface (Computed FPA Relative Energies Are Given in kcal mol⁻¹)



overlooked, as studies have mostly emphasized the Criegee intermediate **4**^{16,17} and dioxirane **3**,¹⁸ which are actually *higher* in energy (Scheme 2).

Here we follow our established route employing high-vacuum flash pyrolysis (HVFP) of oxalic acid (**6**) to first produce and trap **1tt** and **1ct** in a N₂ matrix at 3 K.⁵ To generate **1cc**, **1tt** and **1ct** were prepared first and then selectively irradiated with near-infrared (NIR) light from a narrow-band optical parametric oscillator (OPO) laser. Similar strategies have been used to detect higher-lying rotamers of other matrix-isolated compounds (e.g., formic acid).^{19–22} New electronic structure computations employing focal point analysis (FPA)^{23–27} were executed to obtain definitive energetics for the potential energy surface (PES) surrounding **1** (Figure 1) at the composite AE-CCSD(T)/CBS//AE-CCSD(T)^{28–32}/aug-cc-pCVTZ³³ level of theory.^{34,35} Tunneling half-lives were computed using both AE-CCSD(T)/aug-cc-pCVTZ reaction paths conjoined with the Wentzel–Kramers–Brillouin (WKB) method^{36–39} as well as density functional theory (DFT)^{40–46} curves treated with small-curvature tunneling (SCT) canonical variational theory (CVT).^{47,48}

In our optically transparent matrices resulting from deposition of the pyrolysis products on a cold window, selective vibrational excitation of **1tt** at 7026 ± 4 cm⁻¹ gave **1ct** (Figures S2 and S3), while the back reaction was initiated with NIR irradiation at 6542 ± 4 cm⁻¹ (Figure S3). After NIR irradiation at either of these two absorptions, we also observed new IR bands that vanished over the course of 1.5 h when the matrix was kept in the dark (Figure S4). We assigned these bands to the **1cc** conformer with the help of VPT2//AE-CCSD(T)/aug-cc-pCVTZ^{49,50} vibrational frequency computations (Figure 2); full details of the assignments, including total energy distributions,^{51–53} can be found in Table S3. The

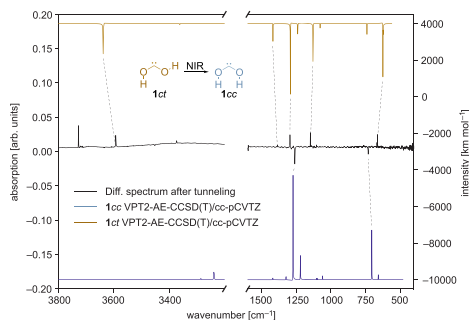


Figure 2. Dihydroxycarbene rotamers **1cc** and **1ct** identified in a N₂ matrix at 3 K. Bottom and top traces: computed VPT2//AE-CCSD(T)/aug-cc-pCVTZ spectra of **1cc** and **1ct**, respectively. Middle trace: difference spectrum obtained from spectra recorded before and after the matrix was irradiated at 7026.0 ± 4 cm⁻¹ (**1ct** band) for 15 min and then at 6542 ± 4 cm⁻¹ (**1cc** band) for 15 min and then kept in the dark for 1.5 h. The full spectrum is shown in Figure S4.^{54–56}

multireference character of **TS4** and **TS5** is marginal (cf. Chapter 4.3 in the Supporting Information (SI)).²⁵

While the bands of **1cc** vanished, the bands of **1ct** simultaneously grew. Because the barrier for this conformational interconversion is 9.4 kcal mol⁻¹ (Figure 1), QMT must be operative for this reaction to occur at 3 K. The disappearance of **1cc** over time (Figure 3) was monitored at

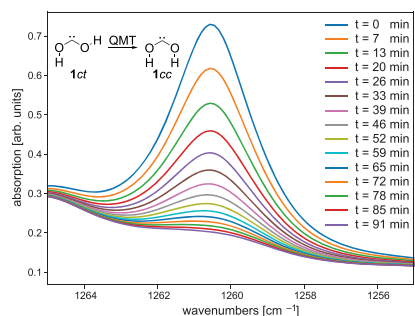


Figure 3. Temporal decay of the most intense IR band (1260.2 cm⁻¹) of **1cc** over 138 min at 3.0 K in a N₂ matrix. Spectra were taken every 98 s with a 4.5 μm low-pass filter in front of the matrix to avoid photoreactions caused by the spectrometer global source. For clarity, only every fourth trace is shown. The temporal profile of the **1cc** band at 730.1 cm⁻¹ is shown in Figure S5.^{54–56}

different temperatures, and our kinetic analyses revealed effective tunneling half-lives in the 17–22 min range over the 3–20 K interval (Table 1). The relative insensitivity of the reaction rate to temperature is also indicative of QMT.

In solid Ar and Ne matrices, we could interconvert **1tt** and **1ct** by NIR irradiation, but the **1cc** rotamer remained undetected (Figures S7–S11). However, the bands of **1ct** could not be depleted completely even after prolonged irradiation, which might hint that **1cc** formed but has an inherent lifetime of less than 2 min in these environments. Our

Table 1. Tunneling Kinetics of *s-cis,s-cis*-Dihydroxycarbene (1cc) in a N₂ Matrix^a

T/K	τ_{ct}/h	τ_{leak}/h	τ_{eff}/h^b	leak fraction	initial 1cc:1ct population ratio
3.0	0.331(1)	0.78(10)	0.363	0.13(2)	2.797(3)
7.5	0.331(1)	0.73(9)	0.359	0.14(3)	2.106(3)
12.5	0.312(1)	0.48(12)	0.325	0.10(7)	3.483(3)
15.0	0.307(1)	0.82(22)	0.331	0.09(3)	4.255(5)
20.0	0.278(1)	0.35(7)	0.291	0.19(18)	3.133(3)

^aStandard errors of the least-squares fits are shown in parentheses in multiples of the last significant digit. See the text and SI for a description of the fitting parameters. ^b τ_{eff} = effective half-life for overall 1cc decay.

best theoretical prediction for the 1cc \rightarrow 1ct tunneling half-life in the gas phase is 1.2 min, which was derived as follows: (a) uniform scaling of the optimized AE-CCSD(T)/aug-cc-pCVTZ potential energy curve (Table S30) by 1.024 to reproduce the converged FPA rotamerization barrier; (b) WKB evaluation of the tunneling half-life on this scaled curve; and (c) application of the SCT correction factor of 0.0363 given by the B3LYP/cc-pVTZ level of theory (Table S29). The resulting prediction is consistent with both the observed lack of 1cc bands in the Ar and Ne matrices and the measured 1cc half-life of 17–22 min in solid N₂, whose appreciable polarizability is known to stabilize reactive intermediates. Khriachtchev et al. reported a similar stabilization of the high-lying HOCO-conformer in N₂.¹⁹ To investigate this effect, we computed N₂ complexes of all three rotamers of 1 (SI Chapter 4.2), similar to those reported for formic acid.²⁰ The AE-CCSD(T)/aug-cc-pCVTZ-optimized complexes display O–H \cdots N₂ interactions that yield binding energies of 1.2–1.8 kcal mol⁻¹ and vibrational frequency shifts as large as 63 cm⁻¹. Such substantial interactions are also evidenced in the experimental IR spectra of 1ct and 1tt, as both species display an O–H stretching frequency in N₂ that differs from the corresponding value in solid Ne (Tables S11 and S12) by almost 60 cm⁻¹.

The QMT kinetics from 3 to 20 K was analyzed by means of a simultaneous nonlinear least-squares fit of two 1cc and three 1ct high-quality IR bands (Table 1). The simplest integrated rate equations capable of accurately fitting the entirety of the kinetic data for 1cc decay and 1ct growth required four adjustable parameters: the rotamerization half-life (τ_{ct}), the 1cc:1ct initial population ratio, a half-life for alternative 1cc decay (τ_{leak}), and a branching fraction for such secondary leaking. Unlike the cases of carbonic⁵⁷ and oxalic acid,⁵⁸ no evidence of frozen molecules or distinct fast and slow conformational tunneling was found. Figures S19–S28 show that if the rate constants for 1cc decay and 1ct growth are set equal to one another, the spectral data cannot be fit precisely, revealing the necessity of the “leak” component. As shown in Table 1, leaking is responsible for roughly 10% of the decay, which is too small to allow the parameters for this unknown process to be pinned down to a high degree. Nonetheless, we believe that the kinetic profiles provide compelling evidence for a secondary, minor process of decay with a half-life less than but on the same order of magnitude as τ_{ct} .

One candidate for the leaking process is suggested by our CVT/SCT tunneling computations (Tables S29–S33) at several levels of theory, including CCSD(T)/aug-cc-pVTZ//B2-PLYP/aug-cc-pVTZ. To wit, the rate for the direct 1cc \rightarrow H₂ + CO₂ decomposition is in the same time regime as the

rotamerization, in agreement with the kinetic analysis. Neither product can be monitored in our experiments because the CO₂ concentration after pyrolysis exceeds our spectrometer limits and H₂ is not IR-active. Continuously populating 1cc by laser irradiation of the other rotamers should lead to overall depletion of 1 to form H₂ and CO₂, but this was not observed after 5 h (Figure S6).

We attempted to probe the behavior of the dideuterated species ²H₂-1 originating from the pyrolysis of ²H₂-oxalic acid⁵ in order to further characterize 1cc and its tunneling decay (which should be quenched by dideuteration). However, bands of ²H₂-1cc were not observed after NIR excitation because the energy of the O–²H overtone of ²H₂-1tt is barely too low (5258 cm⁻¹ = 15.0 kcal mol⁻¹) to overcome the rotamerization barriers (1tt \rightarrow 1ct = 15.9 and 1ct \rightarrow 1cc = 16.1 kcal mol⁻¹).

We tried to prepare monodeuterated 1 through ester pyrolysis of several suitable precursors⁵⁹ (Scheme S1), hoping to use the OH group as an NIR antenna for remote rotamerization.⁶⁰ This would have allowed an indirect probe of the leak process because the heavier ²H-1cc isotopomer could not dissociate by QMT while rotamerization would still occur at approximately 50% of the rate of the parent molecule. However, in all of our attempts the carbene yield was too low through this alternative generation method (see the SI for details).

To conclude, we have isolated and characterized in solid N₂ the higher-lying *s-cis,s-cis* rotamer of dihydroxycarbene, which may be the missing link in the reduction of CO₂ with H₂ to form 1ct⁴ and subsequently formic acid. The 1cc species rapidly rotamerizes even at 3 K and could be identified only in stabilizing N₂ rather than noble gas cryogenic environments. A secondary QMT pathway involving dissociation of 1cc to H₂ + CO₂ is plausible according to theory and might be responsible for the biexponential characteristics measured in our decay profiles.

■ ASSOCIATED CONTENT

Supporting Information

The Supporting Information is available free of charge at <https://pubs.acs.org/doi/10.1021/jacs.0c09317>.

Full-matrix IR spectra after pyrolysis of 6 in N₂, Ar, and Ne; full matrix IR spectra after irradiation with NIR light in N₂, Ar, and Ne; full assignments of 1 in Ne and N₂; full PES around 1 at the FPA//AE-CCSD(T)/aug-cc-pCVTZ level of theory; geometries with all important bond lengths and angles; Cartesian coordinates of all molecules on the PES; detailed results of tunneling computations; details of the kinetic analysis; description of attempts to generate ²H₁-1 (PDF)

■ AUTHOR INFORMATION

Corresponding Authors

Peter R. Schreiner – Institute of Organic Chemistry, Justus Liebig University, D-35392 Giessen, Germany; orcid.org/0000-0002-3608-5515; Email: prs@uni-giessen.de

Wesley D. Allen – Center for Computational Quantum Chemistry and Department of Chemistry, University of Georgia, Athens, Georgia 30602, United States; Allen Heritage Foundation, Dickson, Tennessee 37055, United States; Email: wballen@uga.edu

Authors

Henrik Quanz – Institute of Organic Chemistry, Justus Liebig University, D-35392 Giessen, Germany

Bastian Bernhardt – Institute of Organic Chemistry, Justus Liebig University, D-35392 Giessen, Germany; orcid.org/0000-0002-7734-6427

Frederik R. Erb – Institute of Organic Chemistry, Justus Liebig University, D-35392 Giessen, Germany

Marcus A. Bartlett – Center for Computational Quantum Chemistry and Department of Chemistry, University of Georgia, Athens, Georgia 30602, United States

Complete contact information is available at:
<https://pubs.acs.org/10.1021/jacs.0c09317>

Author Contributions

[†]H.Q. and B.B. contributed equally.

Notes

The authors declare no competing financial interest.

ACKNOWLEDGMENTS

We thank Dennis Gerbig for maintaining our computer clusters and André K. Eckhardt and Hans P. Reisenauer for fruitful discussions. B.B. thanks the Bayer Fellowship Program and the Deutscher Akademischer Austauschdienst for financial support during a research visit at the University of Georgia and the Fonds der Chemischen Industrie for a doctoral scholarship. This work was supported by the Volkswagen Foundation (“What is Life” Grant 92 748 to P.R.S.).

REFERENCES

- Tian, F.; Toon, O. B.; Pavlov, A. A.; De Sterck, H. A Hydrogen-Rich Early Earth Atmosphere. *Science* **2005**, *308*, 1014–1017.
- Kasting, J. F. Earth's early atmosphere. *Science* **1993**, *259*, 920–926.
- Herbst, E. The chemistry of interstellar space. *Chem. Soc. Rev.* **2001**, *30*, 168–176.
- Womack, C. C.; Crabtree, K. N.; McCaslin, L.; Martinez, O.; Field, R. W.; Stanton, J. F.; McCarthy, M. C. Gas-Phase Structure Determination of Dihydroxycarbene, One of the Smallest Stable Singlet Carbenes. *Angew. Chem. Int. Ed.* **2014**, *53*, 4089–4092.
- Schreiner, P. R.; Reisenauer, H. P. Spectroscopic Identification of Dihydroxycarbene. *Angew. Chem. Int. Ed.* **2008**, *47*, 7071–7074.
- Jeans, J. *The Dynamical Theory of Gases*; Cambridge University Press: London, 1916; Vol. 1, p 436.
- Allen, A. G.; Baxter, P. J.; Ottley, C. J. Gas and particle emissions from Soufrière Hills Volcano, Montserrat, West Indies: characterization and health hazard assessment. *Bull. Volcanol.* **2000**, *62*, 8–19.
- Eckhardt, A. K.; Linden, M. M.; Wende, R. C.; Bernhardt, B.; Schreiner, P. R. Gas-phase sugar formation using hydroxymethylene as the reactive formaldehyde isomer. *Nat. Chem.* **2018**, *10*, 1141–1147.
- Schreiner, P. R. Tunneling Control of Chemical Reactions: The Third Reactivity Paradigm. *J. Am. Chem. Soc.* **2017**, *139*, 15276–15283.
- Feller, D.; Borden, W. T.; Davidson, E. R. A theoretical study of paths for decomposition and rearrangement of dihydroxycarbene. *J. Comput. Chem.* **1980**, *1*, 158–166.
- Broderick, B. M.; McCaslin, L.; Moradi, C. P.; Stanton, J. F.; Douberly, G. E. Reactive intermediates in ⁴He nanodroplets: Infrared laser Stark spectroscopy of dihydroxycarbene. *J. Chem. Phys.* **2015**, *142*, 144309–144316.
- Hutschka, F.; Dedieu, A.; Leitner, W. Metathesis as a Critical Step for the Transition Metal Catalyzed Formation of Formic Acid from CO₂ and H₂? An Ab Initio Investigation. *Angew. Chem. Int. Ed. Engl.* **1995**, *34*, 1742–1745.
- Steigerwald, M. L.; Goddard, W. A., III The 2₂ + 2₂ Reactions at Transition Metals. 1. The Reactions of D₂ with Cl₂TiH⁺, Cl₂TiH, and Cl₂SCH. *J. Am. Chem. Soc.* **1984**, *106*, 308–311.
- Woodward, R. B.; Hoffmann, R. The Conservation of Orbital Symmetry. *Angew. Chem. Int. Ed. Engl.* **1969**, *8*, 781–853.
- Woodward, R. B.; Hoffmann, R. Stereochemistry of Electrocyclic Reactions. *J. Am. Chem. Soc.* **1965**, *87*, 395–397.
- Taatjes, C. A.; Meloni, G.; Selby, T. M.; Trevitt, A. J.; Osborn, D. L.; Percival, C. J.; Shallcross, D. E. Direct Observation of the Gas-Phase Criegee Intermediate (CH₂OO). *J. Am. Chem. Soc.* **2008**, *130*, 11883–11885.
- Wadt, W. R.; Goddard, W. A., III Electronic structure of the Criegee intermediate. Ramifications for the mechanism of ozonolysis. *J. Am. Chem. Soc.* **1975**, *97*, 3004–3021.
- Lovas, F. J.; Suenram, R. D. Identification of dioxirane (H₂COO) in ozone-olefin reactions via microwave spectroscopy. *Chem. Phys. Lett.* **1977**, *51*, 453–456.
- Lopes, S.; Domanskaya, A. V.; Fausto, R.; Räsänen, M.; Khriachtchev, L. Formic and acetic acids in a nitrogen matrix: Enhanced stability of the higher-energy conformer. *J. Chem. Phys.* **2010**, *133*, 144507–144514.
- Marushkevich, K.; Khriachtchev, L.; Lundell, J.; Domanskaya, A.; Räsänen, M. Matrix Isolation and Ab Initio Study of *Trans-Trans* and *Trans-Cis* Dimers of Formic Acid. *J. Phys. Chem. A* **2010**, *114*, 3495–3502.
- Pettersson, M.; Lundell, J.; Khriachtchev, L.; Räsänen, M. IR Spectrum of the Other Rotamer of Formic Acid, *cis*-HCOOH. *J. Am. Chem. Soc.* **1997**, *119*, 11715–11716.
- Gerbig, D.; Schreiner, P. R. Hydrogen-Tunneling in Biologically Relevant Small Molecules: The Rotamerizations of α -Ketocarboxylic Acids. *J. Phys. Chem. B* **2015**, *119*, 693–703.
- East, A. L. L.; Allen, W. D. The heat of formation of NCO. *J. Chem. Phys.* **1993**, *99*, 4638–4650.
- Schuurman, M. S.; Muir, S. R.; Allen, W. D.; Schaefer, H. F., III Toward subchemical accuracy in computational thermochemistry: Focal point analysis of the heat of formation of NCO and [H,N,C,O] isomers. *J. Chem. Phys.* **2004**, *120*, 11586–11599.
- Bartlett, M. A.; Liang, T.; Pu, L.; Schaefer, H. F., III; Allen, W. D. The multichannel *n*-propyl + O₂ reaction surface: Definitive theory on a model hydrocarbon oxidation mechanism. *J. Chem. Phys.* **2018**, *148*, 094303.
- Császár, A. G.; Allen, W. D.; Schaefer, H. F., III In pursuit of the ab initio limit for conformational energy prototypes. *J. Chem. Phys.* **1998**, *108*, 9751–9764.
- Gonzales, J. M.; Allen, W. D.; Schaefer, H. F., III Model Identity S_N2 Reactions CH₃X + X⁻ (X = F, Cl, CN, OH, SH, NH₂, PH₂): Marcus Theory Analyzed. *J. Phys. Chem. A* **2005**, *109*, 10613–10628.
- Stanton, J. F. Why CCSD(T) works: a different perspective. *Chem. Phys. Lett.* **1997**, *281*, 130–134.
- Čížek, J. On the Correlation Problem in Atomic and Molecular Systems. Calculation of Wavefunction Components in Ursell-Type Expansion Using Quantum-Field Theoretical Methods. *J. Chem. Phys.* **1966**, *45*, 4256–4266.
- Bartlett, R. J.; Watts, J. D.; Kucharski, S. A.; Noga, J. Non-iterative fifth-order triple and quadruple excitation energy corrections in correlated methods. *Chem. Phys. Lett.* **1990**, *165*, 513–522.
- Purvis, G. D., III; Bartlett, R. J. A full coupled-cluster singles and doubles model: The inclusion of disconnected triples. *J. Chem. Phys.* **1982**, *76*, 1910–1918.
- Raghavachari, K.; Trucks, G. W.; Pople, J. A.; Head-Gordon, M. A fifth-order perturbation comparison of electron correlation theories. *Chem. Phys. Lett.* **1989**, *157*, 479–483.
- Woon, D. E.; Dunning, T. H., Jr. Gaussian basis sets for use in correlated molecular calculations. V. Core-valence basis sets for boron through neon. *J. Chem. Phys.* **1995**, *103*, 4572–4585.
- Kállay, M.; Nagy, P. R.; Mester, D.; Rolik, Z.; Samu, G.; Csontos, J.; Csóka, J.; Szabó, P. B.; Gyevi-Nagy, L.; Hégyely, B.; Ladjánszki, I.; Szegegy, L.; Ladóczki, B.; Petrov, K.; Farkas, M.; Mezei,

- P. D.; Ganyecz, Á. MRCC, a Quantum-Chemical Program Suite. Available at <https://www.mrcc.hu>.
- (35) MOLPRO, a Package of Ab Initio Programs, ver. 2019.2 (see the SI for the full reference). Available at <https://www.molpro.net>.
- (36) Wentzel, G. Eine Verallgemeinerung der Quantenbedingungen für die Zwecke der Wellenmechanik. *Eur. Phys. J. A* **1926**, *38*, 518–529.
- (37) Kramers, H. A. Wellenmechanik und halbzahlige Quantisierung. *Eur. Phys. J. A* **1926**, *39*, 828–840.
- (38) Brillouin, L. La mécanique ondulatoire de Schrödinger: une méthode générale de résolution par approximations successives. *C. R. Acad. Sci.* **1926**, *183*, 24–26.
- (39) Quanz, H.; Schreiner, P. R. TUNNEX: An easy-to-use Wentzel-Kramers-Brillouin (WKB) implementation to compute tunneling half-lives. *J. Comput. Chem.* **2019**, *40*, 543–547.
- (40) Lee, C.; Yang, W.; Parr, R. G. Development of the Colle-Salvetti correlation-energy formula into a functional of the electron density. *Phys. Rev. B* **1988**, *37*, 785–789.
- (41) Becke, A. D. A new mixing of Hartree–Fock and local density-functional theories. *J. Chem. Phys.* **1993**, *98*, 1372–1377.
- (42) Becke, A. D. Density-functional exchange-energy approximation with correct asymptotic behavior. *Phys. Rev. A* **1988**, *38*, 3098–3100.
- (43) Kim, K.; Jordan, K. D. Comparison of Density Functional and MP2 Calculations on the Water Monomer and Dimer. *J. Phys. Chem.* **1994**, *98*, 10089–10094.
- (44) Stephens, P. J.; Devlin, F. J.; Chabalowski, C. F.; Frisch, M. J. Ab Initio Calculation of Vibrational Absorption and Circular Dichroism Spectra Using Density Functional Force Fields. *J. Phys. Chem.* **1994**, *98*, 11623–11627.
- (45) Grimme, S. Semiempirical hybrid density functional with perturbative second-order correlation. *J. Chem. Phys.* **2006**, *124*, 034108.
- (46) Bousquet, D.; Brémond, E.; Sancho-García, J. C.; Ciofini, I.; Adamo, C. Is There Still Room for Parameter Free Double Hybrids? Performances of PBE0-DH and B2PLYP over Extended Benchmark Sets. *J. Chem. Theory Comput.* **2013**, *9*, 3444–3452.
- (47) Fernandez-Ramos, A.; Ellingson, B. A.; Garrett, B. C.; Truhlar, D. G. Variational transition state theory with multidimensional tunneling. *Rev. Comput. Chem.* **2007**, *23*, 125–233.
- (48) Frisch, M. J.; et al. *Gaussian 16*, rev. B.01; Gaussian, Inc.: Wallingford, CT, 2016 (see the SI for the full reference). Available at <https://www.gaussian.com>.
- (49) Allen, W. D.; Császár, A. G. On the ab initio determination of higher-order force constants at nonstationary reference geometries. *J. Chem. Phys.* **1993**, *98*, 2983–3015.
- (50) Allen, W. D.; Császár, A. G.; Szalay, V.; Mills, I. M. General derivative relations for anharmonic force fields. *Mol. Phys.* **1996**, *89*, 1213–1221.
- (51) Pulay, P.; Török, F. *Acta Chim. Acad. Sci. Hungary* **1965**, *44*, 287.
- (52) Keresztury, G.; Jalsovszky, G. An alternative calculation of the vibrational potential energy distribution. *J. Mol. Struct.* **1971**, *10*, 304–305.
- (53) Allen, W. D.; Császár, A. G.; Horner, D. A. The Puckering Inversion Barrier and Vibrational Spectrum of Cyclopentene. A Scaled Quantum Mechanical Force Field Algorithm. *J. Am. Chem. Soc.* **1992**, *114*, 6834–6849.
- (54) Hunter, J.; Matplotlib, D. A 2D Graphics Environment. *Comput. Sci. Eng.* **2007**, *9*, 90–95.
- (55) Behnel, S.; Bradshaw, R.; Citro, C.; Dalcin, L.; Seljebotn, D. S.; Smith, K. Cython: The Best of Both Worlds. *Comput. Sci. Eng.* **2011**, *13*, 31–39.
- (56) van der Walt, S.; Colbert, S. C.; Varoquaux, G. The NumPy Array: A Structure for Efficient Numerical Computation. *Comput. Sci. Eng.* **2011**, *13*, 22–30.
- (57) Wagner, J. P.; Reisenauer, H. P.; Hirvonen, V.; Wu, C.-H.; Tyberg, J. L.; Allen, W. D.; Schreiner, P. R. Tunneling in carbonic acid. *Chem. Commun.* **2016**, *52*, 7858–7861.
- (58) Schreiner, P. R.; Wagner, J. P.; Reisenauer, H. P.; Gerbig, D.; Ley, D.; Sarka, J.; Császár, A. G.; Vaughn, A.; Allen, W. D. Domino Tunneling. *J. Am. Chem. Soc.* **2015**, *137*, 7828–7834.
- (59) Honda, K.; Ohkura, S.; Hayashi, Y.; Kawauchi, S.; Mikami, K. Cationic Chiral Pd-Catalyzed “Acetylenic” Diels–Alder Reaction: Computational Analysis of Reversal in Enantioselectivity. *Chem. Asian J.* **2018**, *13*, 2842–2846.
- (60) Halasa, A.; Reva, I.; Lapinski, L.; Nowak, M. J.; Fausto, R. Conformational Changes in Thiazole-2-carboxylic Acid Selectively Induced by Excitation with Narrowband Near-IR and UV Light. *J. Phys. Chem. A* **2016**, *120*, 2078–2088.

2.4 Further co-authored publications

Allen, W. D.; **Quanz, H.**; Schreiner, P. R. Polytriangulane. *J Chem Theory Comput.* **2016**, *12*, 4707–4716.

Rösel, S.; **Quanz, H.**; Logemann, C.; Becker, J.; Mossou, E.; Cañadillas-Delgado, L.; Caldeweyher, E.; Grimme, S.; Schreiner, P. R. London Dispersion Enables the Shortest Intermolecular Hydrocarbon H···H Contact. *J Am Chem Soc.* **2017**, *139*, 7428–7431.

Lu, Z. P.; **Quanz, H.**; Burghaus, O.; Hofmann, J.; Logemann, C.; Beeck, S.; Schreiner, P. R.; Wegner, H. A. Stable Organic Neutral Diradical via Reversible Coordination. *J Am Chem Soc* **2017**, *139*, 18488–18491.

Lu, Z.; **Quanz, H.**; Ruhl, J.; Albrecht, G.; Logemann, C.; Schlettwein, D.; Schreiner, P. R.; Wegner, H. A. Control of Excited-State Conformations in B,N-Acenes. *Angew Chem Int Ed* **2019**, *58*, 4259–4263.

Schümann, J. M.; Wagner, J. P.; Eckhardt, A. K.; **Quanz, H.**; Schreiner, P. R. Intramolecular London Dispersion Interactions Do Not Cancel in Solution. *J Am Chem Soc* **2021**, *143*, 41–45.

3 Acknowledgement

After a long time, this period of my life is ending. This thesis would not have been possible without the countless help from others. I would like to thank the following people in person:

- **Prof. Dr. Peter R. Schreiner** for his trust in my ability, his scientific advice, and his guidance
- **Dr. Hans Peter Reisenauer** for his knowledge in the arts of spectroscopy
- **Dr. Dennis Gerbig** my mentor and friend without this work would be impossible, and proofreading
- **Dr. Raffael Wende** for a lovely side project with Prof. Vilcinskas, and proofreading.
- **Dr. David Ley** for introducing me to computational chemistry very early on
- **Dr. Artur Marduyukov** for the cooperation in the trifluoromethylhydroxycarbene project
- **Dr. André K. Eckhardt** for the excellent talks in our office, and proofreading
- **Bastian Bernhardt, MSc** for his cooperation in the dihydroxycarbene project, very nice evenings, and proofreading
- **Dr. Wesley Allen** for his thorough proofreading of the dihydroxycarbene paper
- **Frederik R. Erb, MSc** for his fast and reliable precursor synthesis
- To my collages in the office, **Dr. J Philipp Wager, Lijuan Song, PhD**
- To my bachelors **Tizian Müller, MSc** und **Tobias Wagner, BSc**
- **Ms. Richter, Ms. Verch and Dr. Jörg Neudert** for all the help in administrative work
- **The computational center at Gießen and Frankfurt** for making all computations possible
- **The PRS group** for the delightful 8 years
- **Jan M. Schumann, MSc** without whom I would always miss lunchtime ;)
- **Alexander Seitz, MSc, Dr. Marta Larrosa Ferreira, Christian Eschmann, MSc, Dr. Fumito Saito, Dr. Dominik Niedek, Felix Keul, MSc** and **Jean Pohl, MSc** for the some very nice evenings
- **The lunch group** as there was always delightful scientific and unscientific talks
- **My whole semester** for a delightful time during my Bachelor and Master studies
- **My uncle and aunt** Karl Dieter Bleileven and Ingeborg Bleileven for everything they have done since I am in Gießen
- **My Brothers** Mathias Quanz and Frederik Quanz who were always there for me
- **My mother** Friedhilde Riesterer and her husband Hubert Riesterer for the continuous support
- **My father** Dr. Gerhard Quanz and his wife Elke Quanz without whom this thesis would have been impossible